PARALLEL DECODING OF CONCATENATED CODED SPREAD SPECTRUM FREQUENCY-HOPPED COMMUNICATIONS IN PARTIAL BAND JAMMING

Kenneth G. Castor

COMMUNICATIONS & SIGNAL PROCESSING LABORATORY
Department of Electrical Engineering and Computer Science
The University of Michigan
Ann Arbor, Michigan 48109

Technical Report No. 243

January 1987

ABSTRACT

This thesis investigates the use of parallel decoding schemes to mitigate the effects of partial band Gaussian jamming for spread spectrum, M-ary orthogonal, frequency-hopped communication systems which use concatenated error-correcting codes. The motivation for the parallel decoding technique is an ability to capitalize on the powerful error and erasure correction capability and bounded distance decoding characteristics of Reed-Solomon codes which are used exclusive for the outer codes.

General results are presented for the bit error rate of systems which use multiple inner decoders one of which is a complete (hard decisions) decoder and one or more of which are incomplete decoders (i.e., errors and erasures). The system bit error propbability as a function of the per information bit energy-to-jammer noise power ratio and the percentage of hopping bandwidth which is jammed is derived

Specific results for five inner decoding algorithms based on the use of L-diversity repetition codes on M-ary alphabets are given. Two of the decoding schemes use a derived side information quality bit using a ratio thresholding technique defined by Viterbi. Another decoding scheme is based on knowledge of perfect side information. Two decoding algorithms which use no side information are evaluated.

The use of arbitrary binary linear block codes for the inner encoder is considered. We derive general results for evaluating the parallel decoding system performance using such codes with either binary or M-ary channel signalling. Specific results for four inner encoding schemes, two based on shortened Hamming codes and two based on BCH codes are given.

DEDICATION

FOR

my wife:

Virginia L. Castor

my daughter:

Amy R. Castor

my Mom and Dad:

Frances T. Castor and George J. Castor

ACKNOWLEDGEMENTS

Completion of a doctoral dissertation is, for most people, a monumental task. Completion in absentia is more difficult and requires outstanding support of the dissertation advisor, patience and tolerance from ones family, and support and encouragement from ones employer. I am fortunate to have had all of the above.

Dr. Wayne Stark is responsible for conceiving and motivating the original concepts upon which this thesis is based. When necessary, he made his schedule accommodate mine so that progress would not be impeded. He encouraged, he assisted. His criticism was always constructive.

I owe a debt of gratitude to the United States Air Force, the sponsor of my doctoral studies, and to my commanders and supervisers who supported my research. Particular appreciation is due to Dr. Robert Fontana, now retired from the Air Force Institute of Technology, who provided me encouragement and the opportunity to gain momentum with the research effort.

The sacrifices of my wife, Virginia, and my daughter, Amy, have been no less than my own. I thank you both for your support and tolerance of my long and numerous absences.

I thank each of my committee members, Dr. D. Neuhoff, Dr. T. Birdsall, Dr. W. Root and Dr. M. Ristenbatt for their time reading and evaluating the thesis. Special thanks to Ms. Beth Olsen for typing and preparing the manuscript.

TABLE OF CONTENTS

LIST OF FIGURES

LIST OF TABLES

LIST OF APPENDICES

Appendices

CHAPTER 1

INTRODUCTION AND MODELS

The concept of using spread spectrum frequency hopping techniques to achieve anti-jamming capability is very simple: start with a narrowband information signal and move the rf carrier frequency over a very wide bandwidth, in discrete steps, in a very difficult to predict pattern. Initially the jammer's options appear to be limited to two undesirable alternatives: either spread limited power over the full bandwidth of transmission or attempt to follow the changing frequency pattern. However, the design of jamming/anti-jamming systems is like a chess game; each new strategy begets a counter strategy. In this case the counter strategy is partial band jamming. Again a simple concept, with partial band jamming the jammer places power only in a percentage of the transmission bandwidth. The new objective is not to deny all communications, but to create a significant error rate so that the communications is of little or no value.

One concentration of present day research in frequency hopping spread spectrum anti-jamming systems is on the use of error correcting codes to counter the effects of partial band jamming. The objective of this countermeasure is to introduce redundancy so that the receiver may make decisions on the basis of transmissions over multiple frequency bins. Without coding it is well known that an intelligent (e.g., worst case partial band) jammer can cause the bit error probability to be an

inverse linear function of the received signal-to-noise ratio as opposed to an exponentially decreasing function for broadband noise. This can cause a degradation in performance of 30-40 dB.

The obvious countermeasure against partial band jamming is the use of error correcting coding techniques. By introducing redundancy in the transmitted signals the receiver may base data decisions on the results of multiple transmissions. Consequently, the jammer may be forced to spread its power to corrupt a greater portion of the transmissions. As the jammer is forced to a broadband jamming strategy the communicator regains an exponentially improving bit error probability.

Coding techniques for spread spectrum frequency hopped communications are discussed extensively in the literature. The three volume *Spread Spectrum Communications* series [14] summarizes many of the significant results [see in particular Chapter 2 of Volume II]. Researchers recognized early that coding techniques which yielded good performance in additive white Gaussian noise (AWGN) were not directly applicable to partial band jamming. However, if perfect side information is available which identifies whether a received signal is jammed or not, decoding techniques for AWGN can be modified to give good performance in partial band jamming.

For example, with a system using L-diversity repetition codes the communicator can achieve performance that with worst case partial band jamming is within $3dB$ of the performance in equivalent broadband noise with no jamming. However, the repetition code rate $(1/L)$ necessary to achieve this performance may become very small (e.g., $L = 20$ with 32-ary FSK at $P_b = 10^{-5}$). If the communicator knew the percentage of the total hopping bandwidth which would be jammed, the communication strategy (i.e., diversity and modulation) could be improved. However, if the

jammer anticipates this approach and alters the jamming strategy the results could be disastrous for the communication. For example, with 16-ary FSK, $P_b = 10^{-5}$, and 75% of the hopping bandwidth jammed, a conservative design would require $11.11dB$ received signal-to-noise ratio; an optimized design requires $9.23dB$. However, in the later case the jammer could reapportion the jamming power so that $42.56dB$ would be required [14, Section 2.3.2.2].

A technique which provides robust performance against partial band jamming involves parallel decoding of the received signal by decoders which are individually sensitive to extremes of the percentage of bandwidth which is jammed. In [12] Pursley and Stark investigate parallel decoding techniques for systems using concatenated codes in the channel encoder. Their results demonstrate that good performance is achievable in a partial band jamming environment independent of the percentage of bandwidth jammed when perfect side information is available.

The weakness of analysis such as described above is the assumption of perfect side information. In most practical situations perfect side information cannot be generated. The reliability of techniques which produce side information estimates should be included in the analysis of side information dependent systems. Moreover, the reliability should include the susceptibility of the estimator to being spoofed by the jammer.

In this thesis we continue the investigation of the use parallel decoding techniques to mitigate the effect of partial band jamming. Except for one case, used for comparison purposes, perfect side information is not assumed. Our results show that parallel decoding without side information does provide a robust technique for countering a partial band jammer independent of the percentage of bandwidth

jammed. Below we describe in detail the parallel decoder, system models, and assumptions used in the analysis.

In Figure 1.1 we present a general parallel decoding system block diagram showing major processing blocks between the information source and the user output. We will assume that the alphabet of interest to the source and user is the binary alphabet. The source is modelled as being binary and equiprobable. One performance parameter of primary interest will be the probability that an information bit is received in error.

The channel encoder for the system uses two error correcting channel encoders connected in tandem. Such a configuration is called concatenated coding and is widely discussed in the literature (see e.g., [4, Section 8.1] or [10, Section 11.1]). The first encoder, called the outer encoder, will be exclusively an (N_O,K_O) Reed-Solomon encoder. The Reed-Solomon encoder operates on K_O blocks of k bits, each such block is called a symbol. For each input of K_O symbols the encoder produces an output of N_O symbols called a codeword. In general, for Reed-Solomon codes N_O is an element of the set $\{2^k-1,2^k,2^k+1\}$.

In practice, concatenated coding systems have also used Reed-Solomon codes almost exclusively for the outer codes. One of the primary reasons for this fact is that Reed-Solomon codes are the easiest to implement of a class of codes called maximum distance separable codes. Codes which belong to this class are very efficient in use of redundancy and allow for wide ranges of block lengths and symbol sizes. [10,376] Additional details on maximum distance separable codes are given in Chapter 2.

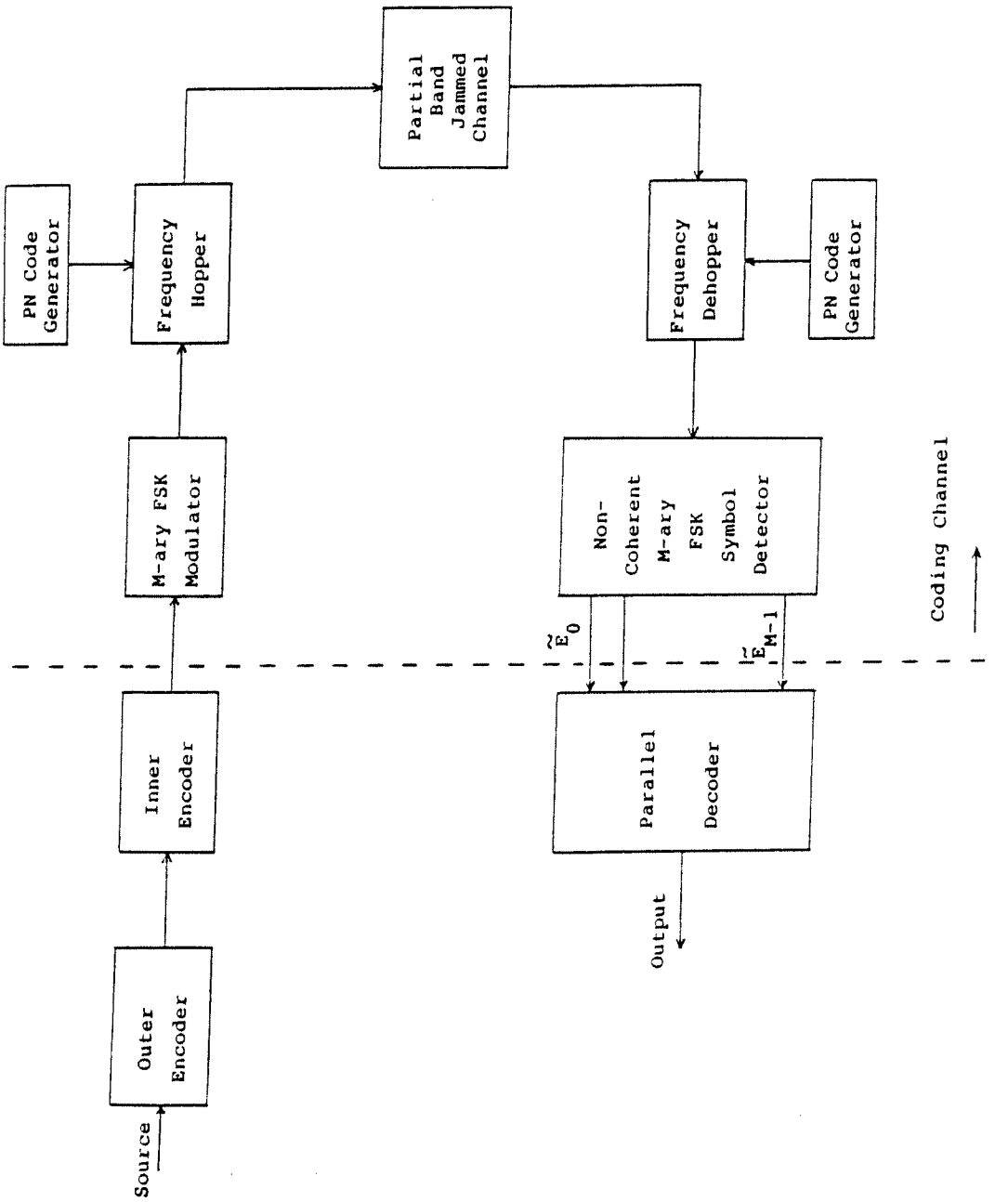

Figure 1.1 Concatenated Coded System With Parallel Decoder

The second channel encoder, called the inner encoder, is an (N_I,K_I) linear block code. For this thesis we consider two types of inner error correcting codes. First, we consider cases when the inner code is an L-diversity repetition code on the same symbol alphabet used by the Reed-Solomon decoder. That is, with $K_I = 1$ and $N_I = L$, for each k bit symbol input to the inner encoder the output is that same symbol repeated L times. Second, we consider the inner encoder to be a binary linear block code where we restrict the input block length, K_I, to be equal to the Reed-Solomon code symbol size, i.e., k bits.

The transmitter accepts the output of the inner encoder and produces an M-ary frequency shift keyed spread spectrum frequency hopped signal. Both binary and M-ary ($M>2$) signalling are considered. The frequency hopped signal is formed as follows. First a conventional M-ary frequency shift keyed signal is generated either at base band frequencies or at a suitable intermediate frequency (IF). Secondly, the signal is heterodyned up to a carrier frequency which is one of a set of possible frequency selected by a suitable algorithm. The carrier frequency is varied at a fixed rate which may range from multiple frequency changes (hops) per symbol to one frequency being used for multiple symbols. The later case, called slow frequency hopping, will be used throughout this thesis.

We note that the use of L-diversity inner codes with one hop per symbol is equivalent to merely hopping L times for each symbol output from the outer encoder. The frequency selection algorithm is often derived from a simple operation on either a linear maximum length recursive sequence or a ciphered bit stream. In either case, the objective is to produce a pseudorandom hopping pattern, that is, a pattern which appears to be random. We will assume that the hopping pattern may be modelled as

an independent, identically distributed random sequence of frequencies and that the receiver successfully synchronizes to this sequence. With this assumption, the results of this thesis are independent of the frequency selection algorithm.

As stated above, with partial band jamming the jammer places his power in only part of the spread spectrum frequency hopped bandwidth. We define ρ as the fraction of the hopped bandwidth which is jammed, $0 \leq \rho \leq 1$. Then with the assumption of a random hopping pattern over the spread bandwidth, the received signal is jammed with probability ρ and not jammed with probability $1-\rho$. We will concentrate on the effects of the jammer and for the analysis described in this thesis we ignore the contribution of thermal noise.

It is assumed that the jammer has power S_J which may be distributed at will uniformly across any portion of the spread spectrum frequency hopping bandwidth, W_{SS}. We let N_J be the noise power spectral density at the receiver when the jammer distributes power S_J uniformly across the full hopped spectrum, $N_J = S_J / W_{SS}$. When the jamming power is uniformly distributed over a fraction ρ of the hopped bandwidth, the received noise spectral density is $S_J / \rho W_{SS} = N_J / \rho$ for those transmissions which hop into the jammed band. In this thesis we assume the jammer is a Gaussian noise process with spectral density N_J / ρ over a bandwidth ρW_{SS}. Furthermore, whenever the transmitted signal hops in the spectrum all possible M-ary FSK signals lie either entirely within or external to the jammed portion of the spread spectrum bandwidth.

To illustrate the nature of the calculations, consider an example using binary signalling with no error corrective coding. The non-coherent receiver for a channel with Gaussian noise spectral density N_J achieves a bit error rate P_b of:

$$P_b = \frac{1}{2}\, e^{-E_b/2N_J} \tag{1.1}$$

where E_b is the received energy per bit. To compute the receiver performance in the partial band Gaussian noise channel where thermal noise is ignored, we first note that:

$$\begin{aligned} P(\text{bit error}) = {} & P(\text{bit error} \mid \text{not jammed})\, P(\text{not jammed}) \\ & + P(\text{bit error} \mid \text{jammed})\, P(\text{jammed}) \end{aligned} \tag{1.2}$$

Without background noise, $P(\text{ bit error} \mid \text{not jammed }) = 0$ and since $P(\text{jammed}) = \rho$ we have,

$$P_b = \frac{1}{2}\, \rho\, e^{-\rho E_b/2N_J} \tag{1.3}$$

The jammer wishes to choose a strategy (i.e., ρ) which maximizes P_b. It is well known [14, Volume II, page 77] that the value of ρ which maximizes P_b is given by $\rho_{\max} = 2N_J/E_b$ if $E_b/N_J \geq 3dB$ and $\rho_{\max} = 1$ otherwise. The corresponding values of P_b are given by:

$$P_b(\max) = \begin{cases} \dfrac{e^{-1}}{E_b/N_J} & E_b/N_J \geq 3dB \\ \dfrac{1}{2}\, e^{-E_b/2N_J} & \text{otherwise} \end{cases} \tag{1.4}$$

The effect of an optimum partial band jamming strategy is illustrated by a simple numerical example. Suppose the communicators objective is to achieve a bit error rate of $P_b = 10^{-4}$. With uniform jamming over the entire frequency hopped spectrum (i.e., $\rho = 1$) a received signal energy-to-jammer noise density ratio of $E_b/N_J = 12.31\ dB$ is required. However, if the jammer maximizes the jamming strategy an E_b/N_J of 35.66 dB is required to achieve the same performance. For the above example ρ_{MAX} is .00054. That is, the jammer needs only to cause errors on a small percentage of the frequency hops to degrade the bit error rate to greater than

10^{-4}. This result is not surprising since to defeat the communicators performance goal the jammer must cause only two or more bit errors for 10000 bits transmitted (even less on an average over many transmissions).

We note that although the general connotation of a jammer refers to a hostile third party, the analysis presented herein is equally applicable to the "friendly" jammer. The same channel model of interference in a fraction of the hopping bandwidth results with multiple-access frequency hopping systems. When two or more users hop to the same frequency that particular hop is in essence jammed.

The transmitted signal and jamming energy is first processed by the frequency dehopper which has been assumed to be synchronized with the hopping pattern. In addition, the dehopper commonly contains band-pass filters which reject any received energy which is not at the current hop frequency. Hence, the input to the non-coherent M-ary FSK symbol detector is an M-ary FSK signal which is noise free with probability $1-\rho$ and contains noise of spectral density N_J/ρ with probability ρ. The symbol detector output is the result of processing the input signal through parallel filters matched to the M possible outputs of the M-ary FSK generator. In Figure A.1 of Appendix A we show a block diagram of a typical non-coherent M-ary FSK symbol detector.

We define the coding channel as that portion of the system model which lies between the output of the inner encoder and the input to the parallel decoder. The inputs to the coding channel are the symbols of the inner decoder which are elements of an M-ary alphabet ($M \geq 2$). For each input symbol of the output of the decoding channel is vector of M independent random variables $(\tilde{E}_0, \ldots, \tilde{E}_{M-1})$ as described above. Assume symbol $k \in \{0,1, \ldots, M-1\}$ is transmitted. Conditioned

on the event that the transmission is not jammed $\tilde{E}_j \equiv 0$ if $j \neq k$ and $\tilde{E}_k = 4E_S^2$. On the other hand, given that the transmission is jammed, standard calculations (e.g., [6, Volume I, Section 4.7] or [11, Section 4.3.2]) yield the following probability distributions on the matched filter outputs.

$$P_{\tilde{E}_j}(\alpha) = \begin{cases} \frac{\rho}{4E_S N_J} \; e^{-\frac{\rho\alpha}{4E_S N_J}} & j \neq k \\ \frac{\rho}{4E_S N_J} \; e^{-\frac{\rho\alpha}{4E_S N_J}} e^{-\frac{\rho E_S}{N_J}} \; I_0\Big(\frac{\rho\sqrt{\alpha}}{N_J}\Big) & j = k \end{cases} \tag{1.5}$$

where I_0 is the 0^{th}-order modified Bessel function; the first distribution is exponential and the second is non-central chi-square with two degrees of freedom. The coding channel is memoryless and successive transmissions are received with distributions given by (1.5).

The M outputs of the symbol detector are the inputs to the parallel decoding system. This system consists of two or more concatenated decoders that is, an inner decoder followed by an outer decoder operating in parallel. In Figures 2.1, 2.2, and 2.3 we show the three parallel decoder configurations which are considered in this thesis. In all cases the outer decoder is an (N_O, K_O) Reed-Solomon decoder. Reed-Solomon codes are chosen because of their powerful error and erasure correction capability. We assume a bounded distance decoder for the Reed-Solomon code which corrects t errors and e erasures provided $2t + e \leq N_O - K_O + 1$.

The uniqueness of the parallel decoding approaches analyzed herein lies primarily in the design of the inner decoders. These inner decoders consist of one complete decoder and one or more incomplete decoders. A complete decoder is one which is restricted to making a hard decision estimate of the transmitted codeword. On the

other hand, the incomplete decoder may indicate an inability to make a clear choice which results in a output referred to as an erasure. The incomplete decoder outputs are either the correct symbol, and erroneous symbol or an erasure. In the most general case, the J-ary parallel decoder of Figure 2.3 contains $J-1$ incomplete inner decoders which have a successively more restrictive algorithms allowing for erasure outputs. Finally, the J^{th} inner decoder is a complete decoder which does not allow for an erasure output.

The general decoding concept is as follows, the N_I symbols corresponding to a transmitted inner code codeword are assembled and input to each of the inner decoders. Each inner decoder output is one symbol (possibly an erasure) of a Reed-Solomon codeword. The N_O symbols which comprise a Reed-Solomon codeword are then assembled for each of the Reed-Solomon decoders. Each Reed-Solomon decoder is implemented as a bounded distance decoder which is also an incomplete decoder. Each of these decoders may output a correct symbol, an erroneous symbol, or indicate a failure to make a clear choice. We require the parallel decoding system to output hard decision estimates of the source information. Hence, we do not allow for erasures. In the events that all Reed-Solomon decoders fail we choose to output the information portion of the Reed-Solomon decoder codeword at the output of the complete decoder (this codeword cannot contain erasures). We initially approached this research with the assumption that a Reed-Solomon decoder with bounded distance decoding will fail with probability one rather than output an erroneous symbol. We have since evaluated the merit of this assumption. The analysis is described in Chapter 2 and numerical results are given in Chapter 5.

We consider six designs for the parallel inner decoding system. We analyze one case where perfect side information of the jamming state is available and the inner decoder erasure criterion is obvious. We consider two algorithms based on a thresholding technique introduced by Viterbi [18,19] which develops a binary qualitative estimate of the signal environment by using a ratio test on the outputs of the noncoherent M-ary FSK symbol detector. In the remaining cases, the inner decoder erasure decisions are derived without reference to perfect or derived sider information.

The different decoding schemes will be evaluated on the basis of their ability to achieve a 10^{-4} bit error probability as a function of the received energy per information bit-to-jammer noise ratio E/N versus the percentage of bandwidth jammed ρ. In Chapter 2 we develop the general model for parallel decoding of concatenated coded spread spectrum frequency-hopping communication systems. We derive general formulas for the symbol and bit error rates for three parallel decoder configurations: one, two, and multiple Reed-Solomon decoders. We initially rely on the assumption that bounded distance decoding by the Reed-Solomon decoders will with high probability yield decoder failures rather than error. Subsequently we evaluate and substantiate the assumption. Finally, we evaluate the relationship of bit errors as function of symbol errors.

In Chapter 3 we concentrate on the case when the inner encoder is an M-ary repetition code. We start by evaluating the case when perfect side information is available. The Viterbi ratio-thresholding technique is introduced with developmental details left to Appendix A. We define two erasure algorithms based on quality estimates provided by ratio test and derive necessary quantities to evaluate their performance with parallel decoding. Finally, we describe techniques called "repetition

thresholding" and "tie thresholding" and again derive the quantities necessary for decoder evaluation.

Next, in Chapter 4, we consider the effects of using binary linear block codes for the inner code. In this case the erasure criterion is a trade-off between the error-detection and error-correction capabilities of the inner code. Among the codes evaluated are a shortened Hamming codes and a BCH code. Where conditions allow, we consider both binary and M-ary signalling schemes. In some case, by appropriate partitioning of the inner code standard array we can meet the criterion established in Chapter 2 for the M-ary parallel decoder. All quantities necessary to evaluate performances of the different decoder configurations are derived.

In Chapter 5 we describe procedures used to normalize the results of decoder performances to allow fair comparison of different configurations and algorithms. Curves of typical best and worst case parallel decoder performances are presented and compared. In addition, we compare our results with those for soft decisions and perfect side information given in [12].

CHAPTER 2

PARALLEL DECODING TECHNIQUES

2.1 Introduction

In this chapter we introduce three models for parallel decoding of concatenated coded spread spectrum frequency-hopped communications. The models are presented in order of increasing complexity which corresponds to their evolvement in the research. In general, each model has one or more incomplete decoders for processing the inner code. In all cases the outer code is assumed to be a Reed-Solomon code. The function of the incomplete inner decoder is to capitalize on the powerful error and erasure correction capability and bounded distance decoding characteristics of the Reed-Solomon decoder. We make no assumptions regarding the particular type of code used for the inner coder nor the algorithms this decoder uses to generate output symbols or erasures. We leave analysis for specific inner codes and erasure algorithms to Chapters 3 and 4.

Figures 2.1, 2.2, and 2.3 illustrate the three parallel decoder models to be analyzed. The 2-ary parallel decoder of Figure 2.2 will be seen to be a special case of the J-ary decoder shown in Figure 2.3. However, for the sake of clarity we will present the analysis for the systems in order of increasing complexity.

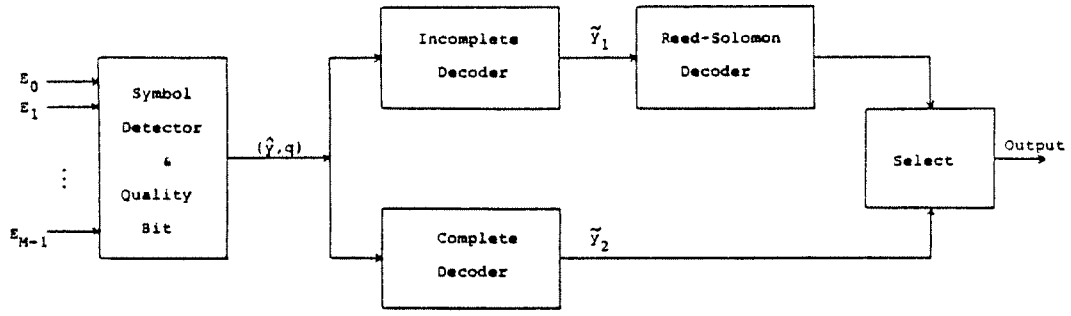

Figure 2.1 Parallel Decoding System With Single Reed-Solomon Decoder

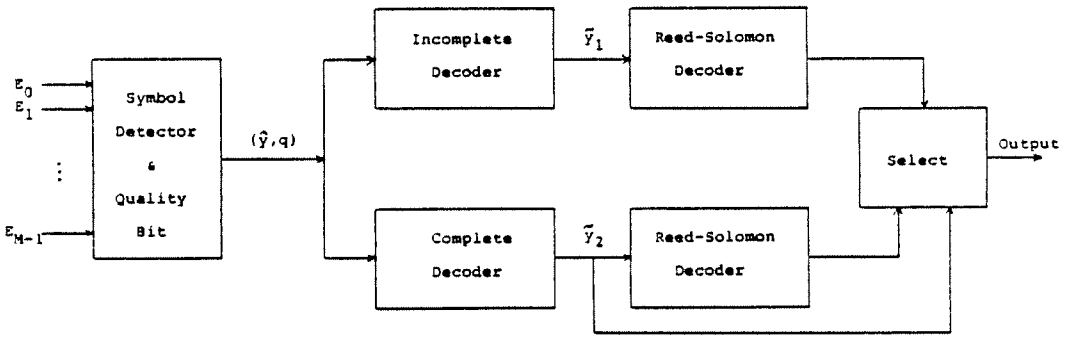

Figure 2.2 Parallel Decoding System With Two Reed-Solomon Decoders

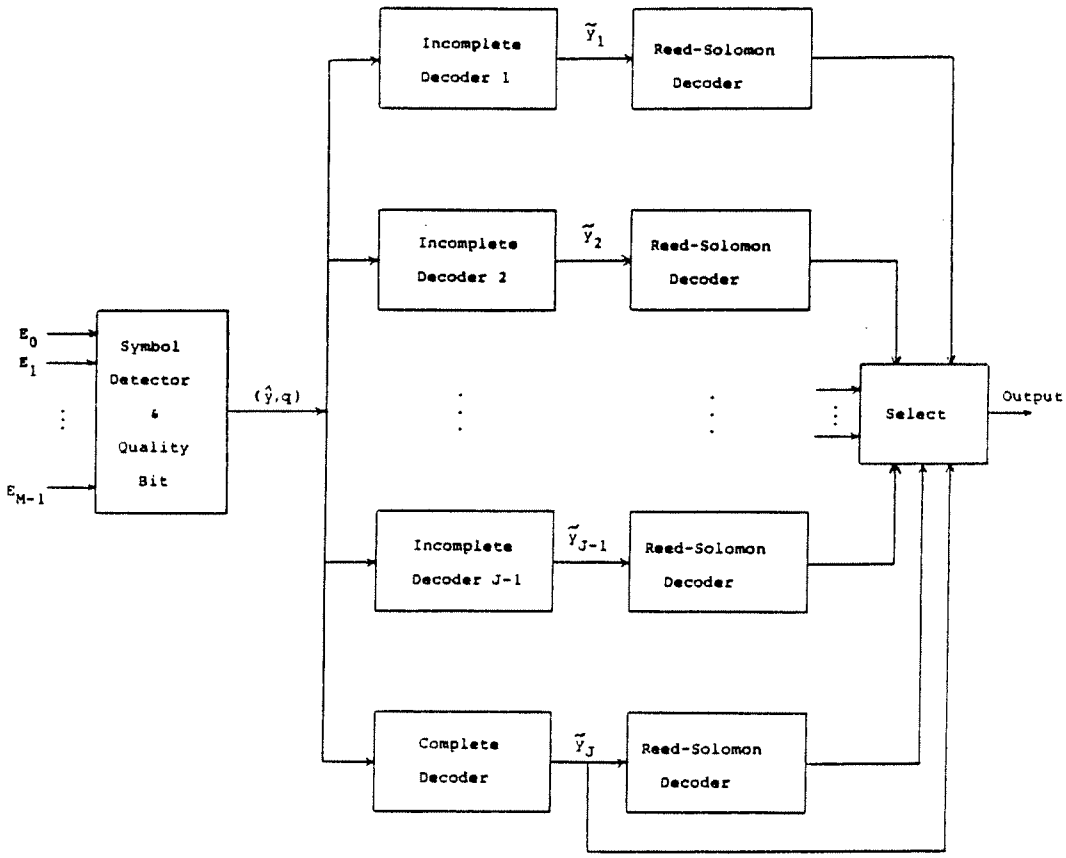

Figure 2.3 Multiple Parallel Decoding System

In general, the inputs to the inner decoders are the same for each system. These inputs are the result of processing the M-tuple of values E_i, $i = 0, 1, \ldots, M-1$ which are the outputs of M energy detectors matched to the orthogonal M-ary signal set; system synchronization and successful dehopping are assumed. In the most general case, the receiver produces a pair of outputs $(\hat{y},q)$ for each M-ary detection. The first element,

$$\hat{y} \in \{0, 1, \ldots, M-1\}$$

is a hard decision estimate of the transmitted symbol corresponding to $E_{\max} = \max\{E_i\}$. The second element, q, is an optional quality bit which may be used to convey side information. In Chapter 3 we will consider a case where q represents perfect side information and another case where q is a binary soft decision metric which gives a quality measure of the symbol estimate.

The inputs to each inner decoder is a N_I-tuple of pairs

$$\{(\hat{y}_j,q_j)\ ;\ j = 1, \ldots, N_I\} \quad .$$

Each incomplete decoder outputs either a codeword estimate or an erasure for each N_I-tuple input. On the other hand, the complete decoder makes a hard decision estimate (no erasures) of the transmitted symbol. Assuming an (N_0,K_0) Reed-Solomon outer code, N_0 outputs of each inner decoder are input to the respective Reed-Solomon decoders to produce K_0 information symbols.

The Reed-Solomon decoders used are bounded distance decoders [10, pages 92-94]. A bounded distance decoder is normally an incomplete decoder which is designed to indicate a decoding failure rather than attempt to exceed its error/erasure correction capability. That is, for each codeword a decoding sphere is defined, the boundary of which is dictated by the codes error/erasure correction capability. In general,

the union of all decoding spheres does not cover all possible input N_0-tuples. In contrast, for maximum-likelihood decoding the decoding spheres are created by decoding each possible received N_0-tuple to the codeword which is most probable given that N_0-tuple was received.

Hence, with bounded distance decoding, when a received N_0-tuple does not lie within a defined coding sphere a decoder failure occurs. When one of the Reed-Solomon decoders fail, the parallel decoder output defers to the next Reed-Solomon decoder output. A primary concern in evaluating the parallel decoder performance is the probability that a Reed-Solomon decoder will produce an erroneous output rather than fail.

The parallel decoder capitalizes on the fact that Reed-Solomon codes are maximum distance separable (MDS for short) codes [7, page 317]. That is, the minimum distance for the code

$$d_{\min} = N_0 - K_0 + 1 \tag{2.1}$$

is the maximum possible for the given code dimensions. For MDS codes with bounded distance decoding, the probability of incorrect decoding becomes very small especially for larger values of $N_0 - K_0$. Initially, we will assume that the probability of incorrect decoding is zero and later we will revisit this assumption to evaluate its merit.

In Sections 2.2, 2.3, and 2.4 we derive the general performance parameters necessary to determine the output symbol error rate for the parallel decoders shown respectively in Figures 2.1, 2.2, and 2.3. In Section 2.5 we derive the bit error rates from each of these decoders as a function of the symbol error rates. Finally, in Section 2.6, we consider the assumption that the Reed-Solomon decoders with bounded

distance decoding will fail rather than incorrectly decode.

2.2 Single Reed-Solomon Decoder

The parallel decoder shown in Figure 2.1 was the first configuration considered. In this section we will derive equations for the symbol error probability of the parallel decoder as a function of the symbol erasure and error rates out of the inner decoders.

With reference to Figure 2.1, we have defined $\tilde{y}_1$ as the output of the incomplete decoder and $\tilde{y}_2$ as the output of the complete decoder. We now define the following six events which partition the joint space of output events for the inner decoders.

$E_1 =$ The event that $\tilde{y}_1$ is an error and $\tilde{y}_2$ is an error.

$E_2 =$ The event that $\tilde{y}_1$ is an erasure and $\tilde{y}_2$ is an error.

$E_3 =$ The event that $\tilde{y}_1$ is correct and $\tilde{y}_2$ is an error.

$E_4 =$ The event that $\tilde{y}_1$ is an error and $\tilde{y}_2$ is correct.

$E_5 =$ The event that $\tilde{y}_1$ is an erasure and $\tilde{y}_2$ is correct.

$E_6 =$ The event that $\tilde{y}_1$ is correct and $\tilde{y}_2$ is correct.

Also define the following events and quantities:

$E_{n1} =$ The event that corresponding to reception of the first symbol of a outer code codeword, the pair $(\tilde{y}_1\tilde{y}_2)$ have the states specified by event E_n, $n = 1, 2, \ldots, 6$.

$S_n =$ The number of symbols in the last $N_0 - 1$ symbols in the outer code codeword which satisfy E_n, $n = 1, 2, \ldots, 6$.

F_S = The event that the first symbol out of the parallel decoding system is in error.

F_b = The event that the first bit out of the parallel decoding system is in error.

p_n = $Pr\{$ A symbol output pair $(\tilde{y}_1, \tilde{y}_2)$ satisfies event $E_n\}$ $n = 1, 2, \ldots, 6$

A compact form for recalling the six events $E_1, \ldots, E_6$ is given in Table 1.1. These events, the related probabilities $p_1, \ldots, p_6$, and the related quantities $S_1, \ldots, S_6$ will be referred to throughout the remainder of the thesis. We also note that due to the memoryless characteristics of the coding channel defined in Chapter 1, $P(E_{n1}) = P(E_n)$ $n = 1, \ldots, 6$.

		Incomplete Inner Decoder Output		
		Error	Erasure	Correct
Complete Inner Decoder Output	Error	E_1	E_2	E_3
	Correct	E_4	E_5	E_6

Table 2.1. Joint Output Events of the Inner Decoders

We have assumed slow frequency hopping with one symbol per hop. The probability that a transmission is jammed is ρ for each symbol independently from symbol-to-symbol. Hence, the inputs $(\hat{y}_j, q_j)$ to the inner decoders are independent and it follows that the symbol statistics out of the inner decoder are independent from symbol-to-symbol.

The first output symbol of the parallel decoding system is in error only if the Reed-Solomon decoder fails and the first output symbol of the complete decoder is in error. We can write:

$$P_S = P(F_S) = \sum_{n=1}^{3} P(F_S \mid E_{n1}) P(E_{n1}) \tag{2.2}$$

The outer code is an (N_0,K_0) Reed-Solomon code with minimum distance given by (2.1). With our assumption on bounded distance decoding, the Reed-Solomon decoder will fail only when the number of erasures and twice the number of errors exceed $N_0 - K_0$ within a received codeword. Thus, given E_{11} the decoder will fail whenever:

$$2(1 + S_1 + S_4) + (S_2 + S_5) > N_0 - K_0 \tag{2.3}$$

Similarly, given E_{21} and E_{31} the conditions for Reed-Solomon decoder failure are respectively:

$$2(S_1 + S_4) + (1 + S_2 + S_5) > N_0 - K_0 \tag{2.4}$$

$$2(S_1 + S_4) + (S_2 + S_5) > N_0 - K_0 \tag{2.5}$$

The expressions for the conditional probabilities $P(F_S \mid E_{n1})$ are similar and take on the general form:

$$P(F_S \mid E_{n1}) = \sum_{i=0}^{N_0-1} \sum_{j=0}^{N_0-1-i} \sum_{k=0}^{N_0-1-i-j} \sum_{l=l(n)}^{N_0-1-i-j-k} P_{i,j,k,l} \tag{2.6}$$

for $n = 1,2,3$ and where:

$$l(n) = \max \left[0, \lceil (N_0 - K_0 - i - j - k - n - 2)/2 \rceil \right]$$

$$P_{i,j,k,l} = P(S_1{=}l,\ S_2{=}k,\ S_4{=}j,\ S_5{=}i)$$

$$= \binom{N_0-1}{i,j,k,l} p_1^l\ p_2^k\ p_4^j\ p_5^i\ (p_3+p_6)^{N_0-1-i-j-k-l}$$

We have evaluated this parallel decoder configuration for two inner decoder algorithms. In both cases the algorithms were based on use of M-ary repetition inner codes with derived side information via an energy threshold test. The results were published in [2] and will be presented in detail in Chapters 3 and 5 of this thesis. Our investigation continued by adding a second Reed-Solomon decoder at the output of the complete decoder. The analysis for this parallel decoder configuration is given in the next section.

2.3 Two Reed-Solomon Decoders

In Figure 2.2 we show the second parallel decoder configuration to be analyzed. With an additional Reed-Solomon decoder on the output of the complete decoder, we must now have failure of two levels of outer decoders before the output defaults to the complete inner decoder.

The events and quantities defined in Section 2.2 as well as (2.2) are applicable for analysis of the parallel decoder with two Reed-Solomon outer decoders. However, the analysis must be modified to account for the conditions under which both outer decoders fail. Given E_{11}, both outer decoders will fail when

$$2(1 + S_1 + S_4) + (S_2 + S_5) > N_0 - K_0 \tag{2.7a}$$

$$2(1 + S_1 + S_2 + S_3) > N_0 - K_0 \tag{2.7b}$$

Similarly, given E_{21}, and E_{31} the conditions for joint failure of the outer decoders are respectively:

$$2(S_1 + S_4) + (1 + S_2 + S_5) > N_0 - K_0 \tag{2.8a}$$

$$2(1 + S_1 + S_2 + S_3) > N_0 - K_0 \tag{2.8b}$$

$$2(S_1 + S_4) + (S_2 - S_5) > N_0 - K_0 \tag{2.9a}$$

$$2(1 + S_1 + S_2 + S_3) > N_0 - K_0 \qquad \textbf{(2.9b)}$$

As before, the expressions for the conditional probabilities $P(F_S \mid E_{n1})$ are similar. In this case they take on the form:

$$P(F_S \mid E_{n1}) = \sum_{i=0}^{I} \sum_{j=0}^{J} \sum_{k=k_n}^{K} \sum_{l=l_n}^{L} \sum_{m=m_n}^{M} P_{i,j,k,l,m} \qquad (2.10)$$

for $n = 1,2,3$ and where:

$$I = N_0 - 1 - \lfloor (N_0 - K_0)/2 \rfloor$$

$$J = N_0 - 1 - j$$

$$K = N_0 - 1 - i - j$$

$$L = \min\left[N_0 - 1 - i - j - k\ ,\ N_0 - 1 - \lfloor (N_0 - K_0)/2 \rfloor + j + k\right]$$

$$M = N_0 - 1 - j - k - l$$

$$k_n = \max\left[0,\ \left\lceil \left(\lfloor 3(N_0 - K_0)/2 \rfloor - 2i - 2j - N_0 - 1 + n \right)/3 \right\rceil \right]$$

$$l_n = \max\left[0,\ N_0 - K_0 - 2i - j - 2k + n - 2\right]$$

$$m_n = \max\left[0,\ \lceil (N_0 - K_0)/2 \rfloor - j - k\right]$$

$$P_{i,j,k,l,m} = P(S_1{=}k, S_2{=}j, S_3{=}m, S_4{=}i, S_5{=}l)$$
$$= \binom{N_0 - 1}{i,j,k,l,m} p_1^k p_2^j p_3^m p_4^i p_5^l p_6^{N_0-1-i-j-k-l-m}$$

Since the limits on the summations are relatively complex, we will illustrate their derivation for the case $n = 2$. In this case, (2.8a) and (2.8b) are applicable; equivalent conditions are given by:

$$2(S_1 + S_4) + (S_2 + S_5) \geq N - K \qquad (2.11a)$$

$$S_1 + S_2 + S_3 \geq \lfloor (N_0 - K_0)/2 \rfloor \qquad (2.11.b)$$

Combining these two equations we arrive at,

$$S_3 + S_5 \geq \lfloor 3(N_0 - K_0)/2 \rfloor - 3S_1 - 2S_2 - 2S_4 \tag{2.12}$$

Note that if $N_0 = 32$, $K_0 = 8$, $S_1 = S_2 = S_3 = 0$ then

$$S_3 + S_5 \geq 36$$

which is impossible. We account for such events by noting that the right side of (2.12) is upper bounded by $N_0 - 1$. Thus,

$$S_1 \geq \frac{1}{3}\left(\left\lfloor \frac{3(N-K)}{2} \right\rfloor - 2S_2 - 2S_4 - N_0 - 1 \right) \tag{2.13}$$

With S_1,S_2 and S_4 as parameters 2.11a yields

$$S_5 \geq N_0 - K_0 - 2S_1 - S_2 - 2S_4 \tag{2.14}$$

Similarly, 2.11b yields

$$S_3 \geq \lfloor (N_0 - K_0)/2 \rfloor - S_1 - S_2 \tag{2.15}$$

Now, to allow (2.11b) to be valid we must have

$$S_4 + S_5 \leq N_0 - 1 - \lfloor (N_0 - K_0)/2 \rfloor \tag{2.16}$$

Equations (2.12) through (2.16) result in the limits established for (2.10) when $n = 2$.

The two Reed-Solomon decoder parallel decoder configuration has been evaluated for both algorithms used in the single decoder configuration. In addition, three other algorithms using repetition codes are evaluated in Chapter 3; linear block code algorithms are analyzed in Chapter 4; results and comparisons are presented in Chapter 5. A subset of these analyses and results were published in [3].

2.4 Multiple Reed-Solomon Decoders

The final configuration for parallel decoding to be considered is the extension to arbitrary multiple decoders as shown in Figure 2.3. This configuration was

motivated by the observation that the erasure criterion for a number of the inner decoders evaluated could be strengthened or weakened by varying a threshold parameter or standard array partition. Our objective was to obtain an optimal envelope performance curve. In this section we will present the analysis of the multiple parallel decoder leading to expressions for output symbol error rate. Specific inner decoding schemes and their performance with multiple parallel decoders will be discussed in Chapters 5.

In general, for the J-ary parallel decoder shown in Figure 2.3 the vector of inputs to the Reed-Solomon decoders $(\tilde{y}_1, \tilde{y}_2, \ldots, \tilde{y}_J)$ may have $2(3^{J-1})$ combinations of errors and erasures. To constrain the magnitude of the analysis we have adopted a set of hierarchical rules for the inner decoders. These rules are not seen as a serious impediment. Almost all of the inner coding schemes we analyzed, particularly the linear block codes, conformed naturally to the hierarchy. The rules are as follows:

Let $\alpha \in \{1, 2, \ldots, J\}$ and assume symbol m is transmitted. Also let e denote a symbol error, $?$ denote an erasure, and c denote a correct symbol. Then,

(1) if $\tilde{y}_\alpha = ?$ then $\tilde{y}_j = ?$ for $j < \alpha$

(2) if $\tilde{y}_\alpha = n \neq m$ then $\tilde{y}_j \in \{n, ?\}$ for $j < \alpha$

(3) if $\tilde{y}_\alpha = m$ then $\tilde{y}_j = m$ for $j > \alpha$
and $\tilde{y}_j \in \{m, ?\}$ for $j < \alpha$

At the beginning of Section 2.2 we defined a set of 6 events which partitioned the joint space of output events for the two inner decoders. For the J-ary parallel decoder with the defined hierarchy we will require $2J$ events $E_1, \ldots, E_{2J}$ to obtain a similar partition. The event E_i, $i \in \{1, \ldots, 2J\}$ corresponds to the case when the

vector of inputs to the Reed-Solomon decoders has the following state:

$$\widetilde{y}_j = \begin{cases} e & j \geq i \qquad\qquad i = 1, \ldots, J \\ ? & \text{otherwise} \\ c & j \geq 2J-i+1 \quad i = J+1, \ldots, 2J \end{cases}$$

The events and quantities E_{1n}, S_n, F_S, F_b, and p_n defined in Section 2.2 are still applicable except that the index n now ranges from 1 to $2J$. Equation (2.2) becomes:

$$P_S = P(F_S) = \sum_{n=1}^{2J} P(E_S \mid E_{n1}) P(E_{n1}) \tag{2.17}$$

Following previous lines of reasoning, the first symbol out of the J-ary parallel decoder will be in error only if all J Reed-Solomon decoders fail and the first symbol out of the complete decoder is in error. Given that the first symbol of an outer code codeword satisfies event E_n (i.e., given event E_{n1}), there is a set of J equations $\{C_1, \ldots, C_J\}$ which describe the conditions necessary for all Reed-Solomon decoders to fail. Each equation will take on one of two forms denoted by c_{j1} and c_{j2} as shown in (2.18a) and (2.18b).

$$c_{j1}: \; 2(1 + \sum_{k=1}^{j} S_k) + \sum_{k=j+1}^{2J-j} S_k > N - K \tag{2.18a}$$

$$c_{j2}: \; 2 \sum_{k=1}^{j} S_k + \sum_{k=j+1}^{2J-j} S_k + 1 > N - K \tag{2.18b}$$

Now, given event E_{n1}

$$C_j = c_{jk} \qquad j = 1, \ldots, J$$

where:

$$\text{if } j \geq n \text{ then } k = 1$$
$$\text{if } j < n \text{ then } k = 2$$

Using these equations we can give a general expression for the conditional error probability $P(F_S \mid E_{n1})$ as a function of the parameter n.

$$P(F_S \mid E_{n1}) = \sum_{S_1=L_1}^{U_1} \sum_{S_2=L_2}^{U_2} \cdots \sum_{S_{2J-1}=L_{2J-1}}^{U_{2J-1}} P\{S_1,S_2,\ldots,S_{2J-1}\} \quad (2.19)$$

where:

$$P\{S_1,S_2,\ldots,S_{2J-1}\} = \binom{N_0-1}{S_1,\ldots,S_{2J-1}} \left(\prod_{i=1}^{2J-1} p_i^{S_i}\right) (p_{2J-1})^{N_0-1-\sum_{i=1}^{2J-1} S_i}$$

$$U_i = N_0 - 1 - \sum_{k=1}^{i-1} S_k \qquad i = 1,\ldots,2J-1$$

$$L_j = \begin{cases} 0 & i < J \\ \max[0, \frac{N_0-K_0}{2} - \sum_{k=1}^{J-1} S_k] & i = J \\ \max[0, N_0-K_0-1-2\sum_{k=1}^{n} S_k - \sum_{k=n+1}^{2J-n-1} S_k] & J < i \leq 2J-n \\ \max[0, N_0-K_0-2\sum_{k=1}^{n} S_k - \sum_{k=n+1}^{2J-n-1} S_k] & i > 2J-n \end{cases}$$

We note that the J-ary parallel decoder for $J = 2$ is not equivalent to the two Reed-Solomon decoder configuration given in Section 2.3. This is due to the fact that events E_3 (Incomplete inner decoder = errors, complete inner decoder = correct) and E_4 (Incomplete inner decoder = correct, complete inner decoder = error) of Section 2.3 do not conform to the hierarchical rules established above. For most of the inner codes evaluated in Chapter 3 and 4, events E_3 and E_4 occur with zero probability and the J=2 reduction is equivalent.

Having evaluated the symbol error rates for the three parallel decoder configurations, we now turn our attention to the relationship of bit error rates to symbol error rates.

2.5 Bit Error Rate Analysis

When the inner encoder is an L-diversity repetition code on the alphabet of the Reed-Solomon decoders, the relationship of the bit error rate to the symbol error rate

is given by:

$$P(F_b) = \frac{M}{2(M-1)} P(F_s) \tag{2.20}$$

The proof of this relationship is dependent upon the decoding algorithm. In this section we will sketch the general proof and derive a sufficient condition for 2.20 to hold true.

We will give the derivation for the parallel decoder configuration of Figure 2.2 and then indicate the slight modifications necessary for the configuration of Figure 2.1. Without loss of generality we assume symbol 0 was transmitted and define the following events:

$A_i =$ event the first output symbol of the parallel decoder equals symbol i, $i \neq 0$

$D_1 =$ event the Reed-Solomon decoder in the incomplete decoder channel fails

$D_2 =$ event the Reed-Solomon decoder in the complete decoder channel fails

$Y_{1j} =$ event $\tilde{y}_1 = j$; $j = 0, \ldots, M$ (M corresponding to erasure)

$Y_{2j} =$ event $\tilde{y}_2 = j$; $j = 1, \ldots, M-1$

The first output symbol is i, $i \neq 0$ iff both decoders fail and $\tilde{y}_2 = i$. Thus,

$$\begin{aligned} P(A_i) &= P(D_1 \cap D_2 \cap Y_{2i}) \\ &= \sum_{j=0}^{M} P(D_1 \cap D_2 \mid Y_{1j} \cap Y_{2i}) P(Y_{1j} \cap Y_{2i}) \end{aligned} \tag{2.21}$$

Consider first the terms $P(D_1 \cap D_2 \mid Y_{1j} \cap Y_{2i})$. If Y_{10} occurs (i.e., j=0) then $D_1 \cap D_2$ occurs only if the next $N-1$ receptions yield:

$$2(\#\text{ of errors}) + (\#\text{ of erasures}) > N - K$$
$$\text{in incomplete decoder channel}$$
$$2(\#\text{ of errors}) + (\#\text{ of erasures}) > N - K - 2$$
$$\text{in complete decoder channel}$$

Since the channel is symmetric and memoryless in all cases, this joint event is independent of the choice of i. A similar argument holds true for all other values of j.

Assume for a moment that we can also show that $P(Y_{1j} \cap Y_{2i})$ is also independent of the choice of $i \neq 0$ for all values of j. Then it would follow that $P(A_i)$ is independent of choice of i. That is:

$$P(A_i) = P(F_S)/(M-1)$$

then,

$$P(F_b) = \sum_{i=1}^{M-1} P(F_b \mid A_i)P(A_i)$$
$$= [P(F_S)/(M-1)] \sum_{i=1}^{M-1} P(F_b \mid A_i)$$

but

$$P(F_b \mid A_i) = \begin{cases} 0 \text{ if first bit of symbol } i \text{ is ``0''} \\ 1 \text{ if first bit of symbol } i \text{ is ``1''} \end{cases}$$

Therefore,

$$P_b = P(F_b) = \frac{M}{2(M-1)} P_S$$

If we consider the single Reed-Solomon decoder parallel decoder of Figure 2.1, the same result follows by eliminating event D_2 and the second of the two conditions for decoder failure. Showing $P(Y_{1j} \cap Y_{2i})$ is independent of $i \neq 0$ for all choices of j will be left to Chapter 3 as each decoding algorithm is analyzed. Except for rare cases of perfect codes, the relationship of (2.20) will not be met for arbitrary linear

block codes. The relationship of bit and symbol error rates for this latter case will be derived in Chapter 4.

2.6 Decoder Error Analysis

Throughout the developments of the previous sections we have assumed that there is zero probability that the Reed-Solomon decoders will output an incorrect symbol rather than fail. In this section we derive a bound of the probability that the Reed-Solomon decoders incorrectly decode rather than default. In Chapter 5 we present numerical results for each parallel decoder configuration and evaluate the merit of our earlier assumptions. We will concentrate on the two Reed-Solomon decoder configuration and discuss how the results may be extended to arbitrary multiple decoders.

In Figure 2.4 we show the nine joint events which may result at the outputs of the Reed-Solomon decoders of Figure 2.2. This analysis assumed that the significant majority (all!) of the probability is concentrated in the four joint events labeled Y. We would like to demonstrate that the total probability of the remaining events is very small. Letting DE be the event that the resultant output of the Reed-Solomon decoders is an erroneous symbol (recall, we default to the complete decoder output if both decoders fail). Then an upper bound for $P(DE)$ is given by

Complete Inner Decoder/R-S Decoder	Incomplete Inner Decoder/ R-S Decoder: Correct	Error	Fail
Correct	Y	N	Y
Error	N	N	N
Fail	Y	N	Y

Figure 2.4 Joint Events at R-S Decoder Outputs

$$P(DE) \leq P(DE_1) + P(DE_2) \tag{2.22}$$

where

$DE_1 =$ event the $R-S$ decoder in the incomplete decoder channel errs.

$DE_2 =$ event the $R-S$ decoder in the complete decoder channel errs

[Note: for the single $R-S$ decoder configuration we have $P(DE) = P(DE_1)$]

$P(DE_2)$ is a function of the probabilities of correct and error events at the Reed-Solomon decoder input. This probability has been derived in [10, Section 7.3] and will be described herein since the procedure must be extended to account for erasure events which contribute to $P(DE_1)$.

Since the Reed-Solomon codes are linear and since the effective channel at the input to the decoder is M-ary symmetric, we may assume, without loss of generality, that the all zero codeword was transmitted. Event DE_2 will occur only if the error pattern which occurs lies within a radius $d_{\min}$ sphere of a nonzero codeword. Hence, we can write

$$P(DE_2) = \sum_{h=d_{\min}}^{N_0} P(DE_2,h) \tag{2.23}$$

where $P(DE_2,h)$ is the probability the decoder errs to a weight h codeword.

If we let A_i, $i = 0, 1, \ldots, N_0$ be the weight distribution of the Reed-Solomon code we can write

$$P(DE_2,h) = A_h \sum_{s=0}^{t} \sum_{k=h-s}^{\min(h+s,N_0)} N_{k,s}(h) \left(\frac{p_e}{M-1} \right)^k q^{N_0-k} \tag{2.24}$$

where

$N_{k,s}(h) =$ the number of weight k error patterns at distance s from a codeword of weight h.

$p_e =$ probability of a symbol error at the input to the Reed-Solomon decoder.

$q =$ $1-p_e$

$t =$ $\lfloor \frac{d_{\min}-1}{2} \rfloor$, the error correcting capability of the Reed-Solomon code.

To determine $N_{k,s}(h)$ it is best to view the transmitted and received N_0-tuples and the target codeword as five fields of symbol vectors as illustrated in Figure 2.5. (For example, e_1 and c_1 are equal, nonzero vectors of m Reed-Solomon code symbols.)

transmitted N_0-tuple	:	0	0	0	0	0
received N_0-tuple	:	$e_1 \neq 0$	$e_2 \neq 0$	0	$e_3 \neq 0$	0
target codeword	:	$c_1 = e_1$	$c_2 \neq e_2$	$c_3 \neq 0$	0	0
field size (symbols)	:	m	j	v	r	$N_0-m-j-v-r$

(note: notation applies to *each* symbol of the vector, e.g., $e_1 \neq 0 \Longrightarrow e_{1i} \neq 0$ $i = 1,2, \ldots, m$)

Figure 2.5 Fields of Symbol Vectors, N_0 Erasures

Using combinatorial analysis and careful manipulation of terms, the following expression for $N_{k,s}(h)$ results [10, (7.16)]:

$$N_{k,s}(h) = \sum_{r=\max\{0,k-h\}}^{\lfloor \frac{k-h+s}{2} \rfloor} \binom{h}{h-s+r,\ h-k+r} \binom{N_0-h}{r} (M-2)^{k-h+s-2r} (M-1)^r \qquad (2.25)$$

Finally, the weight distributions of Reed-Solomon codes are well known. For example, [10, (6.5)] gives:

$$A_h = \binom{N_0}{h} (M-1) \sum_{l=0}^{h-d_{\min}} (-1)^l \binom{h-1}{l} (M-1)^{h-d_{\min}-l}$$

Equations (2.23) through (2.26) may be combined to evaluate $P(DE_2)$.

The derivation of $P(DE_1)$ is similar. However, we must now account for erasures which may also occur at the input to the Reed-Solomon decoder. We begin by noting that each erasure reduces by one the radius of the decoding sphere around each codeword. Hence the error correction capability of the Reed-Solomon code when z erasures occur is $t - \lceil \frac{z}{2} \rceil$. Thus, we can modify (2.23) and (2.24) to account for erasures as follows:

$$P(DE_1) = \sum_{h=d_{\min}}^{N_0} \sum_{z=0}^{d_{\min}-1} P(DE_1,h,z) \qquad (2.27)$$

$$P(DE_1,h,z) = A_h \sum_{s=0}^{t-\lceil \frac{z}{2} \rceil} \sum_{k=h-s}^{\min(h+s,N_0} N_{k,s}(h,z) \left(\frac{p_e}{M-1} \right)^k p_z^z \, q^{N_0-k-e} \qquad (2.28)$$

where

$N_{k,s}(h,z)$ = the number of weight k error patterns at distance s from a codeword of weight h when z erasures occur.

p_z = probability of a symbol erasure at the input to the Reed-Solomon decoder.

$$q = 1 - p_e - p_z$$

The relationship between transmitted and received N_0-tuples and the target weight h codeword must now be viewed as seven fields of symbol vectors as shown in Figure 2.6.

transmitted N_0-tuple	:	0	0	0	0	0	0	0
received N_0-tuple	:	$e_1 \neq 0$	$e_2 \neq 0$	?	0	$e_3 \neq 0$	?	0
target codeword	:	$c_1 = e_1$	$c_2 \neq e_2$	c_3	$c_4 0$	0	0	
field size (symbols)	:	m	j	x	v	r	$z-x$	

(note: notation applies to *each* symbol of the vector, e.g., $? \Longrightarrow x$ erased symbols)

Figure 2.6 Fields of Symbol Vectors, z Erasures

For specific values of m, j, x, v, and r the number of different error vectors which result in the relationships shown in Figure 2.6 is

$$N_{k,s}(h, z, m, j, x, v, r) = \binom{h}{m, j, x} \binom{N_0 - h}{r, z-x} (M-2)^j (M-1)^r \tag{2.29}$$

where the terms $(M-2)^j$ and $(M-1)^r$ result from the fact that each symbol of vectors e_2 and e_3 respectively may be chosen in $(M-2)$ and $(M-1)$ ways. The following relationships exist between the parameters of (2.29) and Figure 2.6.

$$k = m + j + r \tag{2.30a}$$

$$h = m + j + v + x \tag{2.30b}$$

$$s = j + v \tag{2.30c}$$

Solving these equations in terms of h, k, s, r, and x we arrive at

$$m = h - x - s + r \tag{2.31a}$$

$$j = k - h + x + s - 2r \tag{2.31b}$$

Thus, we can rewrite (2.29) as follows

$$N_{k,s}(h,z,r,x) = \binom{h}{h-x-s+r,\,h-x-k+r,\,x} \binom{N_0-h}{r} (M-2)^{k-h+x+s-2r}(M-1)^r \tag{2.32}$$

The range of permissible r values depends on h,k and x. If $h-z$ (codeword weight minus the erased nonzero codeword positions) is greater than or equal to k (error vector weight), then all nonzero error vector positions may align with nonzero codeword positions and $r \geq 0$ is allowable. Otherwise, at least $k - (h-x)$ non zero error vector positions must align with zero codeword positions. Hence,

$$r \geq \max\{0,k-h+x\} = r_1 \tag{2.33}$$

Since $j \geq 0$, using (2.30c) we see that r is upper bounded by

$$r \leq \left\lfloor \frac{k - h + x + s}{2} \right\rfloor = r_2 \tag{2.34}$$

Using the convention that $\sum_{a}^{b} = 0$ if $a < b$ we conclude,

$$N_{k,s}(h,z) = \sum_{x=0}^{z} \sum_{r=r_1}^{r_2} N_{k,s}(h,z,r,x) \tag{2.35}$$

Hence, $P(DE_1)$ may be evaluated using (2.26), (2.27), (2.28), (2.32), (2.33), (2.34) and (2.35). In Chapter 5 we present numerical results for $P(DE)$, $P(DE_1)$, and $P(DE_2)$ for each of the parallel inner decoders described in Chapters 3 and 4 which follow.

CHAPTER 3

PARALLEL DECODING / DIVERSITY INNER CODES

3.1 Introduction

In this chapter we evaluate the performance of the parallel decoding schemes described in Chapter 2 when the inner encoder is an L-diversity repetition code on the same alphabet as the Reed-Solomon code. This is the first of two general classes of inner codes to be used for evaluating the performance of the parallel decoding systems. In Chapter 4 we will consider using binary linear block codes for the inner encoder.

In general, the different decoding schemes are distinguishable by the algorithm used to declare erasures in the incomplete inner decoders. The first two inner decoder erasure algorithms to be analyzed, Sections 3.2 and 3.3, use a derived side information measure of the symbol estimate (a quality bit) which is obtained from a ratio threshold test as described by Viterbi [18,19]. For each of these algorithms we derive the quantities specified in Chapter 2 which are necessary to evaluate the decoder symbol error rates. The analyses is completed for the decoder configurations of Figures 2.1 and 2.2.

Subsequently, we concentrate our attention on the two Reed-Solomon decoder configuration of Figure 2.2 since this decoder will in general provide better perfor-

mance with only a marginal increase in complexity. To provide a baseline for comparing numerical results, we also derive the performance with a hard decision channel which has perfect side information, Section 3.4. Finally, we introduce two techniques which declare erasures based on a histogram of the L received symbols, Sections 3.5 and 3.6.

In general, the input to each of the two inner decoders is an L-tuple of pairs

$$\{(\hat{y}_j, \hat{q}_j)\ ;\ \ j = 1, \ldots, L\}$$

The incomplete decoder output, $\tilde{y}_1$, is either a symbol estimate or an erasure for each L-tuple input. On the other hand, the complete decoder makes a hard decision estimate (no erasures), $\tilde{y}_2$, of the symbol transmitted. The hard decision estimate will be a maximum likelihood estimate on either the L-tuple input or a subset thereof. Our objective is to derive expressions for the quantities necessary to evaluate (2.2) and (2.6) or (2.2) and (2.10).

The first two algorithms to be analyzed base the erasure criterion on the results of a ratio threshold test defined by Viterbi [18,19]. Reference Figures 1.1 and A.1 (Appendix A). The symbol detector outputs $\tilde{E}_0, \tilde{E}_1, \ldots, \tilde{E}_{M-1}$ are the results of processing the received signal through M filters matched to the possible outputs of the M-ary FSK generator. The receiver decides symbol k was transmitted if $\tilde{E}_k = \max\limits_{0 \le j \le M-1} \{\tilde{E}_j\}$. The Viterbi ratio threshold test assigns a quality bit, q, to the decision as follows:

$$q = \begin{cases} 0 & \tilde{E}_k \ge \max\limits_{0 \le j \le M-1} \{\theta \tilde{E}_j\} \\ 1 & \text{otherwise} \end{cases}$$

where $\theta > 1$ is a real variable.

The ratio threshold test is used to assign a quality bit $\{q_j\ ,\ j = 1, \ldots, L\}$ to each of the L symbol estimates. Joint statistics for symbol-quality bit pairs are derived in Appendix A. The analyses which follow in Sections 3.2 and 3.3 are both dependent on the value of θ chosen for the ratio threshold test.

3.2 Viterbi Thresholding, Algorithm A

The first algorithm based on ratio threshold testing will be referred to as algorithm A. The A incomplete decoder will output an erasure if either or both of the following two conditions occur:

I: No symbol of the set $\{\hat{y}_j\ ;\ j = 1, \ldots, L\}$ occurs more than $\lfloor L/2 \rfloor$ times (L assumed odd)

II: The sum of the corresponding L quality bits satisfies:

$$\sum_{j=1}^{L} q_j > \theta_q \tag{3.1}$$

where $\theta_q \in \{\lceil L/2 \rceil, \ldots, L\}$ is a threshold.

Otherwise, the A incomplete decoder output is that symbol which occurred the majority of the time. The A complete decoder ignores the quality bits and makes a maximum likelihood decision based on the L symbol estimates $\{\hat{y}_j\ ,\ j = 1, \ldots, L\}$

Algorithm A / One Reed-Solomon Decoder

Initially we will consider the single Reed-Solomon decoder in the parallel decoder configuration of Section 2.2 and Figure 2.1. Before evaluating the symbol error probability for this configuration we can simplify the general analysis given in Section 2.2. Since the incomplete decoder for algorithm A will be correct only in the event $\lceil L/2 \rceil$ or more correct symbols are received with quality bit $q = 0$, the complete decoder will be correct whenever the incomplete decoder is correct. Thus, event E_3

(incomplete inner decoder = error, complete inner decoder = correct) cannot occur with algorithm A. By the same reasoning, the incomplete decoder will be in error only in the event at least $\lceil L/2 \rceil$ identical erroneous symbols are received each with quality bit $q = 0$. The complete decoder will err whenever the incomplete decoder errs, thus, event E_4 (incomplete inner decoder = correct, complete inner decoder = error) can not occur. Consequently,

$E_1 =$ Event that the incomplete decoder errors.

$E_6 =$ Event that the incomplete decoder is correct.

Using these facts, we can rewrite (2.2) and (2.6) as:

$$P(F_S) = P(F_S \mid E_{11})P(F_{11}) + P(E_S \mid E_{21})P(E_{21}) \tag{3.2}$$

where

$$P(F_S \mid E_{n1}) = \sum_{i=0}^{N_0-1} \sum_{j=\max[0,\lfloor (N_0-K_0-i+n-2)/2 \rfloor]}^{N_0-1-i} p_1^i (1-p_1-p_6)^j \; p_6^{N_0-1-i-j} \tag{3.3}$$

for $n = 1,2$.

Thus, we only need to evaluate the probabilities $p_1 = P(E_{11})$, $p_2 = P(E_{21})$ and p_6 to complete the analyses for algorithm A. To evaluate these terms we need to consider the discrete channel which produces the inputs to the inner decoders. Without loss of generality, we will assume symbol 0 has been transmitted. In Figure 3.1 we illustrate the discrete channel where the outputs are reduced to the four events of interest. The transition probabilities are labelled consistent with the notation of Appendix A.

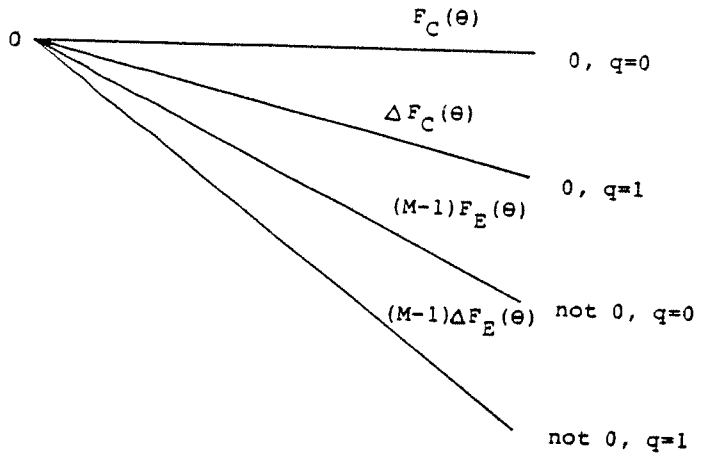

Figure 3.1 Discrete Channel of Input to Inner Decoders

The incomplete inner decoder processes received symbols/quality bits in blocks of L pairs. If we let i be the number of correct symbols received with $q = 0$, j be the number of incorrect symbols received with $q = 0$, and k be the number of correct symbol received with $q = 1$, then the probability the incomplete decoder produces a correct symbol output is given by

$$\begin{aligned} p_6 &= P\{i + k \geq \lfloor L/2 \rfloor + 1\ ,\ i + j \geq L - \theta_q\} \\ &= \sum_{i=0}^{L} \sum_{j=T1}^{L-i} \sum_{k=T2}^{L-i-j} \binom{L}{i,j,k} F_c^i [(M-1)F_E]^j \Delta F_c^k [(M-1)\Delta F_E]^{L-i-j-k} \end{aligned} \tag{3.4}$$

where:

$$T1 = \max\,[0,\ L - \theta_q - i]$$

$$T2 = \max\,[0,\ \lfloor L/2 \rfloor + 1 - i]$$

and where the dependency of p_6, F_c, F_E, ΔF_c, and ΔF_E on θ is suppressed.

Similarly, the probability that the incomplete decoder produces an erroneous symbol output is given by:

(3.5)

$$p_1 = (M-1)\sum_{i=0}^{L}\sum_{j=T1}^{L-i}\sum_{k=T2}^{L-i-j}\binom{L}{i,j,k} F_E^i[F_c+(M-2)F_E]^j \Delta F_E^k[\Delta F_c+(M-2)\Delta F_E]^{L-i-j-k}$$

where $T1$ and $T2$ are the same as in (3.4).

The remaining term to be evaluated is p_2. This term is the probability of the joint event (E_2) that the complete decoder errs and the incomplete decoder erases for a received L-tuple. Let E_d be the event that no symbol of $(\hat{y}_j \ ; \ j = 1, \ldots, L)$ occurs more than $\lfloor L/2 \rfloor$ times. We can write:

$$p_2 = P(E_2) = P(E_2 \cap E_d) + P(E_2 \cap E_d^c) \tag{3.6}$$

When no symbol occurs more than $\lfloor L/2 \rfloor$ times the incomplete decoder will output an erasure independent of the quality bits. Hence, the first term of 3.6 is equivalently the probability that the complete decoder errors and no received symbol occurs more than $\lfloor L/2 \rfloor$ time. This probability can be expressed using the enumeration procedure described in Appendix B and is given by:

$$P(E_2 \cap E_d) = \sum_{n_c=0}^{\lfloor L/2 \rfloor} \sum_{Y} G_1(Y, n_c)\binom{L}{Y} \left[F_c(1)\right]^{n_c} \left[F_E(1)\right]^{L-n_c} \tag{3.7}$$

where

n_c = the number of correct symbol received

Y = $(m_1, m_2, \ldots, m_\alpha)$

= a generic configuration of the $L-n_c$ incorrect symbols such that :

$$m_1 \geq m_2 \geq \cdots \geq m_\alpha > 0$$
$$m_1 + m_2 + \cdots + m_\alpha = L - n_c$$
$$m_1 \geq n_c$$

(example: $L = 5$, $M = 4$, the symbol set $= \{a, b, c, d\}$, if a is sent and $n_c = 2$, the configuration (2,1) accounts for the received L-tuples *aabbc*, *aabbd*, *aaccd*, *aabcc*,

aabdd and *aacdd*, the configuration (1,1,1) accounts for the received L-tuple *aabcd*) letting:

$n_1 =$ the number of terms in the largest grouping of equal terms in Y

$n_2 =$ the number of terms in the next largest grouping of equal terms in Y

. . .

$n_\beta =$ number of terms in the smallest grouping of equal terms in Y

note: $n_1 + n_2 + \cdots + n_\beta = \alpha$

(example: (3,2) has $n_1 = 1$, $n_2 = 1$, $\beta = 2$; (1,1,1) has $n_1 = 3$, $\beta = 1$) Finally, if we define N_e as the number of terms in Y equal to n_e and let

$$r(N_e) = \begin{cases} 1 & \text{if } N_e = 0 \\ N_e/(N_e+1) & \text{if } N_e \neq 0 \end{cases}$$

then,

$$G_1(Y, n_c) = r(N_e)\frac{(M-1)(M-2)\cdots(M-\alpha)}{n_1! n_2! \cdots n_\beta!} \tag{3.8}$$

the term $\binom{L}{Y}$ in (3.7) is a shorthand notation for the multinomial coefficient $\binom{L}{m_1 m_2 \cdots m_\alpha}$. In Appendix B we give example evaluations of (3.7) and (3.8) for $L = 3,5$, and 7.

The second term of (3.6) is the probability of the event that the incomplete decoder erases, the complete decoder errs, and one symbol occurs more than $\lfloor L/2 \rfloor$ times. We further partition this probability by the M events that symbol j, $j = 0, \ldots, M-1$ occurs more than $\lfloor L/2 \rfloor$ times. If the correct symbol is received more than $\lfloor L/2 \rfloor$ times than the complete decoder does not error. Due to the channel symmetry, the remaining $M - 1$ events produce equivalent probabilities and erasure

depends solely on the sum of the quality bits exceeding the threshold θ_q. Hence,

$$P(E_2 \cap E_d^c) = (M-1)\sum_{i=0}^{L}\sum_{j=T3}^{L-i}\sum_{k=T4}^{L-i-j}\binom{L}{i,j,k} F_E^i \Delta F_E^j \left[\Delta F_c + (M-2)\Delta F_E\right]^k \left[F_c + (M-2)F_E\right]^{L-i-j-k} \tag{3.9}$$

where:

$$T_3 = \max[0, \lfloor L/2 \rfloor + 1 - i]$$

$$T_4 = \max[0, \theta_q - j]$$

With thresholds θ and θ_q we can now evaluate the symbol error rate for the single Reed-Solomon decoder parallel decoding system. To show that the bit error rate is given by (2.20), we must show that $P(Y_{1j} \cap Y_{2i})$ is independent of the choice of $i \in \{1,2, \ldots, M-1\}$ for all choices of $j \in \{0,1, \ldots, M\}$ as developed in Section 2.5. Recall Y_{1j} is the event $\tilde{y}_1 = j$; $j = 0, \ldots, M-1$, M (M corresponding to erasure) and Y_{2j} is the event $\tilde{y}_2 = j$; $j = 1, \ldots, M-1$. M

When the incomplete decoder is correct the complete decoder will also be correct as argued earlier in this section. Hence, for $j = 0$ we have $P(Y_{1j} \cap Y_{2i}) \equiv 0$ for any choice of i. Similarly, if the incomplete decoder errs with output symbol $i \neq 0$, that symbol must have occurred $\lceil L/2 \rceil$ or more times and the complete decode will also output symbol i. Thus,

$$P(Y_{1j} \cap Y_{2i}) = \begin{cases} 0 & i \neq j \\ 1 & i = j \end{cases}$$

for any $j \in (1,2, \ldots, M-1)$ and for any choice of $i \neq 0$.

For $j = M$ (corresponding to an erasure), we first note that:

$$P(Y_{1M} \cap Y_{2i}) = P(Y_{1M} \cap Y_{2i} \cap E_d) + P(Y_{1M} \cap Y_{2i} \cap E_d^c) \tag{3.10}$$

where E_4 is defined for Equation 3.6 above. If no symbol occurs more than $\lfloor L/2 \rfloor$ time then

$$\begin{aligned} &P(\text{the complete decoder outputs symbol } i \neq 0) \\ &\quad = P(\text{symbol } i \text{ occurs most frequently}) \\ &\qquad + \frac{1}{2} P(\text{symbols } i \text{ and } j \text{ tie for most frequent occurrence}) \\ &\qquad + \frac{1}{3} P(\text{symbols } i, j \text{ and } k \text{ tie for most frequent occurrence}) \\ &\qquad + \cdots \end{aligned} \tag{3.11}$$

Each of these terms can be written as a multinomial expression on events that occur with equal probabilities. Clearly the terms are independent of the choice of i.

Finally, if one symbol occurs more than $\lfloor L/2 \rfloor$ times the complete decoder will output that symbol. The probability a particular symbol occurs more than $\lfloor L/2 \rfloor$ times and is erased by the incomplete decoder is given by $1/(M-1)$ times the right hand side of (3.9). This result is independent of the choice of $i \neq 0$ and the proof is complete.

These results complete the analysis necessary to evaluate symbol and bit error rates for the decoder of Figure 2.1 using Viterbi thresholding and algorithm A. We now consider the two Reed-Solomon decoder configuration of Figure 2.2 and Section 2.3.

Algorithm A / Two Reed-Solomon Decoders

To evaluate (2.2) and (2.10) we first note that events E_3 and E_4 will not occur by the same rationale used earlier in this section. Hence, we again need to evaluate (3.2). For two Reed-Solomon decoder, (2.10) reduces to

$$P(F_S \mid E_{n1}) = \sum_{i=0}^{N_0-1} \sum_{j=s_1}^{N_0-1-i} \sum_{k=s_2}^{N_0-1-i-j} p_1^i \; p_2^j \; p_5^k \; p_6^{N_0-1-i-j-k} \qquad (3.12)$$

where:

$$n = 1,2$$
$$s_1 = \max[0,\lfloor (N_0-K_0)/2 \rfloor]$$
$$s_2 = \max[0,N_0-K_{N_0-K-i-2j+n-2}]$$

The probabilities p_1, p_2, and p_6 are given respectively by (3.5), (3.6), and (3.4). The remaining probability, p_5, is obtained simply by

$$p_5 = 1 - p_1 - p_2 - p_6 \qquad (3.13)$$

The relationship of bit and symbol error rates is again given by (2.20). The proof given earlier in this section for the single Reed-Solomon decoder system is applicable to the two Reed-Solomon decoder configuration. In both systems the inner decoders are the same; what changes is the manner by which their outputs are processed.

3.3 Viterbi Thresholding, Algorithm B

The second algorithm, B, based on the Viterbi thresholding procedure uses a two step incomplete decoder. First, each symbol having a bad quality bit, $q = 1$, is replaced by an erasure. Secondly, the decoder operates on the expanded alphabet $\{0,1, \ldots, M-1$, erasure $\}$ the output is:

1. Any symbol, including erasure, which occurs more than $\lfloor L/2 \rfloor$ times.

2. An erasure if no symbol occurs more than $\lfloor L/2 \rfloor$ times.

The B complete decoder considers only those symbol estimates of $\{(\hat{y}_j, q_j)\; ;\; j = 1, \ldots, L\}$ which have $q_j = 0$. A maximum likelihood decision is made on this reduced set of estimates. If all symbols have $q_j = 1$, an arbitrary symbol is output, say for example, the first symbol received, $\hat{y}_1$. We now describe the

analysis to evaluate symbol and bit error rates for the single Reed-Solomon decoder system using algorithm B.

Algorithm B / One Reed-Solomon Decoder

The simplifications made for algorithm A also hold for B. That is, events E_3 (incomplete inner decoder = error, complete inner decoder = correct) and E_4 (incomplete inner decoder = correct, complete inner decoder = error) each have probability zero and the symbol error probability is given by (3.2) and (3.3). Hence, we need to derive expressions for p_1, p_2, and p_6.

The incomplete decoder will produce an erroneous symbol output only if that symbol is received more than $\lfloor L/2 \rfloor$ times with quality bit $q = 0$. Thus,

$$p_1 = P\Big(\bigcup_{i=1}^{M-1} \{\text{event symbol } i \text{ received} > \lfloor L/2 \rfloor \text{ times with } q = 0 \text{ given ``0'' transmitted}\Big)$$

$$= (M-1)\, P\left(\text{symbol 1 received} > \lfloor L/2 \rfloor \text{ times with } q = 0 \text{ given ``0'' transmitted}\right)$$

With symbol 0 transmitted, the probability any other symbol is received with quality bit $q = 0$ is $F_E(\theta)$. Hence, suppressing θ we have

$$p_1 = (M-1) \sum_{i=\lfloor L/2 \rfloor + 1}^{L} \binom{L}{i} F_E^i (1 - F_E)^{L-i} \tag{3.14}$$

Similarly, the incomplete decoder produces the correct symbol output only if the correct symbol occurs more than $\lfloor L/2 \rfloor$ times with $q = 0$. Thus,

$$p_6 = \sum_{i=\lfloor L/2 \rfloor + 1}^{L} \binom{L}{i} F_c^i (1 - F_c)^{L-i} \tag{3.15}$$

To evaluate p_2 we begin by partitioning the event of interest using the event F_d that no symbol of $\{\hat{y}_j \ ; \ j = 1, \ldots, L\}$ occurs with quality bit $q = 0$ more than $\lfloor L/2 \rfloor$ times. We obtain

$$p_2 = P(E_2 \cap F_d) + P(E_2 \cap F_d^c) \tag{3.16}$$

The second term of (3.16) is zero since the complete decoder will not erase if any symbol occurs with $q = 0$ more than $\lfloor L/2 \rfloor$ times. Thus, p_2 is equivalently the probability that the complete decoder errs and no symbol occurs with $q = 0$ more than $\lfloor L/2 \rfloor$ times.

Since the complete decoder considers only those symbols which have $q = 0$, we need to evaluate p_2 as the number of non-deleted symbols ranges from 0 to L. When all symbols are deleted the complete decoder makes a random selection which is equally likely to be any of the M possible symbols. Hence, the probability of decoder error is this case is $(M-1)F_X^L/M$ where

$$F_X = F_X(\theta) = \Delta F_c(\theta) + (M-1)\Delta F_E(\theta) \tag{3.17}$$

is the probability a symbol is received with $q = 1$ on any transmission. The remaining terms of p_2 are expressed using the enumeration procedure as in (3.7)

$$p_2 = \frac{M-1}{M} F_X^L + \sum_{l=1}^{L} \sum_{n_c=0}^{\min[l,\lfloor L/2 \rfloor]} \sum_{Y} G_1(Y, n_c) \binom{L}{Y} F_c^{n_c} F_E^{l-n_c} F_X^{L-l} \tag{3.18}$$

where:

l = number of terms received with quality bit $q = 0$

$G_1(Y, n_c)$ is the same as in (3.8) and Y is as defined below (3.7) with additional constraints:

$$\lfloor \frac{L}{2} \rfloor \geq m_1 \geq m_2 \geq \cdots \geq m_\alpha$$

$$m_1 - m_2 + \cdots + m_\alpha = l - n_c$$

$$m_1 \geq n_c$$

In Appendix B we give sample evaluations of (3.18) for $L = 3,5$.

To show that the bit and symbol error rates are related by $P_b = P_s M/2(M-1)$ (2.20) we must prove that $P(Y_{1j} \cap Y_{2i})$ is independent of the choice of $i \in \{1,2,\ldots,M-1\}$ for all choices of $j \in \{0,1,\ldots,M\}$. For algorithm B, the complete decoder will output the same symbol as the incomplete decoder whenever the incomplete decoder does not erase. Hence,

$$P(Y_{10} \cap Y_{2i}) \equiv 0 \quad \text{for all } i$$

$$P(Y_{1j} \cap Y_{2i}) = \begin{cases} 0 & i \neq j \\ 1 & i = j \end{cases} \text{ for } j \in \{1,2,\ldots,M-1\}$$

For $j = M$ we proceed as we did in Section 3.2.

$$P(Y_{1M} \cap Y_{2i}) = P(Y_{1M} \cap Y_{2i} \cap F_d) + P(Y_{1M} \cap Y_{2i} \cap F_d^c) \qquad (3.19)$$

where F_d is defined for (3.15) above. The second term of (3.19) is zero since Y_{1M} will not occur if any symbol occurs with $q = 0$ more than $\lfloor L/2 \rfloor$ times. Finally, if no symbol occurs more than $\lfloor L/2 \rfloor$ times with $q = 0$ the complete decoder makes a maximum likelihood choice on the symbols which have $q = 0$. If all symbol have $q = 1$ then an arbitrary symbol is chosen. In all other cases an equation of the form of (3.11) applies. As before, each term of (3.11) is a multinomial expression on events which occur with equal probabilities. Hence, (3.19) and $P(Y_{1j} \cap Y_{2i})$ are independent of the choice of i for all values of j.

Algorithm B / Two Reed-Solomon Decoders

The analysis for algorithm B used in the two Reed-Solomon decoder configuration may be drawn from the results of the single Reed-Solomon decoder

system. Using (3.12), (3.13), (3.14), (3.15) and (3.18) we may evaluate the symbol error rate. The proof that $P_b = P_S M/2(M-1)$ given earlier in this section remains valid and therefore, we can also evaluate bit error probabilities.

3.4 Hard Decisions, Perfect Side Information

To provide a baseline for comparing numerical results, we derive the performance of the two Reed-Solomon decoder configuration of Figure 2.2 for case of hard decisions and perfect side information. With perfect side information the quality bit, q, is unity when the transmission was jammed and zero otherwise. The incomplete decoder will output the correct symbol in the event any one or more of the L received symbols is not jammed. If all symbols are jammed the incomplete decoder outputs an erasure. The incomplete decoder never errors. The complete decoder functions similarly except that it produces a maximum likelihood estimate in the event all symbols are jammed.

Referring to Section 2.3 and (2.10), events E_1 (both inner decoders err), E_3 (incomplete inner decoder = error, complete inner decoder = correct) and E_4 (incomplete inner decoder = correct, complete inner decoder = error) occur with probability zero. Simplifying (2.10) and substituting into (2.2) we obtain:

$$P_S = p_2 \sum_{i=\lfloor (N_0-K_0)/2 \rfloor}^{N_0-1} \sum_{j=\max[0,N_0-K_0-i]}^{N_0-1-j} \binom{N_0-1}{i,j} p_2^i \, p_5^j \, p_6^{N_0-1-i-j} \qquad (3.20)$$

To facilitate the analysis we define the following events:

E_{Ix} = event the incomplete decoder erases

E_{Ie} = event the incomplete decoder errs

E_{Ic} = event the incomplete decoder is correct

E_{Ce} = event the complete decoder errs

E_{Cc} = event the complete decoder is correct.

Recall that p_2 is the probability that the incomplete decoder erases and the complete decoder errors. Thus,

$$\begin{aligned} p_2 &= P(E_{Iz} \cap E_{Ce}) \\ &= P(E_{Ce} \mid E_{Iz})P(E_{Iz}) \end{aligned}$$

With perfect information about the jammer state, E_{Iz} occurs only when all L transmissions are jammed. Thus,

$$P(E_{Iz}) = \rho^L \tag{3.21}$$

The term $P(E_{Ce} \mid E_{Iz})$ is the symbol error probability of an M-ary repetition code on an M-ary symmetric channel with symbol error probability, p, given by

$$p = \rho\, e^{-\frac{\rho E_s}{N_J}} \sum_{j=2}^{M} \frac{(-1)^{j-1}}{M} \binom{M}{j} e^{\frac{\rho E_s}{jN_J}} \tag{3.22}$$

Calculation of $P(E_{C_e} \mid E_{I_z})$ has been investigated in [16, Appendix A] and is generalized in Appendix B.

We can now calculate p_5 in terms of the above events

$$\begin{aligned} p_5 &= P(E_{Iz} \cap E_{Cc}) \\ &= P(E_{Cc} \mid E_{Iz})P(E_{Iz}) \\ &= [1 - P(E_{Ce} \mid E_{Iz})]P(E_{Iz}) \end{aligned} \tag{3.23}$$

Thus, p_5 and $p_6 = 1-p_2-p_5$ may be calculated using (4.31), (3.23) and the results in Appendix B.

To show $P(Y_{1j} \cap Y_{2i})$ is independent of $i \in (1, \ldots, M-1)$ for all $j \in (0,1, \ldots, M)$ is simple for the case of hard decisions with perfect side

information. First we note that $P(Y_{1j} \cap Y_{2i}) \equiv 0$ for $j \neq M$.

When all L symbols are jammed, the maximum likelihood decoder must select the output in an environment in which all symbols are received over an M-ary symmetric channel. Thus $P(Y_{1M} \cap Y_{2i})$ is independent of i.

Hence, symbol error probabilities are given by (3.20); bit error probabilities are related by (2.20); and the analysis is complete for the case of hard decisions with perfect side information.

3.5 Repetition Thresholding

In this section we introduce and analyze the first of two algorithms for generating erasures in the incomplete decoder without use of side information. The inputs to the incomplete decoder are the L symbol estimates $\{\hat{y}_j \ ; \ j = 1, \ldots, L\}$. The first algorithm, repetition threshold decoding, is defined as follows: Set a threshold T such that $2 \leq T \leq L$. The incomplete decoder output an erasure if no symbol occurs T or more times. Otherwise, the decoder output a maximum likelihood estimate. For example, suppose $L = 5$ and (0,0,1,1,2) is received. If $T = 3$ the decoder output an erasure; if $T = 2$ the decoder makes an arbitrary choice between symbols 0 and 1. The complete decoder is a maximum likelihood decoder.

We will derive the performance parameters for repetition thresholding used in the parallel decoder configuration with two Reed-Solomon decoders. The analysis will be divided into two case $T \geq \lceil L/2 \rceil$ and $T < \lceil L/2 \rceil$.

Case 1: $T \geq \lceil L/2 \rceil$

When $T \geq \lceil L/2 \rceil$ the incomplete decoder erases if no symbol occurs more than $\lfloor L/2 \rfloor$ times. If the incomplete decoder does not erase, both inner decoders will output the same symbol. Hence, events E_3 (incomplete inner decoder = error, complete

inner decoder = correct) and E_4 (incomplete inner decoder = correct, complete inner decoder = error) will not occur and (2.6) reduces to the form given by (3.12). Thus, to complete the analysis of symbol error probability we need to evaluate p_1, p_2, p_5 and p_6 and use (3.2) and (3.12).

Using the notation defined in Section 3.4, we have

$$\begin{aligned} p_1 &= P(E_{Ie} \cap E_{Ce}) \\ &= P(E_{Ie}) \quad (\text{since } E_{Ie} \subset E_{Ce}) \end{aligned} \tag{3.24a}$$

$$p_2 = P(E_{Ix} \cap E_{Ce}) \tag{3.24b}$$

$$\begin{aligned} p_5 &= P(E_{Ix} \cap E_{Ce}^c) \\ &= P(E_{Ix}) - P(E_{Ix} \cap E_{Ce}) \\ &= P(E_{Ix}) - p_2 \end{aligned} \tag{3.24c}$$

$$p_6 = 1 - p_1 - p_2 - p_5 \tag{3.24d}$$

To calculate these terms we need to know the probability of symbol error, p, for non-coherent reception of MFSK signalling with the only noise contribution being partial-band Gaussian interference of a fraction ρ of the bandwidth with power $\rho N_J/2$. If the received signal energy is E_S, p is given by (3.22).

With $T \geq \lceil L/2 \rceil$, the incomplete decoder will output any symbol which occurs T or more time. Letting $q = 1 - p$ we have

$$P(E_{Ic}) = \sum_{i=T}^{L} \binom{L}{i} q^i \left(\frac{p}{M-1}\right)^{L-i} \tag{3.25a}$$

$$P(E_{Ie}) = (M-1) \sum_{i=T}^{L} \binom{L}{i} \left(\frac{p}{M-1}\right)^i \left[q + \left(\frac{M-2}{M-1}\right)p\right]^{L-i} \tag{3.25b}$$

$$P(E_{Ix}) = 1 - P(E_{Ic}) - P(E_{Ie}) \tag{3.25c}$$

The last term to be evaluated, p_2, is best determined using the enumeration tech-

nique of Appendix B.

$$p_2 = \sum_{n_c=0}^{\lfloor \frac{L}{2} \rfloor} \sum_{Y} G_1(Y, n_c) \binom{L}{Y} q^{n_c} \left(\frac{p}{M-1} \right)^{L-n_c} \tag{3.26}$$

where all terms are as defined for (3.7) and (3.8) except that Y is further constrained by the condition $n_c \leq m_1 < T$. See Appendix B for sample evaluations of p_2 for $L = 3,5$ and 7 and for various values of T.

Case: T < ⌈L/2⌉

When $T < \lceil L/2 \rceil$, all of the events E_1 through E_6 defined in Section 2.2 are possible. Equations (2.2) and (2.10) specify the parallel decoder symbol error probability. We require expressions for each of the following terms:

$$p_1 = P(E_{Ie} \cap E_{Ce}) \tag{3.27a}$$

$$p_2 = P(E_{Iz} \cap E_{Ce}) \tag{3.27b}$$

$$\begin{aligned} p_3 &= P(E_{Ic} \cap E_{Ce}) \\ &= P(E_{Ce}) - P(E_{Ce} \cap E_{Ic}^c) \\ &= P(E_{Ce}) - P(E_{Ce} \cap [E_{Ie} \cap E_{Iz}]) \\ &= P(E_{Ce}) - P(E_{Ie} \cap E_{Ce}) - P(E_{Iz} \cap E_{Ce}) \\ &= P(E_{Ce}) - p_1 - p_2 \end{aligned} \tag{3.27c}$$

$$\begin{aligned} p_4 &= P(E_{Ie} \cap E_{Cc}) \\ &= P(E_{Ie}) - P(E_{Ie} \cap E_{Cc}^c) \\ &= P(E_{Ie}) - P(E_{Ie} \cap [E_{Ce}) \\ &= P(E_{Ie}) - p_1 \end{aligned} \tag{3.27d}$$

$$\begin{aligned} p_5 &= P(E_{Iz} \cap E_{Cc}) \\ &= P(E_{Iz}) - P(E_{Iz} \cap E_{Ce}) \\ &= P(E_{Iz}) - p_2 \end{aligned} \tag{3.27e}$$

$$p_6 = 1 - \sum_{i=1}^{5} P_i \tag{3.27f}$$

The set of (3.27a)-(3.27e) require computation of five terms: p_1, p_2, $P(E_{Ce})$, $P(E_{Ie})$ and $P(E_{Iz})$. For the analysis which follows we will assume that ties are decided randomly among the competing signals and decisions made by the two inner decoders are independent.

With the probability of receiving a symbol in error, p, given by (3.22) and with $q = 1 - p$, we begin by partitioning p_1.

$$p_1 = p_{1a} + p_{1b}$$

where,

$p_{1a} =$ p (an error symbol occurs at least $\lceil L/2 \rceil$ times)

$p_{1b} =$ p (no symbol occurs $\lceil L/2 \rceil$ or more times, at least one symbol occurs T or more times, both inner decoders error)

Now,

$$p_{1a} = (M-1) \sum_{i=\lceil L/2 \rceil}^{L} \binom{L}{i} \left(\frac{p}{M-1} \right)^i \left[q + \left(\frac{M-2}{M-1} \right) p \right]^{L-i} \tag{3.28}$$

and

$$p_{1b} = \sum_{n_c=0}^{\lfloor L/2 \rfloor} \sum_{Y} G_2(Y, n_c) \binom{L}{Y} q^{n_c} \left(\frac{p}{M-1} \right)^{L-n_c} \tag{3.29}$$

where (3.29) is an enumeration formula similar to that specified by (3.7) and (3.8) except that we require:

$$n_c \leq m_1, \quad T \leq m_1, \quad m_\alpha < \lceil L/2 \rceil$$

and $r(Ne)$ is replaced by:

$$r(N_e,n_c) = \begin{cases} 1 & \begin{cases} N_e = 0 \quad or \\ n_c < m_1\,,\ N_e \neq 0 \end{cases} \\ \left(\dfrac{N_e}{N_e+1} \right)^2 & n_c = m_1\,,\ N_e \neq 0 \end{cases} \tag{3.30}$$

Next, p_2 is the probability no symbol occurs T or more times and the complete decoder errors. We have

$$p_2 = \sum_{n_c=0}^{T-1} \sum_{Y} G_1(Y,n_c) \binom{L}{Y} q^{n_c} \left(\frac{p}{M-1} \right)^{L-n_c} \tag{3.31}$$

which, except for the upper limit on the first summation, is identical to (3.26).

To calculate the probability that the incomplete decoder errors, we start by partitioning the event space.

$$P(E_{Ie}) = p_{ea} + p_{eb}$$

where

$p_{ea} = p_{1a}$ [given by (3.28)]

$p_{eb} = P$(no symbol occurs $\lceil L/2 \rceil$ or more times , at least one symbol occurs T or more times , the complete decoder errors)

$$= \sum_{n_c=0}^{\lfloor L/2 \rfloor} \sum_{Y} G_1(Y,n_c) \binom{L}{Y} q^{n_c} \left(\frac{p}{M-1} \right)^{L-n_c}$$

where $G_6(Y,n_c,T)$ is the same as specified by (3.8) except we require $n_c \leq m_1$ and $T \leq m_1$.

The probability the incomplete decoder erases is the probability no symbol occurs T or more times which is given by:

$$P(E_{Ie}) = \sum_{n_c=0}^{T-1} \sum_{Y} G_3(Y,n_c) \binom{L}{Y} q^{n_c} \left(\frac{p}{M-1} \right)^{L-n_c} \tag{3.33}$$

where $G_3(Y,n_c)$ is equivalent to (3.8) with the new condition that $r(N_e) = 1$.

Finally, the probability the complete decoder errors, $P(E_{C_e})$, is the probability of error for a L-diversity repetition code. This probability is derived in Appendix B where sample evaluations are also given for each of the enumeration formulas of this section. We have now provided expressions for each of the probabilities p_i; $i = 1, \ldots, 6$ necessary to evaluate the symbol error probability for repetition threshold decoding for all values of $T \geq 2$.

We next consider the bit error probability for this decoder and wish to prove it is given by (2.20). We must show that $P(Y_{1j} \cap Y_{2i})$ is independent of the choice of $i \neq 0$ for all values of j where symbol zero is assumed transmitted. As we did for the decoder performance analysis, we consider the two cases $T \geq \lceil L/2 \rceil$ and $T < \lceil L/2 \rceil$.

When $T \geq \lceil L/2 \rceil$, any time the incomplete decoder output is a symbol, not an erasure, then that symbol occurred at least $\lceil L/2 \rceil$ times and the complete decoder will output the same symbol. Thus,

$$P(Y_{1j} \cap Y_{2i}) = \begin{cases} 0 & j \neq i \\ 1 & j = i \end{cases}$$

where $j \in \{0,1, \ldots, M-1\}$ and $i \neq 0$. For $j = M$, $P(Y_{1j} \cap Y_{2i})$ is the probability the complete decoder outputs symbol $i \neq 0$ when no symbol occurs T or more times. This probability is given by (3.11). We again argue that these events are all multinomial expressions on events that occur with equal probabilities. In fact, we could easily write an enumeration formula for $P(Y_{1M} \cap Y_{2i})$. Hence, for $T \geq \lceil L/2 \rceil$ (2.20) is valid.

The proof is not as simple or as intuitive for $T < \lceil L/2 \rceil$. We need to consider four cases: $j = 0$, $j = i$, $i \neq j \neq M$, and $j = M$ where for each case

$i \in \{1,2,\ldots,M-1\}$. For $j = 0$, $P(Y_{1j} \cap Y_{2i})$ is the probability the incomplete decoder is correct and the complete decoder errs with symbol i output.

$$\begin{aligned} P(Y_{10} \cap Y_{2i}) &= P\{n_I = N_c > T \text{ , incomplete decoder outputs} \\ &\qquad \text{symbol zero , complete decoder outputs } i\} \\ &= \sum_{n_c=T}^{\lfloor L/2 \rfloor} \sum_{Z} H_1(Z,n_c,n_I) \binom{L}{Z,n_c} q^{n_c} \left(\frac{P}{M-1}\right)^{L-n_c} \end{aligned} \tag{3.34}$$

where:

n_I = the number of symbols i received

n_c = the number of correct symbols received

$Z = (m_1, m_2, \ldots, m_\alpha)$

= a generic configuration of the $L-2n_c$ remaining symbols such that

$n_c \geq m_1 \geq m_2 \geq \cdots \geq m_\alpha$

$m_1 + m_2 + \cdots + L - 2n_c$

$\binom{L}{Z,n_c}$ = number of ways of receiving n_c of symbol 0 , n_I of symbol i, m_1 of symbol s_1, m_2 of symbol $s_2 \cdots$; $s_1, s_2 \cdots \neq 0, i$

letting,

Ne = number of terms of Z which equal n_I

$n_1, \ldots, n_\beta$ be as defined for (3.8)

$$H_1(Z,n_c,n_I) = \left(\frac{1}{N_e+2}\right)^2 \frac{(M-2)(M-3)\cdots(M-\alpha-1)}{n_1!n_2!\cdots n_\beta!} \tag{3.35}$$

See Appendix B for development of similar enumeration formulas.

When $j = i$, $P(Y_{1i} \cap Y_{2i})$ is the probability that both decoders error with the same output symbol. Hence,

$$P(Y_{1i} \bigcap Y_{2i}) = P\{n_I > T \text{ , both inner decoders output symbol } i\} \tag{3.36}$$
$$= \sum_{n_I=T}^{L} \sum_{n_c=0}^{\min[L-n_I,n_I]} \sum_{Z} H_2(Z,n_c,n_I) \binom{L}{Z,n_c} q^{n_c} \left(\frac{p}{M-1}\right)^{L-n_c}$$

where all terms are as defined for (3.34) and (3.35) except:

$$Ne = \text{number of terms of } Z \bigcup \{n_c\} \text{ which equal } n_I$$
$$H_2(Z,n_c,n_I) = \left(\frac{1}{N_e+1}\right)^2 \frac{(M-2)(M-3)\cdots(M-\alpha-1)}{n_1!n_2!\cdots n_\beta!} \tag{3.37}$$

When $i \neq j \neq M$, $P(Y_{1j} \cap Y_{2i})$ is the probability both decoders error with different output symbols.

$$P(Y_{1j} \bigcap Y_{2i}) = P\{n_I = n_J \geq T \text{ , complete decoder outputs symbol } i \text{ ,} \tag{3.38}$$
$$\text{incomplete decoder outputs symbol } j\}$$
$$= \sum_{n_I=T}^{\lfloor L/2 \rfloor} \sum_{n_c=0}^{\min[L-2n_I,n_I]} \sum_{Z} H_3(Z,n_I,n_c) \binom{L}{Y,n_c,n_I} q^{n_c} \left(\frac{p}{M-1}\right)^{L-n_c}$$

where all terms are as defined for (3.36) and (3.37) except:

$$n_J = \text{the number of symbols } j \text{ received}$$
$$H_3(Z,n_c,n_I) = \left(\frac{1}{N_e+1}\right)^2 \frac{(M-3)(M-4)\cdots(M-\alpha-2)}{n_1!n_2!\cdots n_\beta!} \tag{3.39}$$

Finally, for $j = M$ the analysis for $T \geq \lceil L/2 \rceil$ is valid. Since none of the derived expressions depend on symbol i being chosen, we have shown that bit and symbol error probabilities are related by (2.20). The analysis for repetition threshold decoding is complete. We now consider another technique called tie thresholding.

3.8 Tie Thresholding

The last of the algorithms we will consider for parallel decoder with L-diversity inner codes is called tie thresholding. With tie thresholding the incomplete decoder output is an erasure symbol whenever there is a tie between symbols which occur most often in a received vector. Otherwise, one symbol must occur more frequently

than another symbol and the incomplete decoder will output that symbol. The complete decoders provides a maximum likelihood decision.

Referring to the general development in Chapter 2, with tie thresholding events E_3 and E_4 cannot occur. The only way one inner inner decoder could err while the other is correct is to have a tie between symbols. However, a tie will produce an erasure in the incomplete decoder. Thus, we can use the form of $P(F_S)$ given by (3.2) and (3.12). In the remainder of this section we will present equations for p_1, p_2, p_5, and p_8 necessary to evaluate $P(F_S)$ and then prove that symbol and bit error probabilities are related by $P_b = P_S M/2(M-1)$.

Event E_1 is the probability that the output of both inner decoders is an erroneous symbol. The probability of E_1, p_1, is equivalently the probability one error symbol occurs more frequently than any other symbol. Since we have an M-ary symmetric, memoryless channel we can write

$$\begin{aligned} p_1 = P(E_1) &= \sum_{i=1}^{M-1} P(E_1 \cap \text{symbol } i \text{ occurs most often}) \\ &= (M-1)P(E_1 \cap \text{symbol 1 occurs most often}) \end{aligned}$$

where, without loss of generality, we have assumed symbol 0 was transmitted. Continuing we write

$$p_1 = p_{1a} + p_{1b}$$

where

$$p_{1a} = (M-1)P(E_1 \cap \text{symbol 1 occurs} \geq \lceil L/2 \rceil \text{ times}) \tag{3.40a}$$

$$p_{1b} = (M-1)P(E_1 \cap \text{symbol 1 occurs} < \lceil L/2 \rceil \text{ times but still most frequently}) \tag{3.40b}$$

Now,

$$p_{1a} = (M-1) \sum_{i=\lceil L/2 \rceil}^{L} \binom{L}{i} \left(\frac{p}{M-1} \right)^{i} \left[q + \left(\frac{M-2}{M-1} \right) P \right]^{L-i} \tag{3.41}$$

where p is given by (3.22) and $q = 1 - p$. Next,

$$p_{1b} = (M-1) \sum_{i=2}^{\lfloor L/2 \rfloor} \sum_{n_c=0}^{i-1} \sum_{Y} G_1(Y, n_c) \binom{L}{Y, n_c} q^{n_c} \left(\frac{p}{M-1} \right)^{L-n_c} \tag{3.42}$$

where $L \geq 5$ and all terms are as defined for (3.8) except we require $m_1 < i$. We note that for diversity $L = 3$, $p_{1b} = 0$.

The probability that the incomplete decoder erases and the complete decoder errors, p_2, is given by

$$\begin{aligned} p_2 &= Pr\{\text{two or more symbols tie and the} \\ &\qquad \text{complete decoder errors}\} \\ &= \sum_{n_c=0}^{\lfloor L/2 \rfloor} \sum_{Y} G_1(Y, n_c) \binom{L}{Y} q^{n_c} \left(\frac{p}{M-1} \right)^{L-n_c} \end{aligned} \tag{3.43}$$

where:

$$\begin{aligned} n_c &= \text{the number of correct symbols received} \\ Y &= (m_1, m_2, \ldots, m_\alpha) \\ & \quad m_1 \geq m_2, \ldots, m_\alpha \\ & \quad n_c \leq m_1, \text{ if } n_c < m_1 \text{ then } m_1 = m_2 \end{aligned}$$

and all other terms are as defined for (3.8). Sample calculations of the enumeration formulas (3.42) and (3.43) are given in Appendix B.

The probability that the incomplete decoder erases and the complete decoder errs, p_5, is the probability the correct symbol and one or more incorrect symbols tie for most frequent occurrence and the complete decoder choses the correct symbol.

$$p_5 = \sum_{n_c=1}^{\lfloor L/2 \rfloor} \sum_{Y} G_1(Y, n_c) \binom{L}{Y} q^{n_c} \left(\frac{p}{M-1} \right)^{L-n_c} \tag{3.44}$$

where, with the change $n_1 = m_c$, G_{10} is equivalent to (3.8). Finally, noting that

$p_6 = 1 - p_1 - p_2 - p_5$, our remaining task is to prove the symbol and bit error probabilities are related by $P_b = P_s M/2(M-1)$.

With reference to Section 2.5, we need to show that $P(Y_{1j} \cap Y_{2i})$ is independent of $i \in \{1, \ldots, M-1\}$ for all choices of $j \in \{0, \ldots, M-1\}$. We begin by noting that whenever the incomplete decoder outputs a symbol other than an erasure, that symbol occurred more often than any other symbol and will also be the output of the complete decoder. Thus,

$$P(Y_{1j} \cap Y_{2i}) = \begin{cases} 0 & j \neq i \\ 1 & j = i \end{cases}$$

where $j \in \{0,1, \ldots, M-1\}$ and $i \neq 0$. For $j = M$, $P(Y_{1j} \cap Y_{2i})$ is the probability that two or more symbols tie and the complete decoder outputs symbol $i \neq 0$. If we modify (3.43) to require that:

$$m_1 = \text{number of times symbol } i \text{ occurs}$$

then we have an expression for $P(Y_{1M} \cap Y_{2i})$. Clearly this expression is independent of the choice of i and we have completed the proof.

CHAPTER 4

PARALLEL DECODING/LINEAR BLOCK INNER CODES

4.1 Introduction

In the previous chapter, we considered various inner code decoding schemes based on L-diversity repetition inner codes. We now turn our attention to a more general class of inner codes and consider binary linear block codes. Two system implementations will be considered with the binary linear block inner coders. First, the case when binary FSK signalling is used will be evaluated. Next, we will consider the case when M-ary signalling is used where herein M will be restricted to the alphabet size of the outer Reed-Solomon code. The analysis may be easily extended for other values of M.

The linear block codes to be analyzed have dimensions (N_I,K_I) where K_I is equal to the binary symbol size of the Reed-Solomon code. For example, a $(N_0{=}32,K_0{=}16)$ Reed-Solomon outer code will have a $(N_I,K_I{=}5)$ binary linear block inner code. In the complete inner decoder, the linear block codes will be used in an error correction only mode with standard syndrome decoding procedures.

For the incomplete inner decoders, will evaluate use of linear block inner codes for error detection only and for combined error detection/error correction. In the case of error detection only, the incomplete decoder output is an erasure whenever an

error is detected. For combined error detection/error correction, the erasure criteria for the incomplete inner decoders will be obtained by partitioning the standard array for the code. If a received vector results in a zero syndrome, the data portion of the codeword (one symbol) will be input to the Reed-Solomon decoder. Otherwise, depending on where the received vector lies in the standard array, either error correction will be attempted by adding the appropriate coset leader to the received vector or an erasure will be declared. For larger minimum distance codes, we will be able to define a greater variety of partitions on the standard array.

Throughout the analysis we assume a slow frequency hopping system so that each inner code codeword is transmitted on the same hop. With this assumption, the symbol statistics into the outer decoders are independent and identically distributed. Our objective is to compute the bit error probability for the parallel decoding system as a function of the percentage of hopping bandwidth jammed and the received signal energy to jammer noise ratio.

In Section 2 of this chapter we present a general analysis of the parallel decoding algorithms using linear block inner codes. In Sections 3 and 4 respectively we describe the system analysis for cases of binary and 2^{K_I}-ary signalling. The chapter concludes with a description of the codes used to evaluate the parallel decoder performance.

4.2 General Development

The analysis of Chapter 2 will be used in deriving the performance of the parallel decoder using binary linear block inner codes. We will use only inner decoders with an input block length equal to the outer encoder symbol size. Thus, each inner code codeword contains a single outer code symbol plus parity bits. To determine

symbol statistics at the inputs to the outer decoders, we need only determine the probabilities of inner decoder error and erasure.

For the two Reed-Solomon decoder parallel decoder of Section 2.3 and Figure 2.2, (2.2) and (2.10) described the probability of a symbol error out of the parallel decoder system. The complete decoder will perform error-correction standard syndrome decoding. The incomplete decoder will be used either to only detect (i.e., erase) errors or to both detect and correct errors. Figures 4.1, 4.2 and 4.3 illustrate the general partitioning of the standard arrays for each inner decoder configuration where the all zero codeword is assumed to be transmitted. The top line of each figure is the codeword set and the leftmost element of this line is the all zero vector. The leftmost column is the set of coset leaders. The labelings error, erasure, and correct indicate the condition of the decoder output in the event the received vector lies in that portion of the standard array.

With reference to Figures 4.1 and 4.2 we can simplify (2.10) by showing that in either case events E_3 and E_4 cannot occur and thus $p_3 = p_4 = 0$. Hence, (2.10) reduces to the simpler form of (3.12) and we need to determine the probabilities p_1, p_2, p_5, and p_6 to evaluate the parallel decoder performance.

The event E_3 is the event that the incomplete decoder produces a correct output when the corresponding output from the complete decoder is an error. If the incomplete decoder is used for error detection only, it will produce a correct output only when the correct codeword is received. Hence, the complete decoder will also yield the correct output. Similarly, if the incomplete decoder is used for both detection and correction, it will produce a correct output only if the correct codeword is received or if a detectable error pattern occurred. In either case, the complete

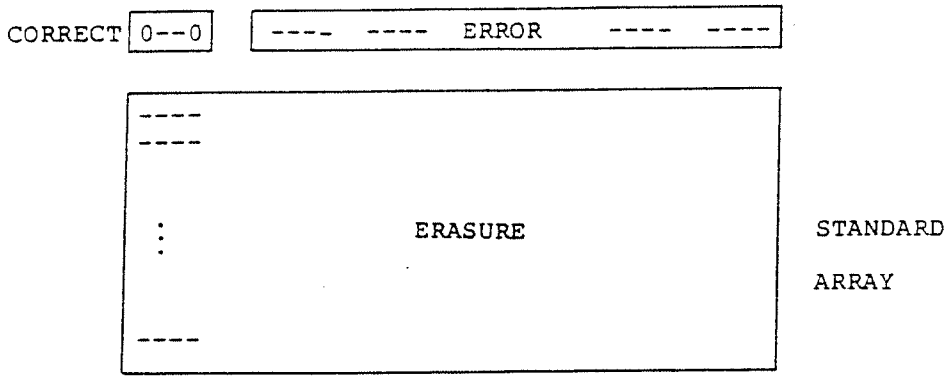

Figure 4.1 Incomplete Decoder: Error Detection Only

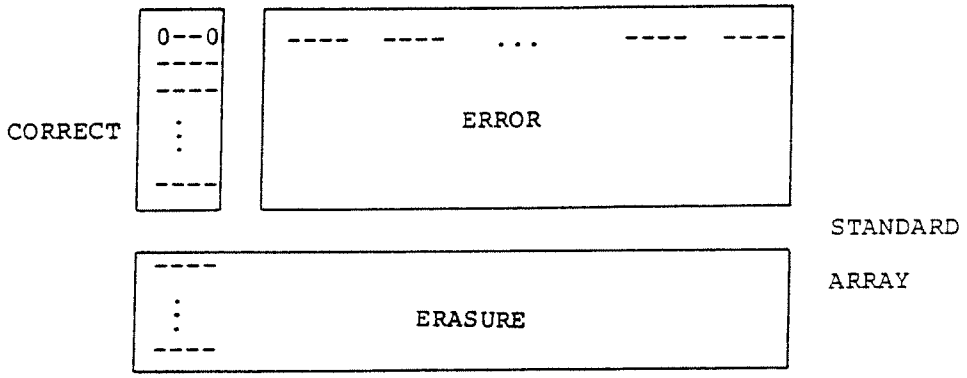

Figure 4.2 Incomplete Decoder: Error Detection and Correction

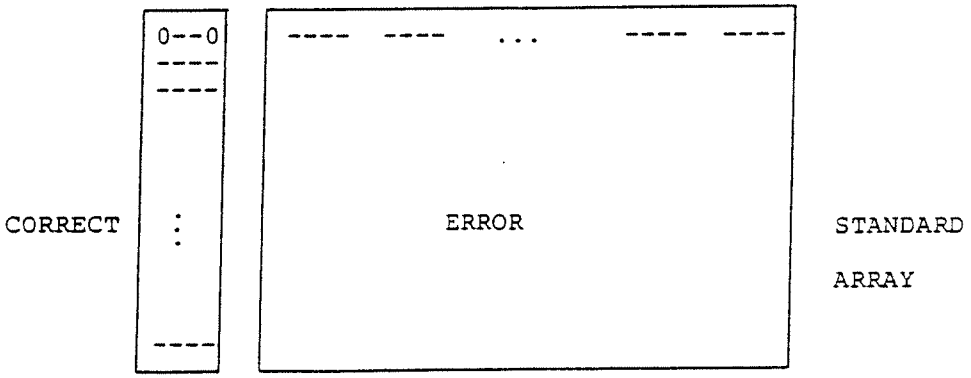

Figure 4.3 Complete Decoder: Error Correction Only

decoder will output the correct symbol.

E_4 is the event that the incomplete decoder errs and the complete decoder is correct. For either decoder configuration, the complete decoder is correct only if the correct codeword is received or if a detectable error pattern occurred. If the correct codeword is received the incomplete decoder is correct. If a correctable error pattern occurs, the error detection only decoder will erase and the detection/correction decoder will either erase or correct. In neither case is an error by the incomplete decoder possible.

Where possible, we will evaluate the parallel decoder performance with binary linear block inner codes and two types of channel signalling. In all cases we will consider the performance with binary FSK signalling and noncoherent detection. When the ratio N_I/K_I is an integer, we will also evaluate performance with 2^{K_I}-ary FSK signalling and noncoherent detection.

If we use slow frequency hopping so that all of the bits or symbols of an inner code codeword are transmitted on a given hop, we have in general.

$$p(E_i) = (1-\rho)\, p(E_i \mid \text{ not jammed }) + \rho\, p(E_i \mid \text{ jammed }) \tag{4.1}$$

where $i = 1, \ldots, 6$. With the assumption of no background noise, $p(E_i \mid$ not jammed) is unity if $i = 6$ and zero otherwise. Thus, we have

$$p_i = \rho\, p_{i \mid J} \quad i = 1,2, \ldots, 5 \tag{4.2a}$$

$$p_6 = 1 - \rho + \rho\, p_{6 \mid J} \tag{4.2b}$$

where $p_{i \mid J}$ is shorthand notation for the conditional probability of the event E_i given the signal was jammed, $i = 1, \ldots, 6$.

In the next two sections. we consider evaluation of $p_{i \mid J}$ when respectively

binary and 2^{K_I}-ary signalling is used. We also derive the parallel decoder bit error probabilities for each of these cases.

4.3 Case: Binary Signalling

Each of the probabilities $p_{i|J}$ we wish to compute are the probabilities of joint events on the incomplete and complete inner decoders assuming the received signal was jammed. Without loss of generality, we may assume the all zero codeword was transmitted. In this case the probabilities of the joint events of interest are equivalently the probabilities that the received vector lies in the intersection of the standard arrays for the appropriate incomplete and complete inner decoders as shown in Figures 4.1, 4.2, and 4.3. With this approach we easily see that $p_3 = p_4 = 0$ since the correct and error events of the complete decoder have null intersections with the error events of either incomplete decoder.

4.3.1 Incomplete Decoder Used For Error Detection Only

Considering first the subcase when the incomplete decoder is used only for error detection, $p_{\delta|J}$ is the probability that both inner decoders produce the correct output. Visualizing the intersection of the standard arrays of Figures 4.1 and 4.3, we see that both decoders will be correct only when the all zero error pattern occurs.

Let r be the probability of a received bit error given the channel is jammed and s be the probability a bit is received correctly given the channel is jammed ($2=1-r$). Then,

$$r = \frac{1}{2}\, e^{-\rho E_b / 2N_J} \tag{4.3}$$

where E_b is the received energy per bit. Thus, the probability that the all zero vector is received is given by

$$p_{6|J} = s^{N_I} \tag{4.4}$$

The probability that both decoders will error, event E_1, is the probability that the received vector is a non-zero codeword. Let the set $\{A_i\ ,\ i = 0, \ldots, N_I\}$ be the weight enumerators of the inner code where A_i is the number of codewords of Hamming weight i. Then,

$$p_{1|J} = \sum_{i=1}^{N_I} A_i\ r^i\ s^{N_I - i} \tag{4.5}$$

The incomplete decoder erases and the complete decoder is correct, event E_5, only if the received N-tuple is a coset leader other than the all zero vector. Similar to the code weight enumerators we define the coset leader weight enumerator $\{L_i\ ,\ i = 0,1, \ldots, N_I\}$ such that L_i is the number of coset leaders of weight i. Hence,

$$p_{5|J} = \sum_{i=1}^{N_I} L_i\ r^i\ s^{N_I - i} \tag{4.6}$$

Finally, we note

$$p_{2|J} = \rho - p_{1|J} - p_{5|J} - p_{6|J} \tag{4.7}$$

4.3.2 Incomplete Decoder Used For Detection and Correction

The analysis proceeds similarly for the subcase when the incomplete decoder is used for both error detection and correction. Figure 4.2 depicts the incomplete decoder actions for given received vectors. By visualizing the intersections of Figures 4.2 and 4.3 we can characterize the quantities required to evaluate $p_{i|J}$ for $i = 1,2,5,6$.

Both decoders are correct only if the incomplete decoder is correct. That is, the received vector must be a coset leader in the correctable event portion of the

standard array for the incomplete decoder. Define $\{L_{ei}\ ,\ i = 0,1, \ldots, N_I\}$ as the weight enumerators of the coset leaders which result in erasure events for the incomplete decoder. Then it follows that

$$p_{6|J} = \sum_{i=0}^{N_I} (L_i - L_{ei})\ r^i\ s^{N_I - i} \tag{4.7}$$

Similarly, $p_{5|J}$ is the probability of the event that the incomplete decoder erases and the complete decoder is correct given the channel is jammed. Referring to the standard arrays, we see that this is equivalently the probability that the received vector is a coset leader in the erasure portion of the standard array for the incomplete decoder. Hence,

$$p_{5|J} = \sum_{i=1}^{N_1} L_{ei}\ r^i\ s^{N_I - i} \tag{4.8}$$

The probability that both decoders err given the channel was jammed, $p_{1|J}$, is equivalently the probability that the received vector is either a non-zero codeword or lies in the error portion of the standard array for the incomplete decoder excluding the coset leaders. This result is not obtained as easily as the previous results. We start by making an assumption that incomplete decoder error correction will be limited to the codes error correction capability given by

$$t = \lfloor (d_{\min} - 1)/2 \rfloor \tag{4.9}$$

For example, a two bit error correcting code $(t - 2)$ will be used either to correct all one bit errors and detect other errors or to correct all one and all two bit errors and detect any other errors as allowed. The general result will be motivated by first considering one and two bit error correction.

If the incomplete decoder corrects all single bit errors then the coset leaders include all possible vectors containing a single "1" and N_I -1 zeros. Hence, in the standard array column below a codeword of weight W there will be

$$\begin{aligned} W &\text{ vectors of weight } W - 1 \\ N_I - W &\text{ vectors of weight } W + 1 \end{aligned}$$

Hence, if $\{A_i\ ,\ i = 1, \ldots, N_I\}$ are the weight enumerators of the code then $\{C_{1i}\ ,\ i = 1, \ldots, N_I\}$ is the joint weight enumerator of all N_I-tuples in cosets having weight one coset leaders where

$$C_{1i} = (N_I - i+1)A_{i-1} + (i+1)A_{i+1} \tag{4.10}$$

(note: A_{N_I+1}=0). Or equivalently, if we let $A(z)$ be the weight enumerator polynomial for the code,

$$A(z) = \sum_{i=0}^{N_I} A_i z^i \tag{4.11}$$

then the joint weight enumerator polynomial for the cosets having weight one coset leaders is

$$\begin{aligned} C_1(z) &= \sum_{i=1}^{N_I} A_i[iz^{i-1} + (N_I-i)z^{i+1}] \\ &= \sum_{i=1}^{N_I} C_{1i} z^i \end{aligned} \tag{4.12}$$

If r is the probability of a bit error at the input to the inner decoders and $s = 1 - r$, then the probability a received vector is in a coset having a weight one coset leader is

$$\sum_{i=1}^{N_I} C_{1i} r^i s^{N_I-i} \tag{4.13a}$$

$$= \sum_{i=0}^{N_I} A_i \left[i r^{i-1} s^{N_I-i+1} + (N_I - i) r^{i+1} s^{N_I-i-1} \right] \qquad \textbf{(4.13b)}$$

where we assume $T \geq 1$. To exclude the weight one coset leaders in (4.13b) the summation is started at $i = 1$.

If a code has $t \geq 2$ ($d_{\min} \geq 5$, then it can correct at least all one and two bit error patterns. The coset leaders include all N_I-tuples with one and two 1's. Considering cosets with weight two coset leaders, in a column below a codeword of weight W there will be,

$$\binom{W}{2} \text{ vectors of weight } W - 2$$

$$\binom{W}{1}\binom{N_I - W}{1} \text{ vectors of weight } W$$

$$\binom{N_I - W}{2} \text{ vectors of weight } W + 2$$

where we define $\binom{a}{b} = 0$ if $b > a$. Letting $C_2(z)$ be the joint weight enumerator polynomial of all cosets having weight two coset leaders we have,

$$C_2(z) = \sum_{i=0}^{N_I} \left[\binom{i}{2} z^{i-2} + \binom{i}{1}\binom{N_I - i}{1} z^i + \binom{N_I - W}{2} z^{i-2} \right] \qquad (4.14)$$

Thus, the pattern becomes clear. If a code has a t bit error correcting capability, the joint weight enumerator polynomial of all cosets having weight t; $1 \leq t' \leq t$, coset leaders is given by,

$$C_{t'}(z) = \sum_{i=0}^{N_I} A_i \sum_{j=0}^{t'} \binom{i}{t'-j}\binom{N_I - i}{j} z^{i+2j-t'} \qquad (4.15)$$

The probability a received vector lies in a coset having a coset leader of weight t' or less is given by,

$$\sum_{i=0}^{N_I} \sum_{j=1}^{t'} \sum_{k=0}^{j} A_i \binom{i}{j-k} \binom{N_I-i}{k} r^{i-2k-j} s^{N_I-i-2k-j} \tag{4.16}$$

As before, we can exclude the coset leaders by starting the outer summation at $i = 1$.

We are now prepared to give a general result for $p_{1|J}$.

$$\begin{aligned} p_{1|J} &= \sum_{i=1}^{N_I} A_i r^i s^{N_I-i} + \sum_{i=1}^{N_I} \sum_{j=1}^{t'} \sum_{k=0}^{j} A_i \binom{i}{j-k} \binom{N_I-i}{k} r^{i+2k-j} s^{N_I-i-2k+j} \\ &= \sum_{i=1}^{N_I} \sum_{j=0}^{t'} \sum_{k=0}^{j} A_i \binom{i}{j-k} \binom{N_I-i}{k} r^{i+2k-j} s^{N_I-i-2k+j} \end{aligned} \tag{4.17}$$

where we have assumed that the incomplete decoder corrects all error patterns of weight t' or less. Hence, using (4.7) we have completed the analysis for the subcase when the incomplete decoder is used to both detect and correct errors.

Considerations for the Multiple Parallel Decoder

The linear block inner codes may be used in the multiple parallel decoder configuration described in Section 2.4. For example, consider an inner code with $d_{\min} = 5$. One way of designing a 4-ary parallel decoder is to have incomplete decoder #1 detect errors only, incomplete decoder #2 correct one bit errors and detect all others, incomplete decoder #3 correct two bit errors and detect all others, and the complete decoder attempt all corrections (See Figure 2.3).

We first note that the hierarchical rules set forth in Chapter 2 are met. If any decoder erases, all decoders above it in the hierarchy will also erase. If any decoder is correct then all decoders below it in the hierarchy will be correct and all decoders above it in the hierarchy will either be correct or erase.

Evaluation of the eight event probabilities $p_1, \ldots, p_8$ proceeds in the same manner as for the 2-ary parallel decoder of this section. We consider the four

standard arrays for the inner decoders and evaluate the probabilities of the appropriate intersections. The coset joint weight enumerator polynomial (4.16) is a very useful tool for finding the probabilities of many of the intersections of interest. In Chapter 5 we will discuss the conditions under which we would expect to use the multiple parallel decoder configuration.

Bit Error Probability Analysis

We have calculated the quantities necessary to evaluate $P(F_S)$ of (2.2) and (3.12). In effect we should redefine $P(F_S)$ as the probability of incorrect decoding by the complete decoder following failure of the Reed-Solomon decoders. The complete decoder processes the input N_I-tuple using the standard syndrome decoding procedure of adding the appropriate coset leader to the received vector. In general, the bit error probability does not conform to the relationship of (2.20) as did the repetition codes.

In [4,Sec.1.3] and [10,Sec.7.2] there are procedures for determining the post-decoding bit error probability for linear block codes. Below we present an equivalent development which allowed calculation of $P(F_b)$ based on quantities that are easy to generate simultaneously with computer computation of code and code coset/coset leader weight distributions.

We begin by noting that

$$P(F_b) = P(F_b \mid F_S)P(F_S) \tag{4.18}$$

where $P(F_S)$ is given by (2.2), 3.12, and earlier developments in this section. Without loss of generality we assume that all zero codeword was transmitted. With reference to Figure 4.3, when a received vector lies in row j, column k ($j,k \neq 1$) of the standard array, the syndrome will point to the coset leader of the head at row j

and the codeword of the head of column k will be selected by the decoder. The information bit portion of that codeword will be output and may contain up to K_I bit errors.

If we define $N(w,j)$ as the number of N_I-tuples in the standard array having Hamming weight w and which result in j information bits in error. Then,

$$P(F_b \mid F_S) = \sum_{j=1}^{K_I} \sum_{w=1}^{N_I} \frac{j}{K_I} N(w,j) r^w s^{N_I - w} \tag{4.19}$$

When the code size is not so large as to prohibit computation of $N(w,j)$, this technique provides an easy method to evaluate $P(F_b \mid F_S)$. Otherwise, the references cited give a combinatoric technique for exact calculation and bounds which are tight under most circumstances.

In Section 4.5 we describe the binary block codes to evaluate the parallel decoder performance. We also provide a brief description of the algorithm used to determine weight distributions and $N(w,j)$. In Appendix C we give the resulting weight statistics for the codes evaluated.

4.4 Case 2^{K_I}-ary Signalling

When the ratio $(N_I/K_I) = \beta$ is an integer we have the option of transmitting the binary codewords as β 2^{K_I}-ary symbols rather than N_I bits. Use of 2^{K_I}-ary FSK with frequency hopping systems increases the instantaneous bandwidth per hop that a jammer must cover. We would expect that higher values of ρ would be required by the jammer to insure the same decrease in performance when compared to binary FSK signalling.

The analysis of the parallel decoder performance when we use 2^{K_I}-ary signalling proceeds in the same manner as for binary signalling in Section 4.3. We will see that

many of the formulas are applicable with a minor modification. Again reference is made to the standard arrays of Figures 4.1, 4.2, and 4.3, except now we must think of each element as a β-tuple of symbols from an alphabet of size 2^{K_I}. The argument of Section 4.3 that $p_3 = p_4 = 0$ is still valid. Thus, the objective of the remainder of this section is to derive expressions for p_1, p_2, p_5, p_6 and $P(F_b \mid F_S)$. We continue to assume, without loss of generality, that the zero codeword is transmitted.

4.4.1 Incomplete Decoder Used For Error Detection Only

If the incomplete decoder is used for error detection only, both decoders will produce the correct output only if the all zero vector (β zero symbols) is the error pattern. Thus,

$$p_{6|J} = q^{\beta} \tag{4.20}$$

where $q = 1 - p$ and p is the probability a symbol is received in error given the signal is received from a jammed portion of the partial-band jammed channel. With non-coherent processing of the 2^{K_I}-ary orthogonal signals.

$$p = e^{-\frac{\rho E_s}{N_J}} \sum_{j=2}^{M} \frac{(-1)^{j-1}}{M} \binom{M}{j} e^{\frac{\rho E_s}{jN_J}} \tag{4.21}$$

Both decoders will err, event E_1, only if the received vector is a non-zero codeword. Let $\{A_i^{'}, i=0,1, \ldots, \beta\}$ be the 2^{K_I}-ary weight enumerators of the inner code where the weight of a β-tuple of 2^{K_I}-ary symbols is merely the number of non-zero symbols. Hence, the probability the error pattern is a non-zero codeword is given by

$$p_{1|J} = \sum_{i=1}^{\beta} A_i^{'} \left(\frac{p}{M-1} \right)^i q^{\beta-i} \tag{4.22}$$

In the same manner we define the coset leader 2^{K_I}-ary weight enumerators $\{L_i^{'}, i = 0,1, \ldots, \beta\}$ such that $L_i^{'}$ is the number of coset leaders of 2^{K_I}-ary weight

i. By the same argument as in Section 4.3 we have

$$p_{\bar{5}|J} = \sum_{i=1}^{\beta} L'_i \left(\frac{p}{M-1} \right)^i q^{\beta-i} \tag{4.23}$$

Using (4.7) the analysis for this subcase is complete.

4.4.2 Incomplete Decoder Used For Detection and Correction

By defining $\{L'_{ei}\ , i = 1, \ldots, \beta\}$ as the 2^{K_I}-ary weight enumerators of the cosets which result in erasure events for the incomplete decoder, we can apply the arguments of Section 4.3 to extend (4.4) and (4.6).

$$p_{\delta|J} = \sum_{i=0}^{\beta} (L'_j - L'_{ej}) \left(\frac{p}{M-1} \right)^i q^{\beta-i} \tag{4.24}$$

$$p_{\bar{5}|J} = \sum_{i=1}^{\beta} L'_{ei} \left(\frac{p}{M-1} \right)^i q^{\beta-i} \tag{4.25}$$

Unfortunately, there is no extension of (4.17) to yield $p_{1|J}$ for 2^{K_I}-ary signalling. Since we are using binary block inner codes, an error correction capability of one bit does not equate to a one symbol error correcting capability. We note that (4.17) could be modified for 2^{K_I}-ary block codes.

Consequently we need to evaluate $p_{1|J}$ by brute force. We start by recalling the $p_{1|J}$ is the probability that both decoders error given that the channel was jammed. As before, this is equivalently the probability that the received vector is either a non-zero codeword or lies in the error correction portion of the standard array for the incomplete decoder excluding the coset leaders. We define $\{C'_{ji}\ , i = 1, \ldots, \beta\}$ as the joint 2^{K_I}-ary weight enumerators of all cosets minus coset leaders which have binary weight j coset leaders. If the inner code is a t bit error correcting code then we define coset 2^{K_I}-ary weight enumerators for $1 \leq j \leq t$.

If the incomplete inner code is used to correct t' or less binary errors, $1 \leq t' \leq t$, then $p_{1|J}$ is given by,

$$p_{1|J} = \sum_{i=1}^{\beta} \left[A_i' + \sum_{j=1}^{t'} C_{ji}' \right] \left(\frac{p}{M-1} \right)^i q^{\beta-i} \tag{4.26}$$

Using (4.7), we complete the derivation of terms necessary to evaluate $P(F_S)$ when 2^{K_I}-ary signalling is used with binary block inner codes and incomplete inner decoder detects and corrects errors.

Bit Error Probability Analysis

The arguments of Section 4.3 for analyzing the bit error probability for binary signalling apply equally to the case of 2^{K_I}-ary signalling. The relationship of $P(F_b)$ to $P(F_S)$ is given by (4.18). We have just completed the analysis of $P(F_S)$ above. We extend (4.19) to the 2^{K_I}-ary signalling case as follows. We let $N'(w,j)$ be the number of β-tuples of 2^{K_I}-ary symbols in the standard array which have 2^{K_I}-ary weight w and result in decoding to a vector which has j information bits in error. Then,

$$P(F_b \mid F_S) = \sum_{j=1}^{K_I} \sum_{w=1}^{\beta} \frac{j}{K_I} N'(w,j) \left(\frac{p}{M-1} \right)^w q^{\beta-w} \tag{4.27}$$

We determine $N'(w,j)$ as well as all the 2^{K_I}-ary weight enumerators of this section via a computer algorithm which simultaneously computes the corresponding values for the binary signalling case. We briefly describe the algorithm in Section 4.5 and give the weight enumerators for codes evaluated in Appendix C.

4.5 Codes Used for Analysis

In this section we describe the linear block codes used as inner codes for analysis of the parallel decoder performance. For the analysis using L-diversity repetition codes as inner codes we used $(32,K_0)$ Reed-Solomon codes and $L = 3,5,7$. We will continue the use of $(32,K_0)$ Reed-Solomon outer codes and thus, will use $(N_I,5)$ linear block codes to allow matching of outer code symbol size to inner code information block size.

The four codes used in the analysis are Code I: $(9,5,d_{\min} = 3)$ code which is a shortened (15,11) Hamming Code; Code II: $(10,5,d_{\min} = 4)$ code which is Code I extended; Code III: $(13,5,d_{\min} = 5)$ code which is a shortened (15,7) BCH code; and Code IV: $(15,5,d_{\min} = 7)$ BCH code. All four codes are evaluated using binary signalling. Code II with $\beta = 2$ and code IV with $\beta = 3$ are also evaluated when 2^{K_I}-ary signalling (M=32) is used. The results are discussed and compared in Chapter 5.

In the remainder of this section we describe each of the four codes listed above. We conclude by briefly describing the software algorithm used to generate the binary and 2^{K_I}-ary weight enumerators defined in Sections 4.3 and 4.4.

Code I: $(9,5,d_{\min} = 3)$

To obtain code I we began with a (15,11) Hamming code which has parity check matrix.

$$H = \begin{bmatrix} 1\,0\,0\,0\,1\,1\,1\,1\,0\,0\,0\,0\,1\,1\,1 \\ 0\,1\,0\,0\,1\,0\,1\,0\,1\,1\,1\,1\,0\,0\,1 \\ 0\,0\,1\,0\,0\,1\,1\,0\,0\,1\,0\,1\,1\,1\,1 \\ 0\,0\,0\,1\,0\,0\,0\,1\,1\,0\,1\,1\,1\,1\,1 \end{bmatrix}$$

In general, shortening of a code is accomplished by setting a number of information bits to zero. The resulting codewords are a subspace of the original code and hence,

the shortened code will have minimum distance at least as great as the original code. The codeword bits set to zero need not be transmitted. Thus, both dimensions of the original code are reduced in the shortened code [7, Section 1.9 and 10, Section 4.3.4].

For the Hamming code given above, we can equivalently eliminate columns from the parity check matrix to achieve the desired shortening. Thus, to obtain $K_I = 5$ we choose to delete 6 columns and arrive at the parity check matrix for code I shown below:

$$H_I = \begin{bmatrix} 1\,0\,0\,0\,1\,1\,1\,0\,0 \\ 0\,1\,0\,0\,1\,0\,0\,1\,0 \\ 0\,0\,1\,0\,0\,1\,0\,1\,1 \\ 0\,0\,0\,1\,0\,0\,1\,0\,1 \end{bmatrix} \tag{4.28}$$

The code and coset weight enumerators for code I are given in Appendix C.

Code II: $(10,5,d_{min} = 4)$

In general, a binary (N,K,d_{min}) code which has an odd d_{min} may be extended to an $(N+1,K,d_{min}+1)$ code by appending an additional parity check to each codeword which is the sum of all other codeword components [1,57]. Thus, we can extend code I by this procedure to obtain a $(10,5,d_{min}=4)$ code which will be named code II. The parity check matrix for code II is shown below.

$$H_{II} = \begin{bmatrix} 1\,0\,0\,0\,0\,1\,1\,1\,1\,1 \\ 0\,1\,0\,0\,0\,1\,1\,1\,0\,0 \\ 0\,0\,1\,0\,0\,1\,0\,0\,1\,0 \\ 0\,0\,0\,1\,0\,0\,1\,0\,1\,1 \\ 0\,0\,0\,0\,1\,0\,0\,1\,0\,1 \end{bmatrix} \tag{4.29}$$

Since $(N_I/K_I) = 2 = \beta$ an integer, code II may be used with either binary or 2^{K_I}-ary signalling. Both binary and 2^{K_I}-ary code and coset weight enumerators are given for code II in Appendix C.

Code III: $(13,5,d_{min} = 5)$

We obtained code III, a $(13,5 d_{min} = 5)$ code by shortening a (15,7) BCH code. We began with the generator polynomial for the (15,7) code [10, Table 4.7]

$$g(x) = 1 + x^4 + x^6 + x^7 + x^8 \tag{4.30}$$

We shortened the code by setting to zero the two high order information bits when a systematic implementation of the code is used.

That is, if

$$u(x) = b_0 + b_1 x + \cdots + b_{K_I-2} x^{N_I-K_I-1} + b_{K_I-1} x^{N_I-K_I} \tag{4.31}$$

is the polynomial of information symbols, then the systematic form of the code has codewords given by

$$c(x) = [x^{N_I-K_I} u(x)] mod\ g(x) + x^{N_I-K_I} u(x) \tag{4.32}$$

Thus, by setting $b_{K_I-2} = b_{K_I-1} = 0$ we obtain a simple shortening of the code. The code could be simply decoded by inserting two zeros at the receiver and using standard BCH decoding procedures. See Appendix C for code and coset weight enumerators.

Code IV: $(15,5,d_{min} = 7)$

The final code used to evaluate the parallel decoder is the $(15,5 d_{min} = 7)$ BCH code which has generator polynomial [10, Table 4.7]

$$g(x) = 1 + x + x^2 + x^4 + x^5 + x^8 + x^{10} \tag{4.33}$$

We used the systematic implementation given by (4.32) for cases of both binary and 2^{K_I}-ary signalling. The weight enumerators for both cases are given in Appendix C.

Generation of Code/Coset Weight Enumerators

Evaluation of the parallel decoding system with binary linear block codes using the analysis of this chapters requires knowledge of binary and 2^{K_I}-ary weight enumerators for codes, coset leaders, and cosets as well as a matrix of bit errors which result from given weight error vectors. Below we give a brief description of the computer algorithm used to generate this data, results are given in Appendix C.

Step I: Create a $1 \times 2^{N_I} - 1$ array of bits which may be addressed or masked as needed. This array corresponds to the $2^{N_I} - 1$ non-zero N_I-tuples which occupy the standard array. The address of each bit is its decimal position in the array. Set all bits to zero, call this the check-off array

Step II: Read in a $(2^{K_I} - 1) \times N_I$ array of bits where each row is a codeword. As each codeword is read in perform the following tasks:

(1) Determine binary and 2^{K_I}-ary weights and add to code weight enumerator tallies.

(2) Convert the N_I-tuple to a decimal number and change zero to one in the corresponding bit of the check-off array.

(3) Determine the number of bit errors associated with the codeword (assuming a zero codeword sent) and store in an array indexed to the codeword array.

Step III: Let t be as given in (4.9), in succession generate all binary weight 1,2, . . . , t N_I-tuples. As each N_I-tuple (i.e., a coset leader) is formed do the following:

(1) Determine binary and 2^{K_I}-ary weights and add to coset leader weight enumerator tallies.

(2) Perform step II(2).

(3) In sequence add the coset leader bit-by-bit to each codeword performing the following on the sum vector.

(a) Step II(2).

(b) Determine binary and 2^{K_I}-ary weights and

(i) Add to joint coset leader enumerator tallies

(ii) Using the bit error index of the codeword increment the $N(w,j)$ and $N'(w,j)$ tallies

Note: At this point we have accounted for weights and bit errors associated with all codewords and *a priori* known coset leaders. The remaining zero bits of the check-off array are the N_I-tuples with which the standard array must be completed. Of course, we want minimum weight coset leaders.

Step IV: Search the check-off array for zero bits. If that position's binary equivalent is a binary weight $t+1$ N_I-tuple then performs steps III(1), III(2), III(3) for that vector. Continue to search the check-off array for binary weight $t+1$ N_I-tuples each time repeating steps III(1), III(2), III(3) when a vector is found. When the search is complete go to step V.

Step V: Repeat step IV for binary weight $t+2$, then $t+3$, etc. N_I-tuples. When a pass is made through the check-off array and all bits are one, the algorithm is complete.

CHAPTER 5

COMPUTER ANALYSES AND PERFORMANCE CURVES

5.1 Introduction

In this chapter we present the results of computer evaluation of the performance of the parallel decoding schemes described and analyzed in the previous chapters. Reed-Solomon codes are used exclusively for the outer codes; the decoders are distinguishable by the techniques used in the inner decoders. We initially consider each of the decoding schemes individually and present results for various values of thresholds and coding parameters. Subsequently, we compare performance across the different inner decoding schemes.

Our assumptions remain those which are described in the earlier chapters. Transmission is accomplished using an M-ary ($M \geq 2$) orthogonal signal set, slow frequency-hopping, and noncoherent processing of received signals. The receiver is synchronized to the hopping pattern; each symbol is received with energy E_S in a noise environment which consists solely of partial band jamming of power density $\rho N_J / \rho$ in a fraction ρ of the hopping bandwidth. The primary performance measure is the decoded bit error probability which is analyzed as a function of the energy per information bit-to-jammer noise ratio E_b/N_J versus the percentage of jammed bandwidth ρ.

In Section 5.2 we describe the methods used to calculate the per information bit related performance statistics as a function of received symbol energy to jammer noise power ratios. We also describe the technique for normalizing the coding rates to allow proper comparison of the different decoding techniques. In Sections 5.3 and 5.4 we present the results of the computer analyses and draw conclusions regarding the relative merits of the parallel decoding techniques.

5.2 Normalizing Rates and SNRs

The parallel decoding systems described in this paper use concatenated error-correcting codes where the outer code is an (N_O,K_O) Reed-Solomon code and the inner code has dimensions (N_I,K_I). The computer analyses used to evaluate decoder performance evaluated the received symbol signal-to-jammer noise ratio necessary to achieve a specified bit error rate for given values of ρ, the percentage of bandwidth jammed. The energy per information bit-to-jammer noise ratio is calculated from the received symbol signal-to-jammer noise ratio, E_S/N_J, as follows.

$$\frac{E_b}{N_J} = \frac{E_S}{N_J}\left(\frac{X \text{ received symbols}}{1 \text{ outer code symbol}}\right)\left(\frac{N_O \text{ outer code symbols}}{K_O \text{ information symbols}}\right)\left(\frac{1 \text{ information symbol}}{\log_2 M \text{ information bits}}\right)$$

where X is a quantity dependent on the selected inner code. For the case of L-ary repetition codes, $X = N_I = L$. When binary block inner codes are used with M-ary signalling by the scheme described in Section 4.4, $X = \beta = N_I/K_I$. Finally, when binary block codes are used with binary signalling as described in Section 4.3, E_S is equivalently the received energy per transmitted bit and $X = N_I$ received bits per outer code symbol. Hence, we arrive at the following two forms for relating received signal-to-noise ratio to information signal-to-noise ratio per bit.

$$\frac{E_b}{N_J} = \frac{E_S}{N_J} \frac{1}{R_I R_O \log_2 M} \text{ (M-ary signalling)} \tag{5.1}$$

$$\frac{E_b}{N_J} = \frac{E_S}{N_J} \frac{1}{R_I R_O} \text{ (binary signalling)} \tag{5.2}$$

where $R_I = K_I/N_I$ and $R_O = K_O/N_O$ are respectively the code rates for the inner and outer codes and for (5.2) we used the fact that $K_I = \log_2 M$.

In the next two sections we present performance curves and discuss the analyses of the various decoding algorithms. We will initially be concerned with individual decoder performance as a function of threshold values and a code parameters. Secondly, we will compare the relative performance of the decoding systems. Since the various coding schemes transmit different numbers of symbols (or bits) per information symbol, we must be careful to make a fair comparison.

Pursley and Stark [12] provide a proper basis for comparing the performance of two different coded systems. They suggest that the following parameters be held constant in any comparison: energy per information bit E_b, RF bandwidth, information bit rate, and total interference power.

Our analysis has been predicated on maintaining total interference power through the definition of the partial band jamming environment. The jammer power was defined as N_J/ρ where the percentage of bandwidth jammed is ρ. Thus, the total interference power for any jamming environment is $\rho(N_J/\rho) = N_J$.

To yield a fair comparison restraining all of the parameters suggested by Pursley and Stark, we should compare systems which have the same overall information rate, R, in bits per dimension. Given the inner and outer code dimensions described above, we can make a simple extension of the results in [12] to arrive at the following expression of information rate in bits per dimension for the parallel decoding systems

described in this paper:

$$R = \frac{R_I' R_O \log_2 M}{D} \tag{5.3}$$

where D is the dimensionality of the transmitted orthogonal signal set and R_I' is the code rate of the inner code in outer code symbols per transmitted symbol. $R_I' = 1/N_I$ for binary signalling and K_I/N_I for M-ary signalling. We note that the definition of R_I' is necessary to deal with the special blocking of inner code input block length to match the outer code symbol size.

5.3 Results of Computer Analyses

In this section we discuss the results of computer analyses of the performance of the parallel decoding schemes which are defined in Chapters 3 and 4. As described above, the primary performance measure of interest is the ratio of the average received energy per information bit to jammer noise power required to obtain a given bit error rate for a specified percentage of frequency hopping bandwidth jammed. All of the analyses were performed based on achieving a bit error probability of 10^{-4}. The values of P_b and corresponding E_b/N_J were calculated for all values of $\rho \geq \rho^*$ where ρ^* is that value of ρ for which 10^{-4} bit error probability is achieved with $(E_b/N_J) = 1$ (i.e., $0dB$).

To allow easy reference, all performance curves are grouped together in Section 5.4 at the end of this chapter. Labeling of the curves follows the following conventions detailed in Figure 5.1. Particular parameters, such as threshold values, and identification of special cases are indicated with the graph labeling.

Before discussing the performance of the individual decoders, some general comments on the desired performance are in order. We have defined ρ^* as that value of

ρ for which the decoder achieves the desired bit error rate with a received E_b/N_J of $0dB$. It will be seen that the slope of the performance curves approach 90° in the vicinity of ρ^*, hence, for $\rho < \rho^*$ the specified bit error rate is achieved independent of the jammer power. Similarly, we let ENR^* be the maximum value of E_b/N_J over $0 \leq \rho \leq 1$ which will guarantee the required bit error rate in partial band Gaussian noise. For any encoder, the optimum performance is provided by the decoder which provides the largest value of ρ^* and the smallest value of ENR^*.

In Figures 5.2 through 5.5 we show the performance curves for Algorithm A using Viterbi thresholding. The decoder for this algorithm was described and analyzed in Section 3.2. We note that for both the single and double Reed-Solomon decoder configurations, the uniformly optimum performance occurs when the ratio threshold is set at $\theta = 1.0$. However, this is the case when neither the ratio thresholding or the incomplete decoder thresholding is used. The optimum performance for the double Reed-Solomon decoder is superior to the single Reed-Solomon decoder for $L=5$ (Figure 5.4, curves a and c) and $L=7$ (Figure 5.5, curves a and b) and equivalent for $L=3$ (Figure 5.3, curve a).

When θ is set at other than 1.0, the optimum performance for the double Reed-Solomon decoder occurs for $\theta_q = L$. For this case the incomplete decoder does not use the quality bit and the ratio threshold test is unnecessary. For $L=7$, (Figure 5.5, curve a) the performance varied by less than $.1dB$ for all values of θ. Different threshold settings resulted in variations in performance for the single Reed-Solomon decoder configuration, but, in all cases the $\rho = 1.0$ curve was equal or superior.

The evaluation of the parallel decoder using algorithm B with Viterbi thresholding (Section 3.3), is illustrated in Figures 5.6 through 5.10. In Figures 5.6 and 5.7 we

Decoder A: Viterbi Thresholding, Algorithm A

A_1 = Case: one Reed-Solomon decoder configuration

A_2 = Case: two Reed-Solomon decoder configuration

Decoder B: Viterbi Thresholding, Algorithm B

B_1 = Case: one Reed-Solomon decoder configuration

B_2 = Case: two Reed-Solomon decoder configuration

Decoder C: Repetition Thresholding

Decoder D: Tie Thresholding

Decoder E: Hard Decisions/Perfect Side Information

Decoder I(c): (9,5) Shortened Hamming, Binary Signalling; Correct c bit errors, c =0,1

Decoder IIb(c): (10,5) Code (Extension of I), Binary Signalling; Correct c bit errors, c =0,1

Decoder IIm(c): (10,5) Code (Extension of I), M-ary Signalling; Correct c bit errors, c =0,1

Decoder III(c): (13,5) Shortened BCH Code, Binary Signalling; Correct c bit errors, c =0,1,2

Decoder IVb(c): (15,5) BCH Code, Binary Signalling; Correct c bit errors, c =0,1,2,3

Decoder IVm(c): (15,5) BCH Code, M-ary Signalling; Correct c bit errors, c =0,1,2,3

Notes:

(1) Unless otherwise indicated, all curves are for a (32,16) Reed-Solomon outer code.

(2) All results except for A_1 and B_1 are for the parallel decoder configuration with two Reed-Solomon decoders.

(3) Other parameters are indicated with the graph labeling.

Figure 5.1 Labeling of Performance Curves

show the performance curves for $L=5$, $L=7$ and respectively the double and single Reed-Solomon decoder systems. The single Reed-Solomon decoder system has uniformly optimum performance for $\theta = 1.0$. However, for the double Reed-Solomon decoder configuration, we see that optimum ENR^* is provided by the $\theta = 1.0$ decoder, and the optimum ρ^* occurs with $\theta = 2.0$.

The curves for $L=3$ and $L=7$ are similar and are not presented. Rather, in the somewhat busy graphs of Figures 5.8 and 5.9 we show minimum and maximum performance curves for each decoder configuration and diversity length. We note that in both cases the value of ρ^* increases as L increases. The values of ENR^* should be compared only for the same value of L since the system code rates are not equivalent. Finally, in Figure 5.10 we show that the maximum and minimum performance of the double Reed-Solomon decoder configuration are superior to the same curves for the single Reed-Solomon decoder system for $L=5$. Again, these results are typical of the $L=3$ and $L=7$ performance curves.

At this point in the research we decided to concentrate the investigation on parallel decoding systems which use two or more Reed-Solomon decoders. Unless stated otherwise, all results and discussions which follow are relative to the two Reed-Solomon decoder configuration.

In Figures 5.11, 5.13, and 5.15 we plot the performance curves respectively for the $L=3$, $L=5$, and $L=7$ hard decision, perfect side information decoders and the repetition threshold decoders. In each case the perfect side information decoder has the optimum ρ^* and the $T=2$ (and $T=3$ for $L=7$) repetition threshold decoder has the best ENR^*. Amongst the repetition threshold decoders, the $T=2$ threshold setting provides uniformly optimum performance.

In Figures 5.12, 5.14. and 5.16 we show the effect of the Reed-Solomon code rate on the performance of the perfect side information and repetition threshold decoders. For $L=3$, 5, and 7 respectively, each graph plots the optimum curve for the ratio threshold and perfect side information decoders for (32,8), (32,16), and (32,24) Reed-Solomon outer codes. The general observation is that ρ^* and ENR^* both increase as code rate decreases.

In Figure 5.17 we give a different perspective on the parallel decoder performance by plotting the relationship of the input symbol error probability to the output bit error probability. The curves of Figure 5.17 are the best and worse cases for the repetition threshold decoder when the diversity is 3, 5, and 7. The separation between the best and worst case curves decreases as L increases. We postulate that for large L the effect of the threshold setting will become negligible.

The last of the proposed decoders for the L-diversity repetition inner codes uses the tie thresholding algorithm described in Section 3.6. In Figure 5.18 we plot the performance of the parallel decoder using tie thresholding for $L=3$, 5, and 7 as well as the curves for the respective perfect side information. The tie threshold decoder yields nearly identical performance at 10^{-4} bit error rate as the optimum repetition threshold decoder. For $L=3$, the two decoders perform identically. At $L=5$, the tie threshold decoder curve lies below the optimum repetition threshold decoder by less than $.05dB$. At $L=7$ the difference increases to about $0.5dB$. The difference would be barely noticeable if plotted on a curve such as Figure 5.18. However, we note in Figure 5.19 that as the required output bit error probability decreases the advantage of the tie threshold decoder becomes more significant.

In Tables 5.1 and 5.2 we chart values of ρ^* and ENR^* for various parallel decoder configurations using linear diversity inner codes. Once again, the superiority of the $\theta = 1.0$ threshold setting is evident for the ratio threshold based decoding algorithms. Similarly the $T = 2$ threshold setting is superior in both ρ^* and ENR^* for the ratio threshold decoding algorithm. Decoder F is a soft decisions perfect side information decoder with linear diversity inner codes. These results were provided by Stark and the analysis for such decoding schemes is described in [12]. We note that the ρ^* value is equal to the case for hard decisions with perfect side information, decoder E while the ENR^* values are approximately $2dB$ lower for soft decisions. These observations are consistent for different Reed-Solomon code rates and bit error rates.

We now consider the performance curves for the case of binary linear block inner codes as described in Chapter 4. In Figures 5.20 through 5.23 we present results when the decoders are used with binary channel signalling and in Figures 5.21 and 5.22 we plot results when M-ary signalling is used. Each incomplete decoder may be used in either error detection only mode or in combined error detection/error correction mode. We indicate the number of bit errors corrected by each incomplete decoder in parentheses following the decoder identifier, e.g., II(0). Decoders II and IV allow for both binary and M-ary channel signalling and the labeling is annotated by b or an m (e.g., IIb (1)) to identify the decoder application.

In Figure 5.20 we plot performance curves for the case when the inner code is a (9,5) shortened Hamming code and the outer code is a (32,8), (32,16), or (32,24) Reed-Solomon code and binary channel signalling is used. In each case, the inner decoder used in error detection only mode is uniformly superior to the single bit error

Decoder	L	θ	θ_1	ρ^*	$ENR^*(dB)$
A_1	3	1.0	--	.345	8.00
	3	2.0	3	.324	8.27
	5	1.0	--	.391	9.63
	5	2.0	5	.376	12.37
	7	1.0	--	.419	10.77
	7	2.0	7	.419	10.77
A_2	3	1.0	--	.345	8.00
	3	2.0	3	.324	8.26
	5	1.0	--	.436	9.38
	5	2.0	5	.436	9.18
	7	1.0	--	.522	9.82
	7	2.0	7	.522	9.84
B_1	3	1.0		.345	7.99
	3	2.0		.346	11.07
	5	1.0		.389	9.64
	5	2.0		.394	12.69
	7	1.0		.419	10.77
	7	2.0		.426	13.79
B_2	3	1.0		.449	6.90
	3	2.0		.422	10.08
	5	1.0		.435	9.18
	5	2.0		.568	10.95
	7	1.0		.523	9.81
	7	2.0		.657	11.69

Table 5.1 Values of ρ^* and ENR^* for Decoders A and B with $(32,16)R$-S Code and $P_b = 10^{-4}$.

Decoder	L	T	ρ^*	$ENR^*(dB)$
C	3	2	.324	8.26
		3	.222	9.87
	5	2	.495	8.63
		3	.435	9.18
		5	.413	9.40
	7	2	.557	9.49
		3	.559	9.49
		7	.521	9.83
D	3		.324	8.22
	5		.492	8.66
	7		.569	9.39
E	3		.623	8.84
	5		.752	9.30
	7		.816	9.83
F	3		.620	6.80
	5		.750	7.36
	7		.820	7.82

Table 5.2 Values of ρ^* and ENR^* for Decoders C,D,E and F with (32,16)R–S Code and $P_b = 10^{-4}$.

correction mode. As the minimum distance of the outer decoder increases so does the ρ^* value for the decoder. However, the (32,16) decoder has the optimum ENR^* value. Moreover, for large values of ρ, the (32,24) code performs best at lower values of ENR. However, this comparison is not perfectly fair since the ENR values are on a per information bit basis and the code rates for the decoders are not equal. We make comparisons of this type later in this section.

Analogous observations may be made for the case when the inner code is a (10,5) Hamming code and binary signalling is used. Performance curves for decoders

using this inner code and the same outer codes listed above are plotted in Figure 5.21. Again the error detection only mode is superior but not uniformly so for the case of a (32,8) $R-S$ outer code. The same relative relationships of performance curves versus outer code minimum distance exists for all the decoder values, hence, we will consider only (32,16) Reed-Solomon outer codes for the next two decoders.

In Figure 5.22 we show the results for the case when the inner code is a (13,5) *BCH* code having minimum distance 5. We plot curves for the cases when the incomplete decoder is used for error detection only [III(0)], single bit error correction [III(1)] and two bit error correction [III(2)]. Although not uniformly superior, the error detection only mode provides the best ρ^* and all *ENR* values are within $.25dB$ of the best curve. Similarly, the performance for the (15,5), $d_{\min} = 7$ *BCH* inner code shown in Figure 5.23 has nearly optimal performance from the error detection only mode. These results are evidence of the Reed-Solomon decoder robustness in correcting up to twice as many erasures as errors.

We can make the same comparative conclusions for the parallel decoder performance when M-ary channel signalling is used. Performance curves for the (10,5) shortened Hamming and (15,5) *BCH* code with M-ary signalling are given respectively in Figures 5.24 and 5.25. We see the same relative performance observed for the binary signalling case except that the received signal-to-noise ratios are between one and two dB lower.

In Table 5.3 we chart values of ρ^* and ENR^* for the parallel decoders using binary linear block inner codes. The given values illustrate the numerical magnitudes of the performance differences discussed above.

In (5.3) we define the parallel decoder information rate in terms of transmitted bits per signalling dimension. We now consider comparison of the different decoding algorithms for systems which have nearly equal information rates. First, in Figure 5.26 we compare the systems which use binary channel signalling. Parings of: (9,5) inner and (32,14) outer codes; (10,5) inner and (32,16) outer codes; (13,5) inner and (32,20) outer codes; and (15,5) inner and (32,24) outer codes give information rates respectively of .121, .125, .120, and .125. The decoder using three bit error correcting with the (15,5) inner code has excellent performance despite having the lowest ρ^* value. The simple error detection only, (9,5) inner code system has the best ρ^* but requires as much a $3dB$ more received signal-to-noise ratio at high values of ρ.

Decoder	ρ^*	$ENR^*(dB)$
I(0)	.277	10.52
I(1)	.154	10.54
IIb(0)	.292	10.45
IIb(1)	.195	10.66
IIm(0)	.291	7.77
IIm(1)	.281	8.97
III(0)	.303	12.20
III(1)	.278	11.92
III(2)	.190	12.26
IVb(0)	.309	10.25
IVb(1)	.300	10.19
IVb(2)	.256	10.19
IVb(3)	.162	11.05
IVm(0)	.306	9.44
IVm(1)	.306	9.41
IVm(2)	.275	9.89
IVm(3)	.160	10.10

Table 5.3 Values of ρ^* and ENR^* for Decoders I, II, III and IV with (32,16)R-S Code and $P_b = 10^{-4}$.

Similarly, we compare the performance of the codes using M-ary channel signalling in Figures 5.27 and 5.28. In this case all codes have information rates which are either .015 or .016 bits per dimension. Surprisingly, the simple $L=7$ tie thresholding and $L=5$, $T=2$ repetition threshold decoders with L-diversity inner codes provide nearly optimum performance. The (10,5) shortened Hamming code seems to yield the best $ENR^* - \rho^*$ compromise.

We conclude this section by analyzing the assumption that the parallel Reed-Solomon decoders will fail rather than output an erroneous symbol. In Section 2.6 we derive a bound on the probability of joint Reed-Solomon decoder error, PDE, which is the sum of the probabilities that each of the individual decoders error. To evaluate (2.23) and (2.27) we require knowledge of the symbol error and erasure statistics at the input to each of the Reed-Solomon decoders. These values may be easily determined using the joint probabilities $p_1, \ldots, p_6$ which were derived to calculate bit decoder error probabilities. We note that for the incomplete decoder channel:

$$\begin{aligned} P(\text{error}) &= p_1 + p_4 \\ P(\text{erasure}) &= p_2 + p_5 \\ P(\text{correct}) &= p_3 + p_6 \end{aligned}$$

and for the complete decoder channel:

$$\begin{aligned} P(\text{error}) &= p_1 + p_2 + p_3 \\ P(\text{correct}) &= p_4 + p_5 + p_6 \end{aligned}$$

In Tables 5.4 and 5.5 we give results of the analysis of the bound on joint decoder error probability. We note that in many cases the Reed-Solomon decoder in

Decoder	L	θ	θ_2	T	ρ	PDE_1	PDE_2	PDE
A_2	3	1.0	2		.345	.318E-31	.165E-08	.165E-08
	3	1.0	2		.730	.487E-32	.720E-10	.720E-10
	3	2.0	2		.329	.334E-18	.116E-08	.116E-08
	5	1.0	2		.436	.440E-43	.847E-11	.847E-11
	5	1.0	2		.890	.440E-43	.842E-11	.842E-11
	5	2.0	5		.436	.675E-29	.909E-11	.909E-11
	7	1.0	2		.522	.655E-55	.195E-11	.195E-11
	7	1.0	2		1.000	.651E-55	.200E-11	.200E-11
	7	2.0	4		.522	.380E-47	.195E-11	.195E-11
B_2	3	1.0			.449	.192E-15	.233E-11	.233E-11
	3	1.0			.880	.193E-15	.240E-11	.240E-11
	3	2.0			.421	.219E-40	.408E-11	.408E-11
	3	2.0			.760	.584E-53	.323E-11	.323E-11
	5	1.0			.434	.643E-29	.789E-11	.789E-11
	5	1.0			.870	.670E-29	.889E-11	.889E-11
	5	2.0			.568	.000E+00	.170E-11	.170E-11
	7	1.0			.523	.560E-41	.192E-11	.192E-11
	7	1.0			1.000	.559E-41	.195E-11	.195E-11
	7	2.0			.657	.000E+00	.165E-11	.165E-11
C	3			2	.324	.630E-17	.105E-08	.105E-08
	3			2	.650	.638E-17	.106E-08	.106E-08
	3			3	.221	.239E-49	.175E-11	.175E-11
	5			2	.495	.148E-10	.381E-09	.396E-09
	5			2	1.000	.148E-10	.381E-09	.396E-09
	5			5	.413	.000E+00	.165E-11	.165E-11
	7			2	.558	.265E-08	.305E-10	.269E-08
	7			2	1.000	.279E-08	.322E-10	.282E-08
	7			7	.521	.000E+00	.166E-11	.166E-11
D	3				.324	.573E-33	.172E-19	.172E-19
	3				.630	.798E-38	.452E-25	.452E-25
	3				1.000	.194E-41	.285E-29	.285E-29
	5				.492	.598E-26	.243E-20	.243E-20
	5				1.000	.219E-36	.140E-31	.140E-31
	7				.570	.315E-24	.292E-21	.293E-21
	7				1.000	.183E-36	.863E-34	.864E-34
E	3				.623	.000E+00	.681E-18	.681E-18
	3				.830	.000E+00	.202E-34	.202E-34
	3				1.000	.000E+00	.198E-37	.198E-37
	5				.750	.000E+00	.628E-18	.628E-18
	5				1.000	.000E+00	.361E-38	.361E-38
	5				.840	.000E+00	.146E-27	.146E-27
	5				.816	.000E+00	.809E-18	.809E-18
	7				1.000	.000E+00	.143E-38	.143E-38

Table 5.4 Reed-Solomon Decoder Error Probabilities for L-Diversity Inner Codes With (32,16) R-S Outer Code.

Decoder	ρ	PDE_1	PDE_2	PDE
I(0)	.27700	.122E-14	.504E-07	.504E-07
	.51000	.153E-18	.335E-07	.335E-07
	1.00000	.836E-24	.719E-07	.719E-07
I(1)	.15400	.557E-07	.558E-09	.563E-07
	.31000	.566E-06	.605E-08	.572E-06
	1.00000	.147E-04	.145E-06	.149E-04
IIb(0)	.29200	.143E-17	.714E-07	.714E-07
	.52000	.210E-21	.176E-06	.176E-06
	1.00000	.141E-30	.787E-06	.787E-06
III(0)	.30300	.150E-26	.894E-07	.894E-07
	.48000	.739E-33	.143E-07	.143E-07
	1.00000	.335E-47	.554E-07	.554E-07
III(2)	.19000	.297E-08	.328E-08	.626E-08
	.36000	.105E-07	.134E-07	.240E-07
	1.00000	.521E-07	.764E-07	.129E-06
IVb(0)	.31000	.204E-32	.103E-06	.103E-06
	.52000	.171E-37	.253E-06	.253E-06
	1.00000	.000E+00	.978E-06	.978E-06
IVb(3)	.16200	.307E-07	.877E-09	.316E-07
	.33000	.114E-05	.398E-07	.118E-05
	1.00000	.337E-05	.114E-05	.4501-05
IIm(0)	.29100	.151E-17	.708E-07	.708E-07
	.50000	.153E-17	.602E-06	.602E-06
	1.00000	.134E-30	.136E-05	.136E-05
IIm(1)	.28100	.641E-16	.569E-07	.569E-07
	.38000	.409E-11	.209E-06	.209E-06
	1.00000	.918E-13	.134E-05	.134E-05
IVm(0)	.30600	.199E-32	.974E-07	.974E-07
	.47000	.104E-33	.524E-06	.524E-06
	1.00000	.000E+00	.139E-05	.139E-05
IVm(3)	.16000	.350E-07	.802E-09	.358E-07
	.30000	.278E-05	.676E-07	.284E-05
	1.00000	.402E-05	.140E-05	.542E-05

Table 5.5 Reed-Solomon Decoder Error Probabilities for Binary Linear Block Inner Codes With (32,16) R–S Outer Code.

the errors and erasures incomplete decoder channel has significantly lower probability of producing and erroneous output. Hence, in these cases performance would be improved by choosing that decoders output in the event the outer decoders produce different symbols. The worst case is for the (9,5) shortened Hamming inner code with single bit error correction which we have already noted is uniformly outperformed by the same decoder with error detection only. Our assumption of negligible Reed-Solomon decoder error probability is vindicated by these results.

We did not perform a computer analysis of the multiple parallel Reed-Solomon decoder configuration. Most of the decoders had a single configuration which was uniformly superior or nearly so. In such situations we could not justify the added complexity of the multiple decoder. In general, the multiple parallel decoder would give at least the performance of the lower envelope of the double parallel decoder curves. We justify this argument by illustration for the case of three parallel decoders. The probability of joint Reed-Solomon decoder error is given by

$$\begin{aligned} P(DE) &= P(DE_1 \bigcap DE_2 \bigcap DE_3) \\ &\leq P(DE_1 \bigcap DE_3) \\ &\leq P(DE_2 \bigcap DE_3) \end{aligned}$$

Hence, since the same symbol error and erasure statistics will exist at the inputs to the Reed-Solomon decoders as do for the double parallel decoders, the multiple parallel decoder system will select the optimum channel output or default to the complete inner decoder.

5.4 Performance Curves

For easy reference we have grouped all of the parallel decoder performance curves at the end of the chapter. Figure 5.1 gives a quick summary of the notation used to identify the different decoding algorithms.

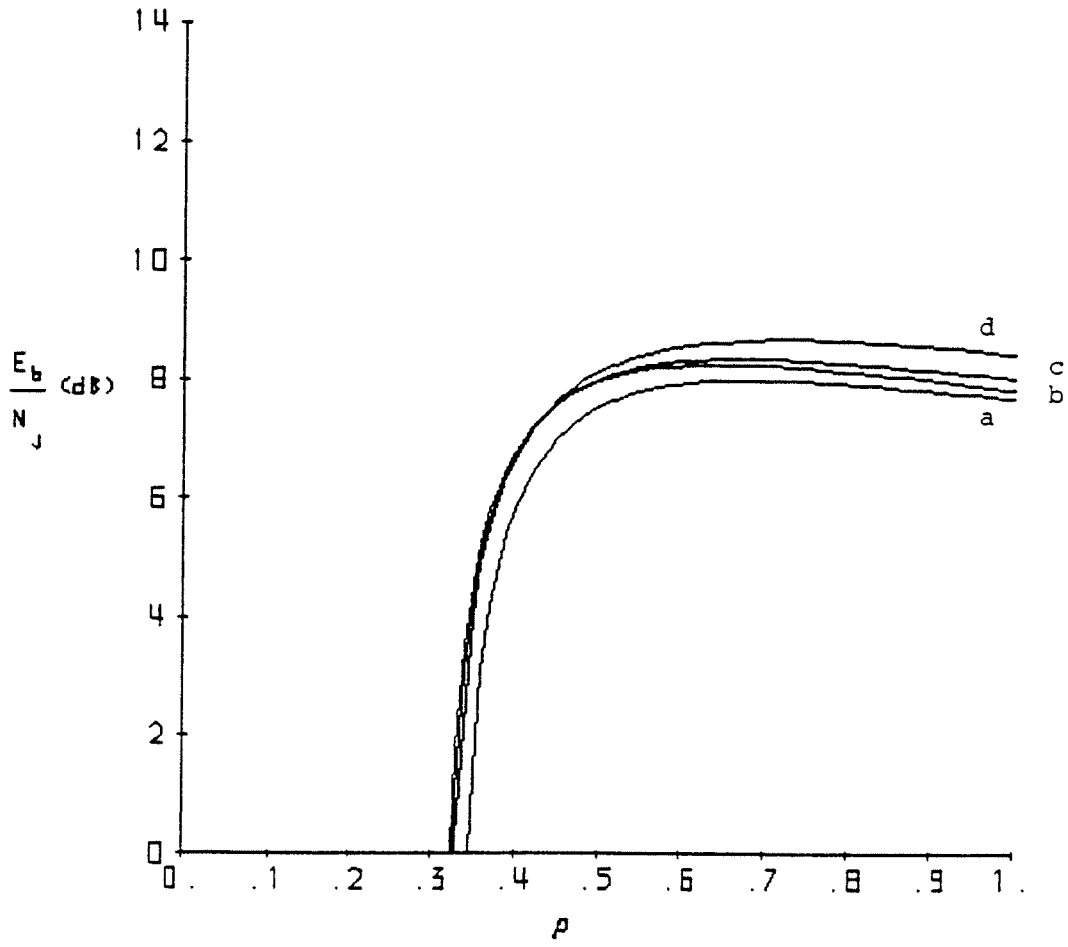

Figure 5.2 $P_b=10^{-4}$, $(32,16)R$-S, Decoder A_2, $L=3$: (a) $\theta=1.0$; (b) $\theta=1.1$, $\theta_q=2$ and $\theta \geq 1.1$, $\theta_q=3$; (c) $\theta=1.5$, $\theta_q=2$; (d) $\theta=2.0$; $\theta_q=2$

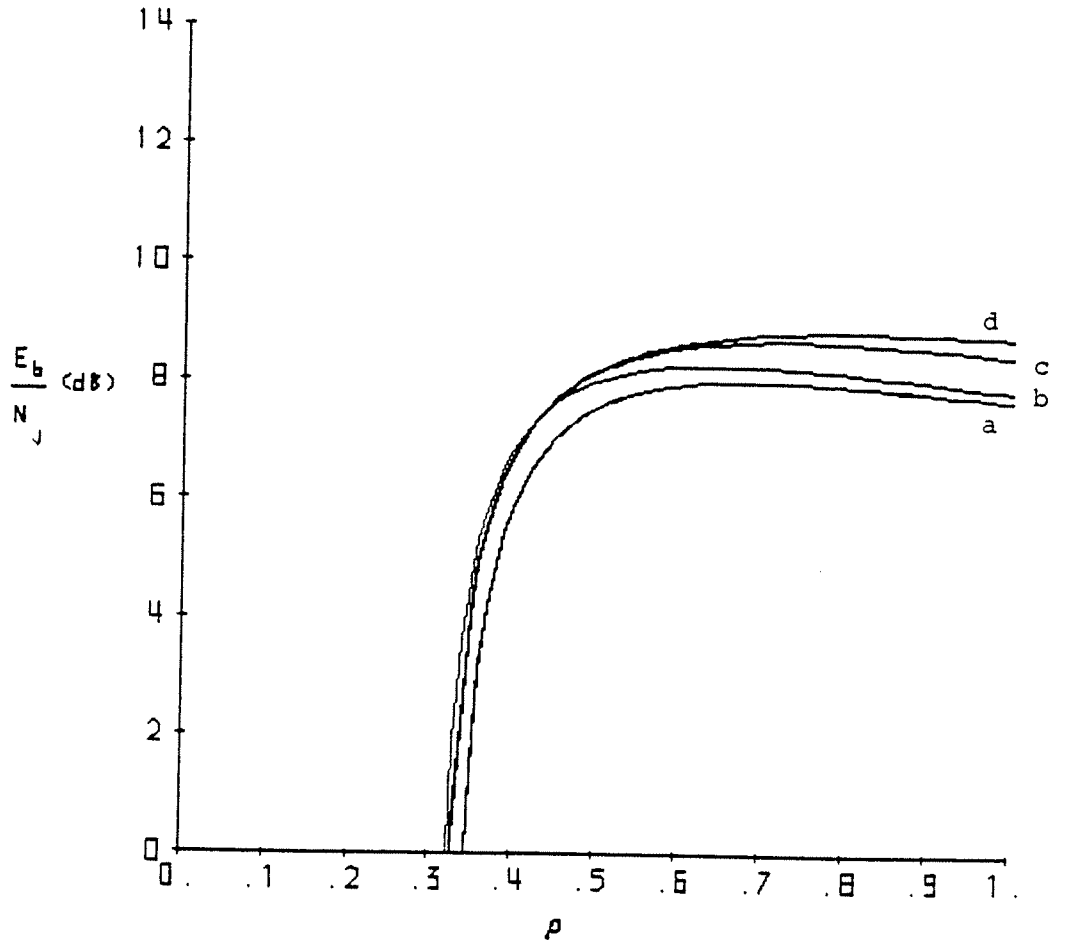

Figure 5.3 $P_b = 10^{-4}$, (32,16)R-S, Decoders A_1 and A_2, $L = 3$: (a) A_1, $\theta = 1.0$ and A_2, $\theta = 1.0$; (b) A_1, $\theta = 1.5$, $\theta_q = 3$; (c) A_2, $\theta = 2.0$, $\theta_q = 2$; (d) A_1, $\theta = 2.0$, $\theta_q = 2$

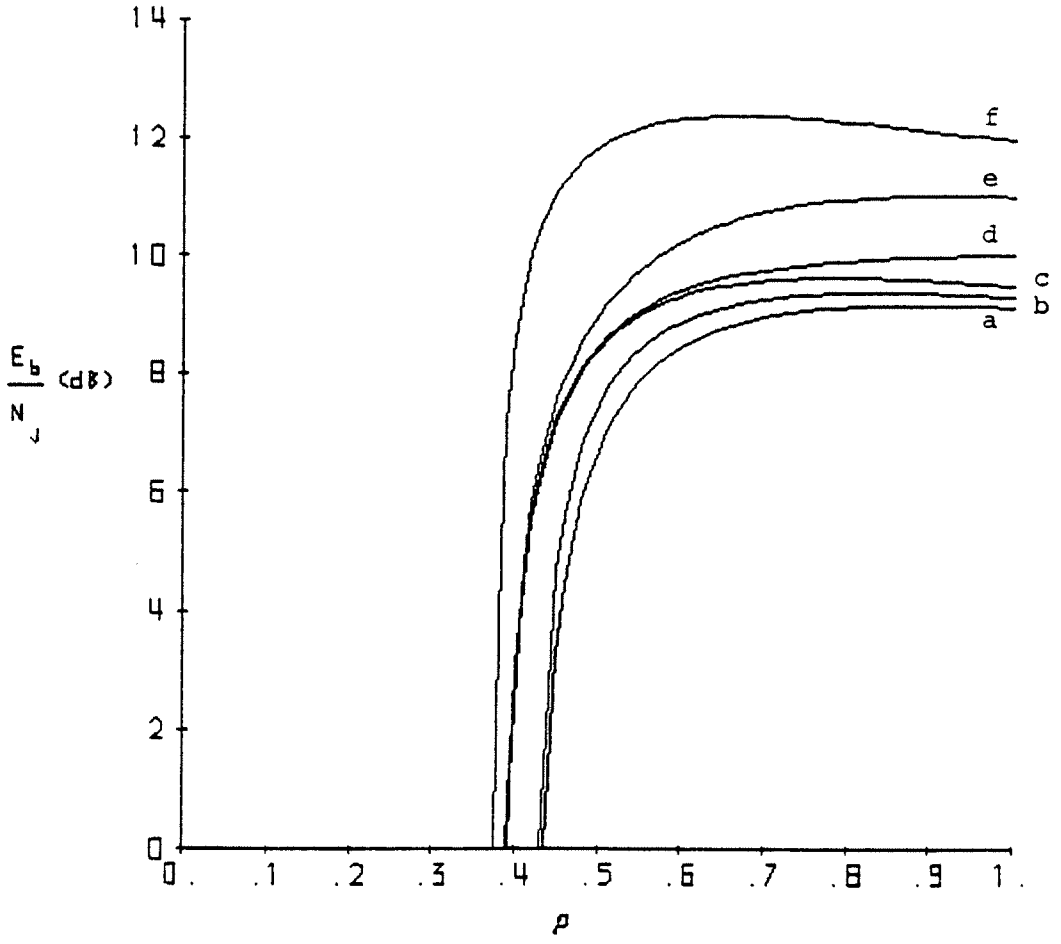

Figure 5.4 $P_b=10^{-4}$, $(32,16)R$-S, Decoders A_1 and A_2, $L=5$: (a) A_2, $\theta=1.0$; (b) A_2, $\theta=2.0$, $\theta_q=5$; (c) A_1, $\theta=1.0$; (d) A_1, $\theta=2.0$, $\theta_q=4$; (e) A_1, $\theta=2.0$, $\theta_q=3$; A_1, $\theta=2.0$, $\theta_q=5$

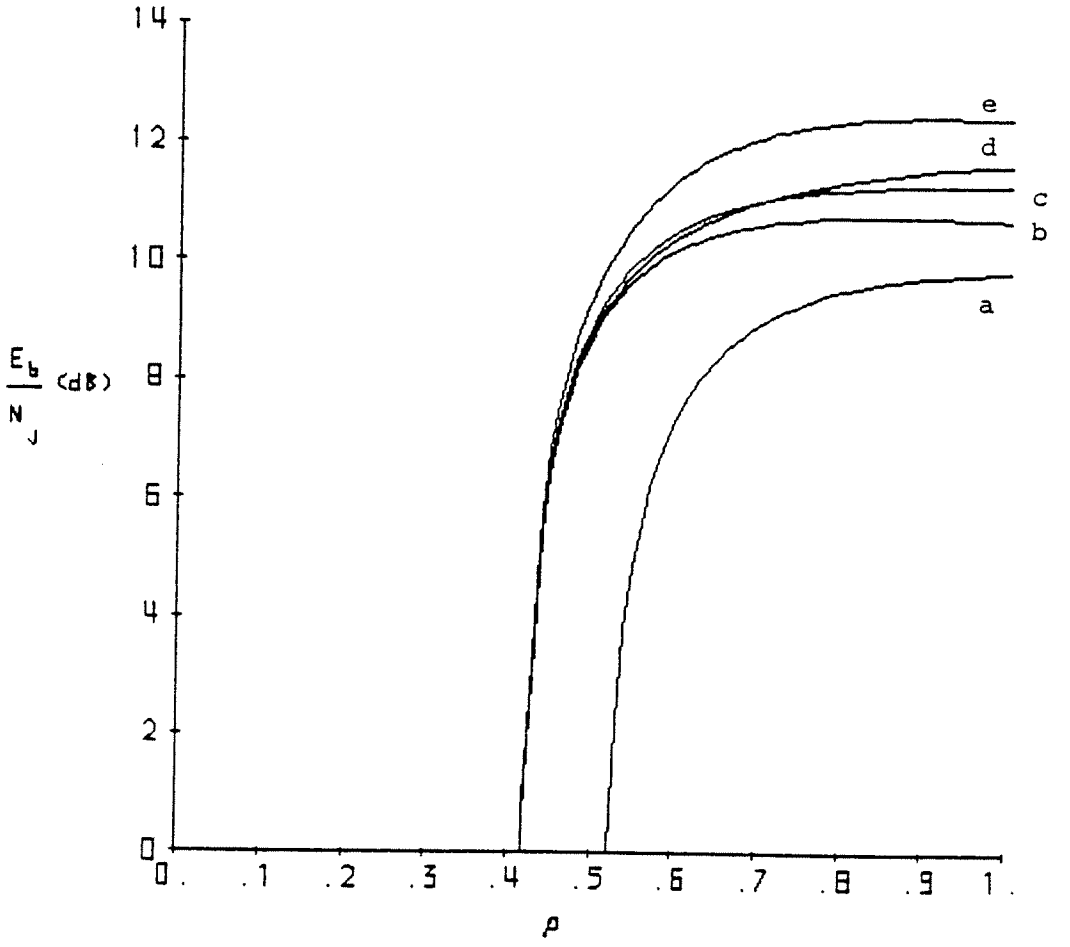

Figure 5.5 $P_b = 10^{-4}$, $(32,16)R\text{-}S$, Decoders A_1 and A_2, $L=7$: (a) A_2, all θ, all θ_q; (b) A_1, $\theta=1.0$; (c) A_1, $\theta=1.5$, $\theta_q=4$; (d) A_1, $\theta=2.0$, $\theta_q=4$; (e) A_1, $\theta=2.0$, $\theta_q=7$

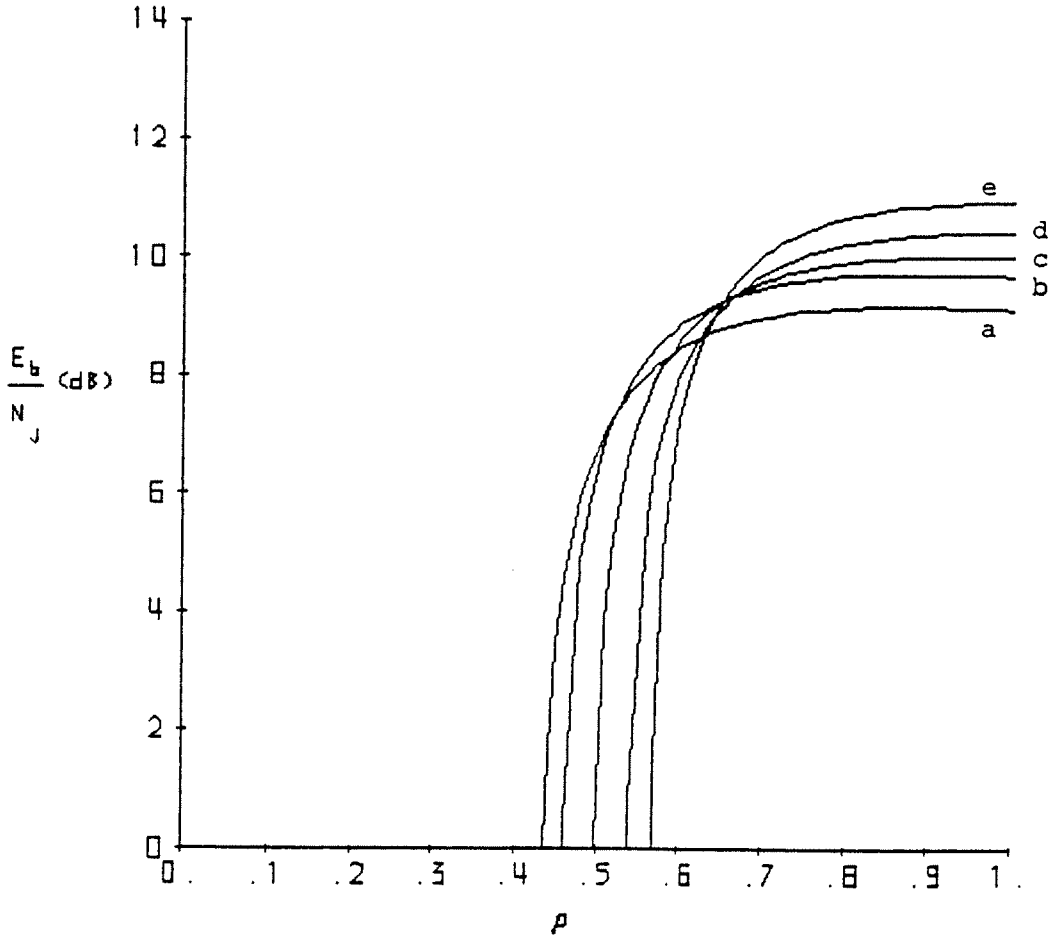

Figure 5.8 $P_b=10^{-4}$, $(32,16)R$-S, Decoder B_2, $L=5$: (a) $\theta=1.0$; (b) $\theta=1.25$; (c) $\theta=1.5$; (d) $\theta=1.75$; (e) $\theta=2.0$

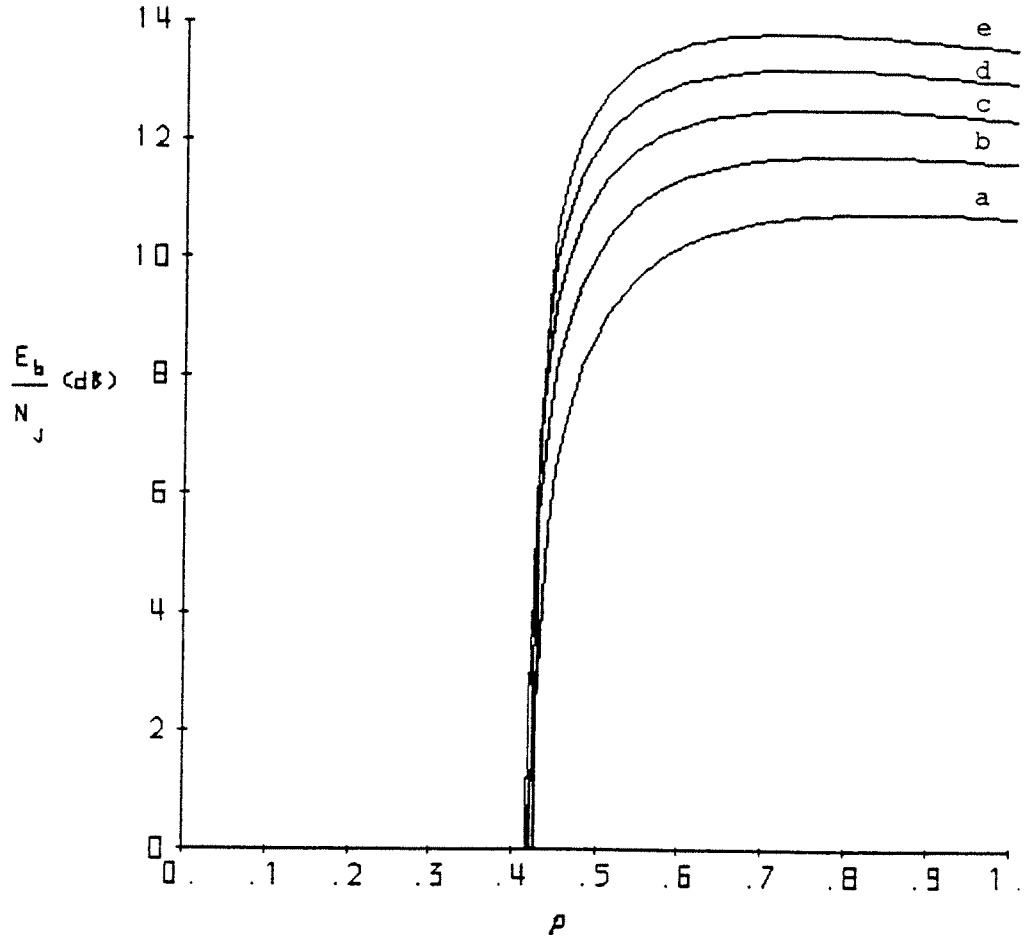

Figure 5.7 $P_b = 10^{-4}$, $(32,16)R\text{-}S$, Decoder B_1, $L = 7$: (a) $\theta_{1.0}$; (b) $\theta_{1.25}$; (c) $\theta_{1.5}$; (d) $\theta_{1.75}$; (e) $\theta_{2.0}$

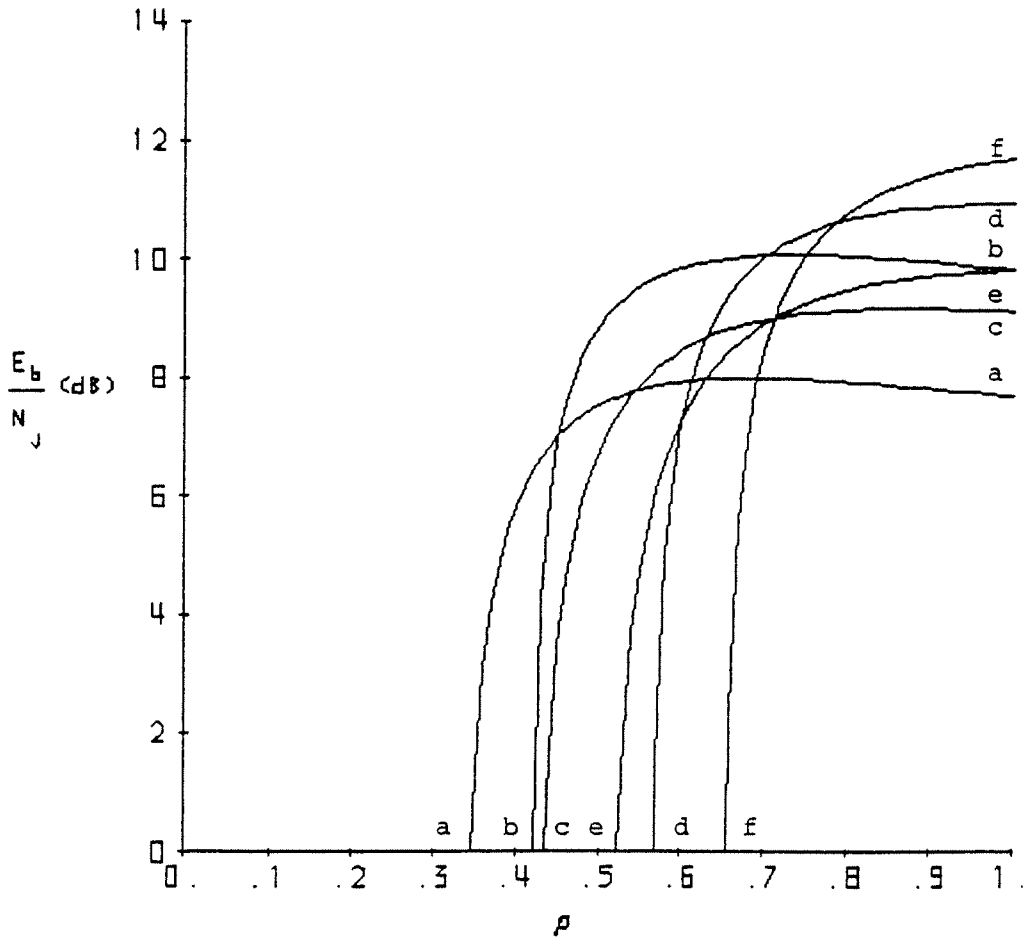

Figure 5.8 $P_b = 10^{-4}$, $(32.16)R$–S, Decoders B_2: (a) $L=3$, $\theta=1.0$; (b) $L=3$, $\theta=2.0$; (c) $L=5$, $\theta=1.0$; (d) $L=5$, $\theta=2.0$; (e) $L=7$, $\theta=1.0$; (f) $L=7$, $\theta=2.0$

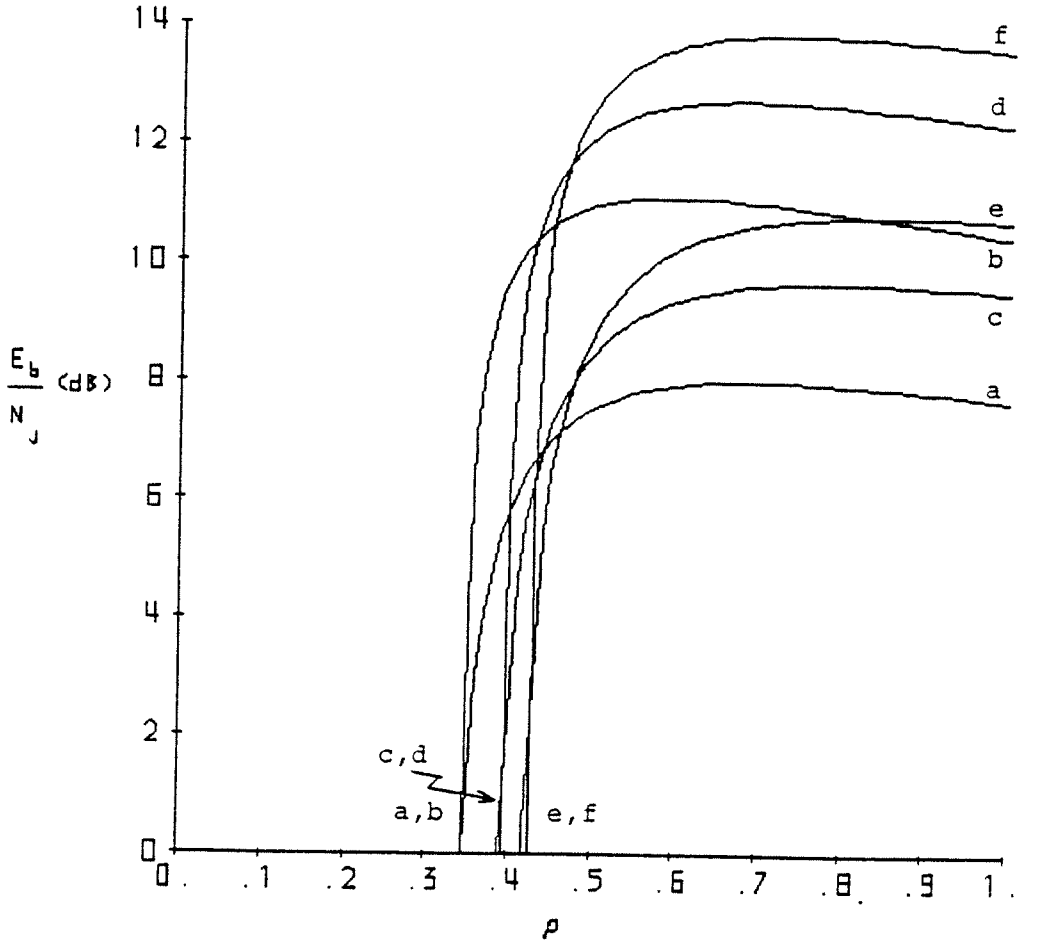

Figure 5.9 $P_b = 10^{-4}$, $(32,16)R\text{-}S$, Decoder B_1: (a) $L=3$, $\theta=1.0$; (b) $L=3$, $\theta=2.0$; (c) $L=5$, $\theta=1.0$; (d) $L=5$, $\theta=2.0$; (e) $L=7$, $\theta=2.0$

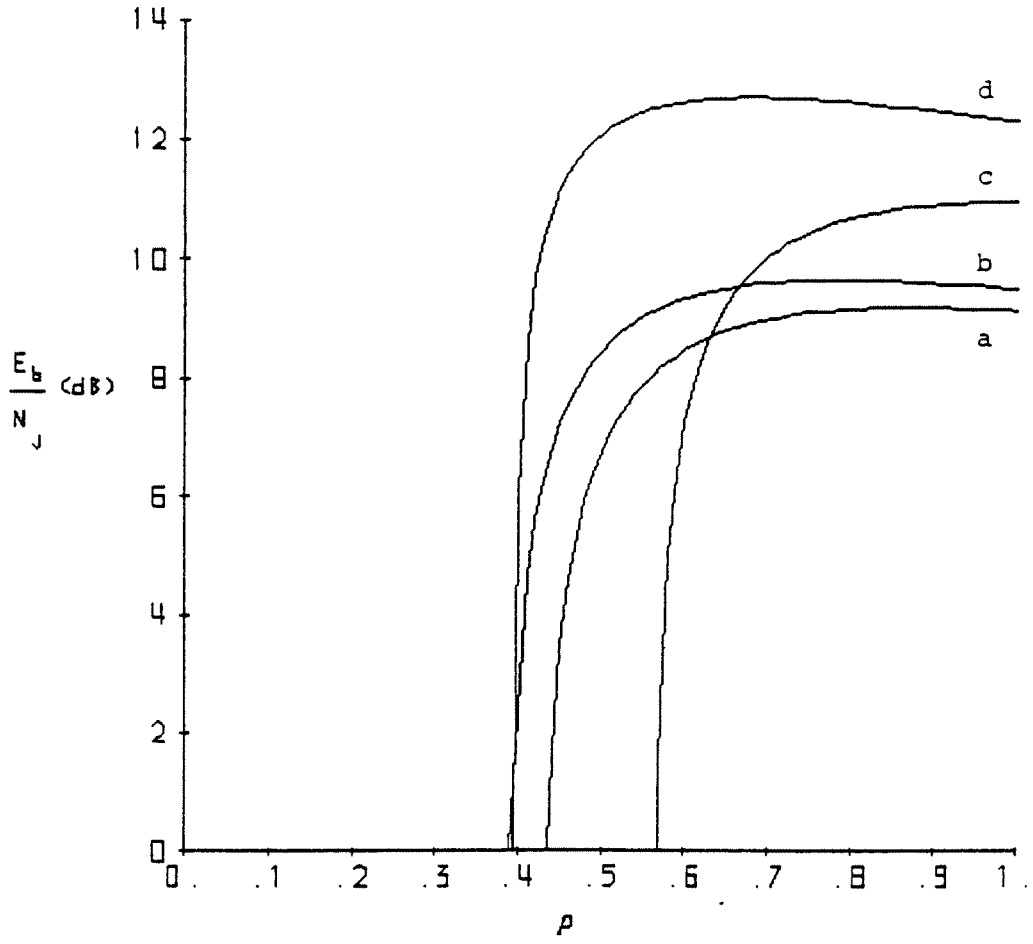

Figure 5.10 $P_b = 10^{-4}$, (32.16)R-S, Decoders B_1 and B_2, $L = 5$: (a) B_2, $\theta = 1.0$; (b) B_1, $\theta = 1.0$; (c) B_2, $\theta = 2.0$; (d) B_1, $\theta = 2.0$

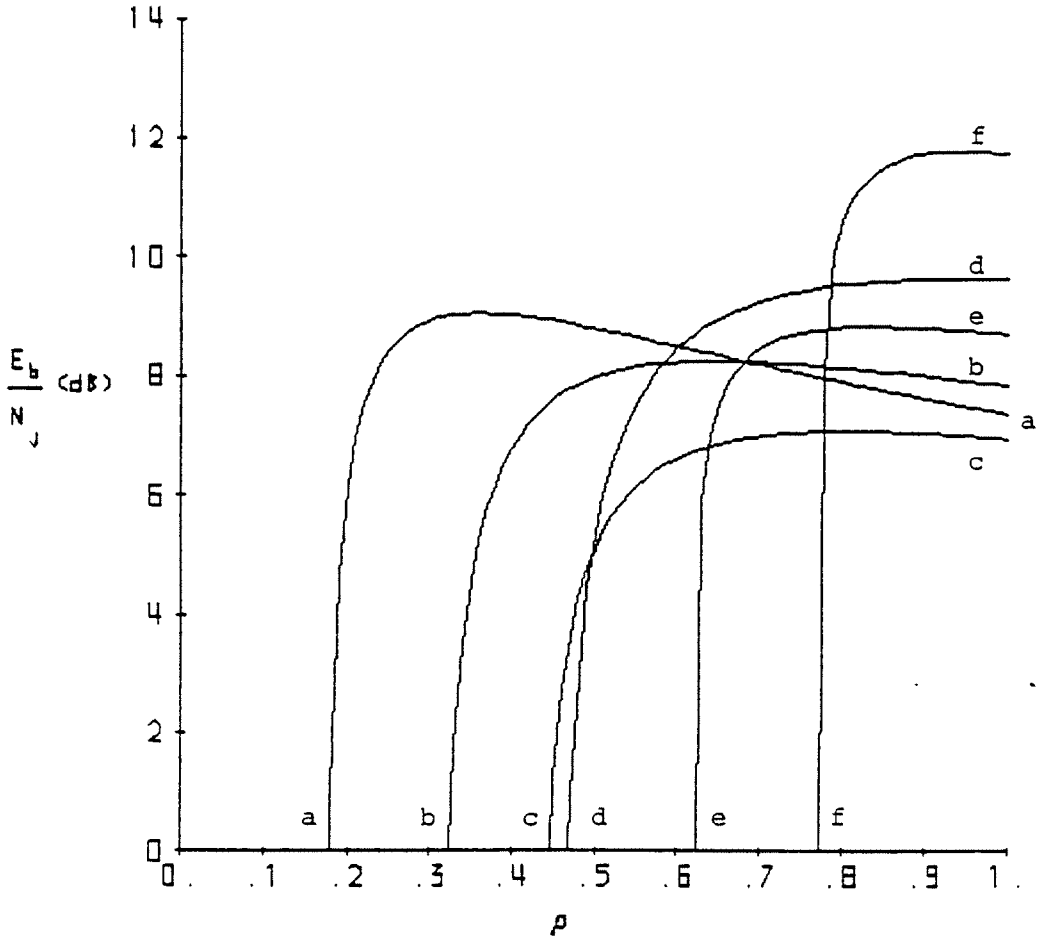

Figure 5.12 $P_b = 10^{-4}$, Decoders C and E, $L = 3$, $T = 2$: (a) C, $(32,24)R$-S; (b) C, $(32,16)R$-S; (c) E, $(32,24)R$-S: (d) C, $(32,8)R$-S; (e) E, $(32,16)R$-S; (f) E, $(32,8)R$-S

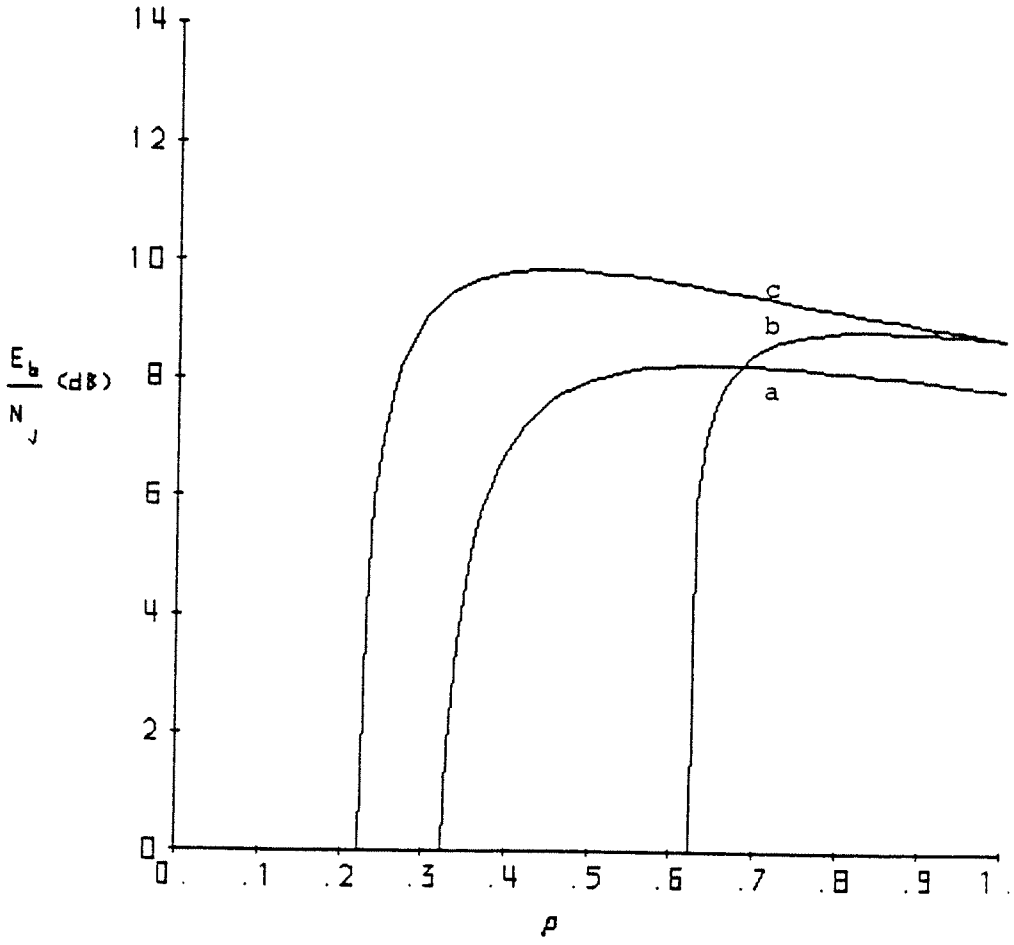

Figure 5.11 $P_b = 10^{-4}$, $(32,16)R$-S, Decoders C and E, $L = 3$: (a) C, $T = 2$: (b) E; (c) C, $T = 3$

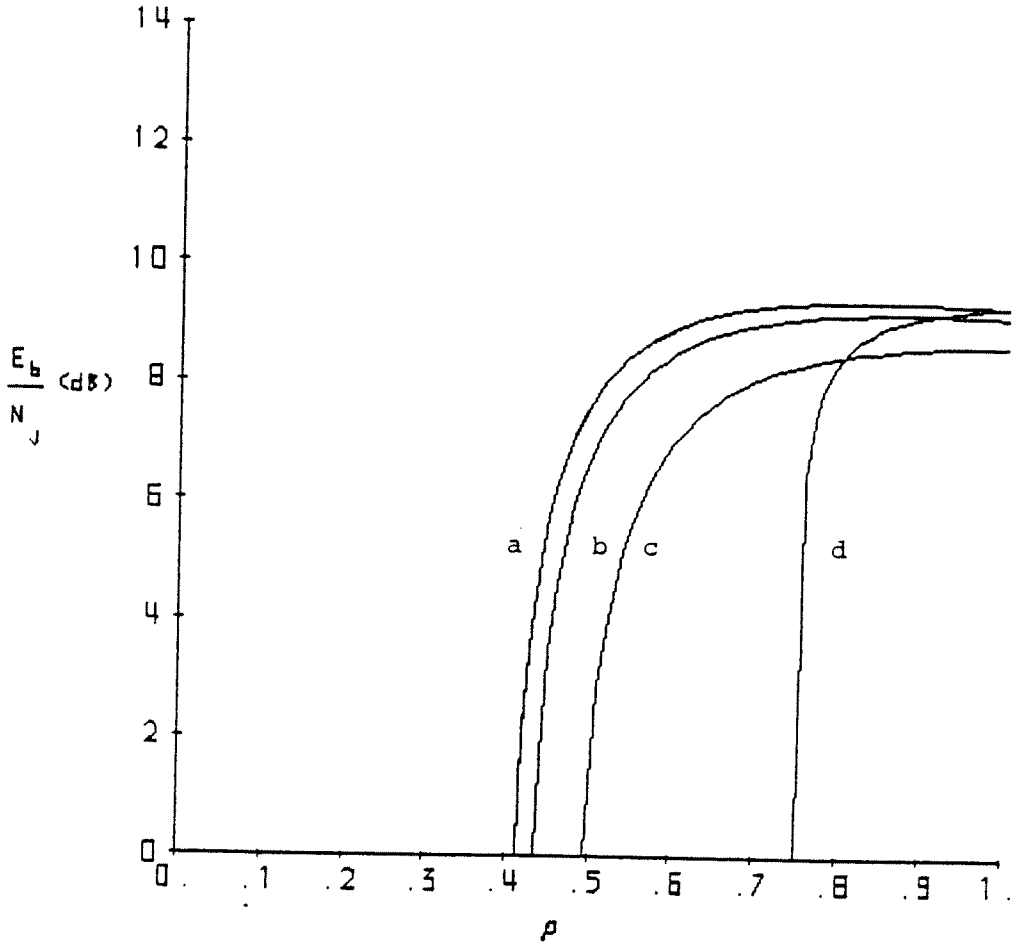

Figure 5.13 $P_b = 10^{-4}$, $(32,16)R$-S, Decoders C and E, $L = 5$: (a) C, $T = 4$ or 5; (b) C, $T = 3$; (c) C, $T = 2$; (d) E

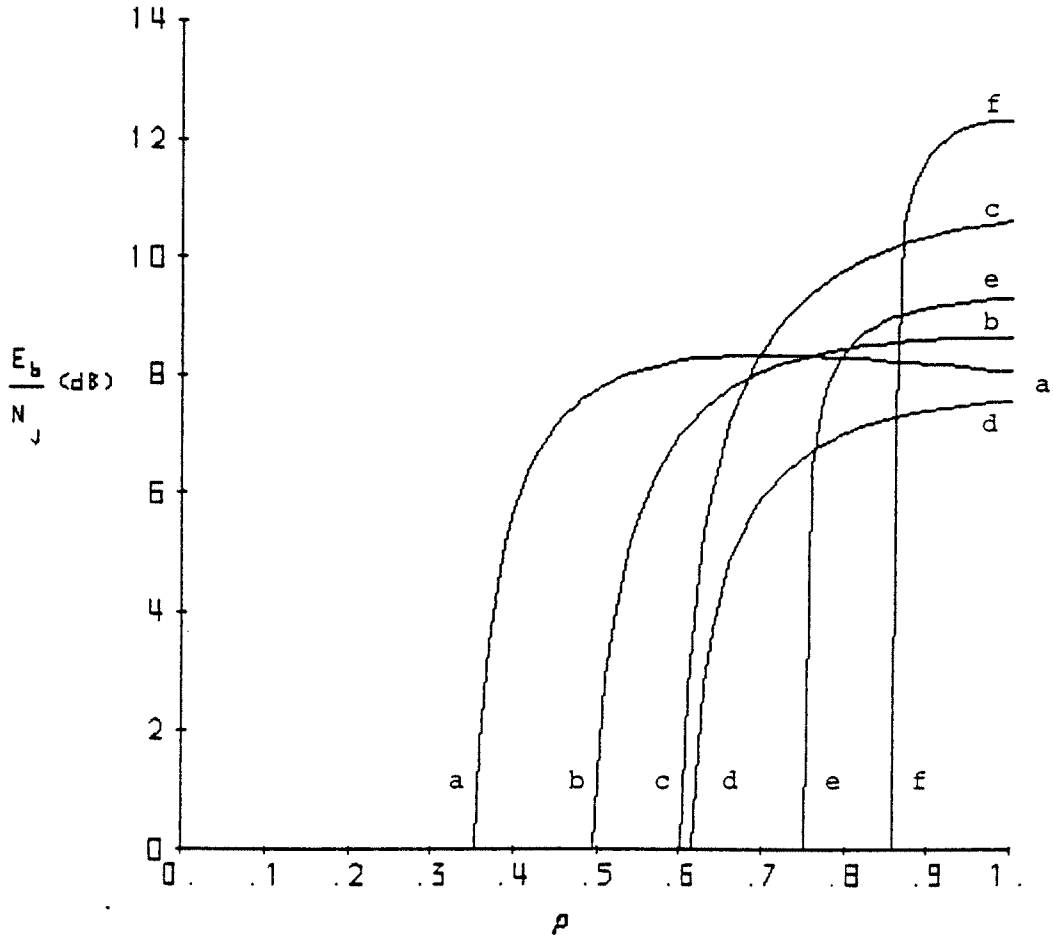

Figure 5.14 $P_b = 10^{-4}$, Decoders C and E, $L = 5$, $T = 2$: (a) C, $(32,24)R$-S; (b) C, $(32.16)R$-S: (c) C, $(32,8)R$-S; (d) E, $(32,24)R$-S; (e) E. $(32,16)R$-S; (f) E, $(32,8)R$-S

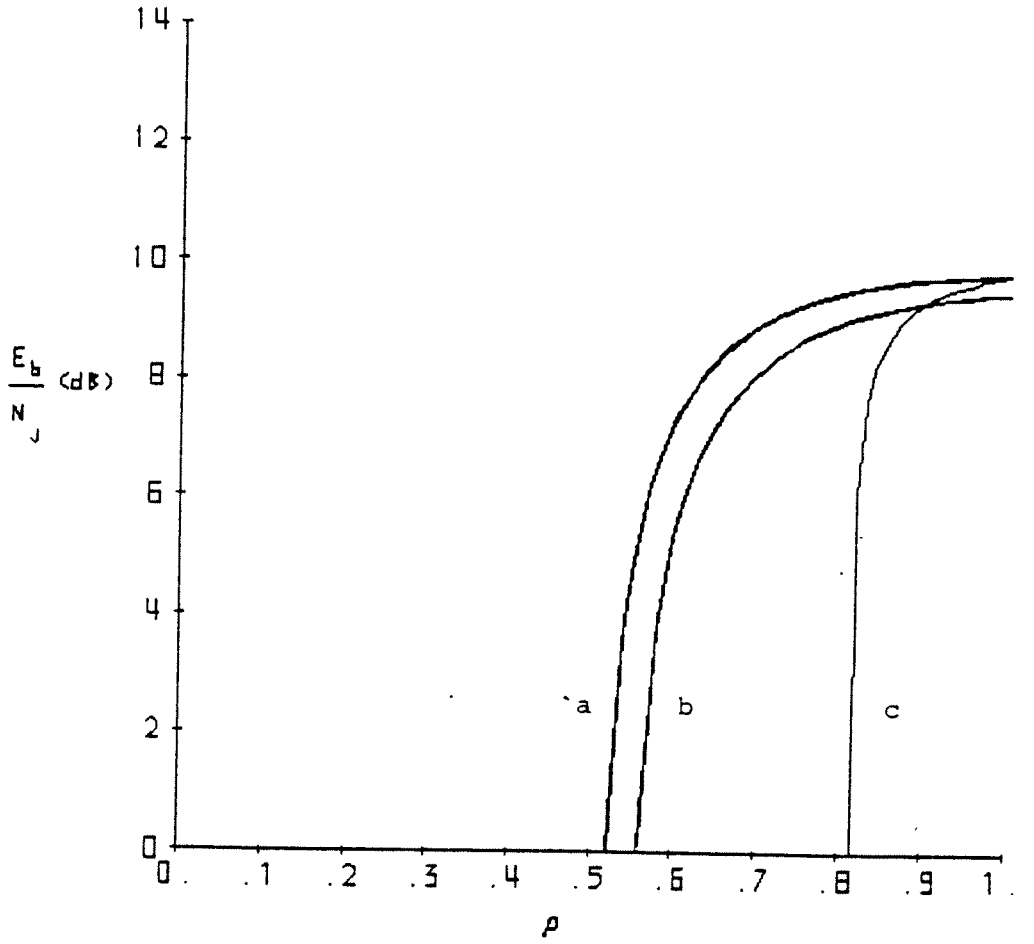

Figure 5.15 $P_b = 10^{-4}$. (32,16)R-S, Decoders C and E, $L = 7$: (a) C, $T = 4,5,6$ or 7; (b) C, $T = 3$ or 3; (c) E

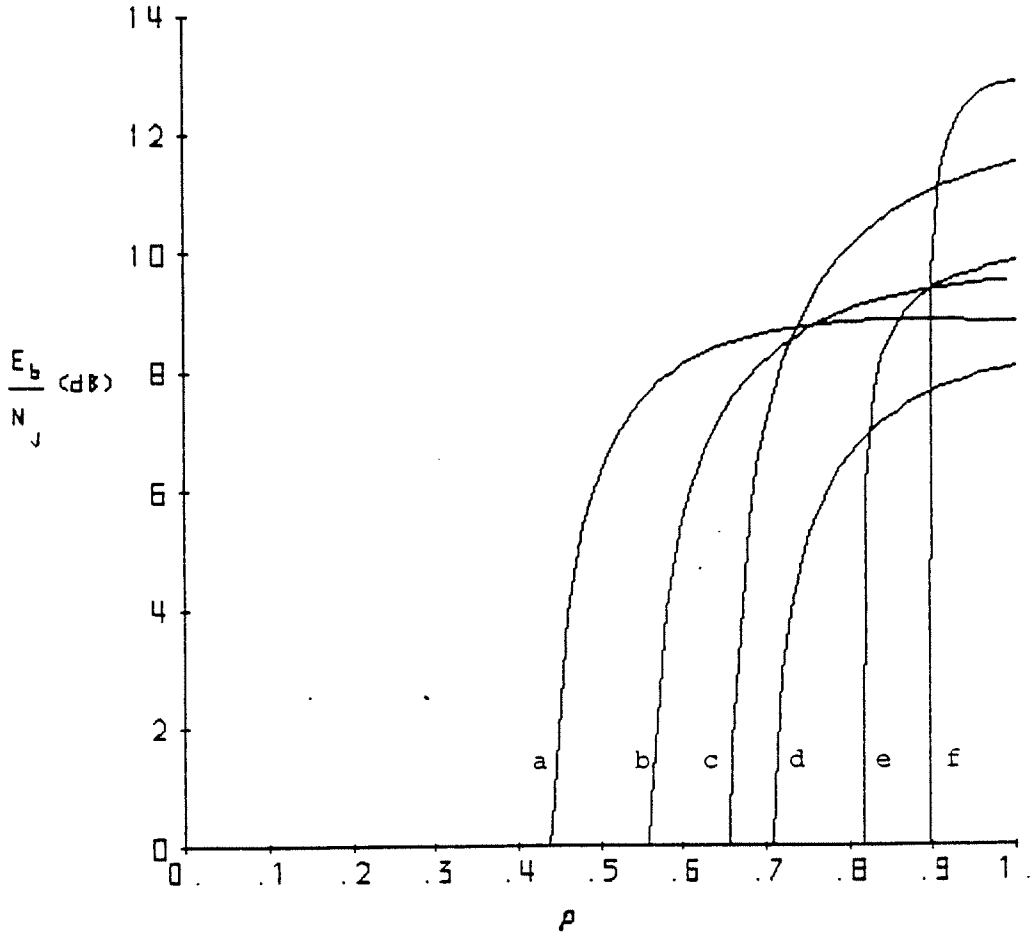

Figure 5.16 $P_b = 10^{-4}$, Decoders C and E, $L = 7$, $T = 2$: (a) C, $(32,24)R\text{-}S$; (b) C, $(32,16)R\text{-}S$; (c) C, $(32,8)R\text{-}S$; (d) E, $(32,24)R\text{-}S$; (e) E, $(32,16)R\text{-}S$; (f) E, $(32,8)R\text{-}S$

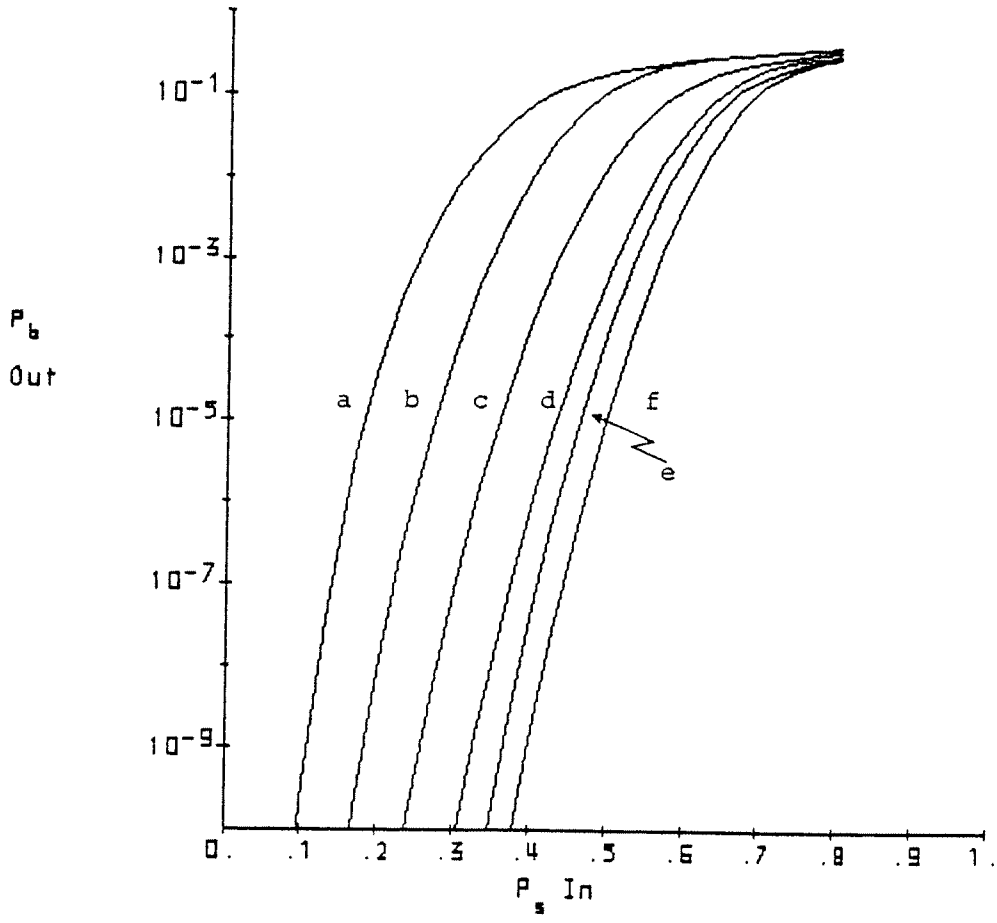

Figure 5.17 (32,16)R-S, Decoder C: (a) $L=3$, $T=3$; (b) $L=3$, $T=2$; (c) $L=5$, $T=5$; (d) $L=5$, $T=2$; (e) $L=7$, $T=7$; (f) $L=7$, $T=2$

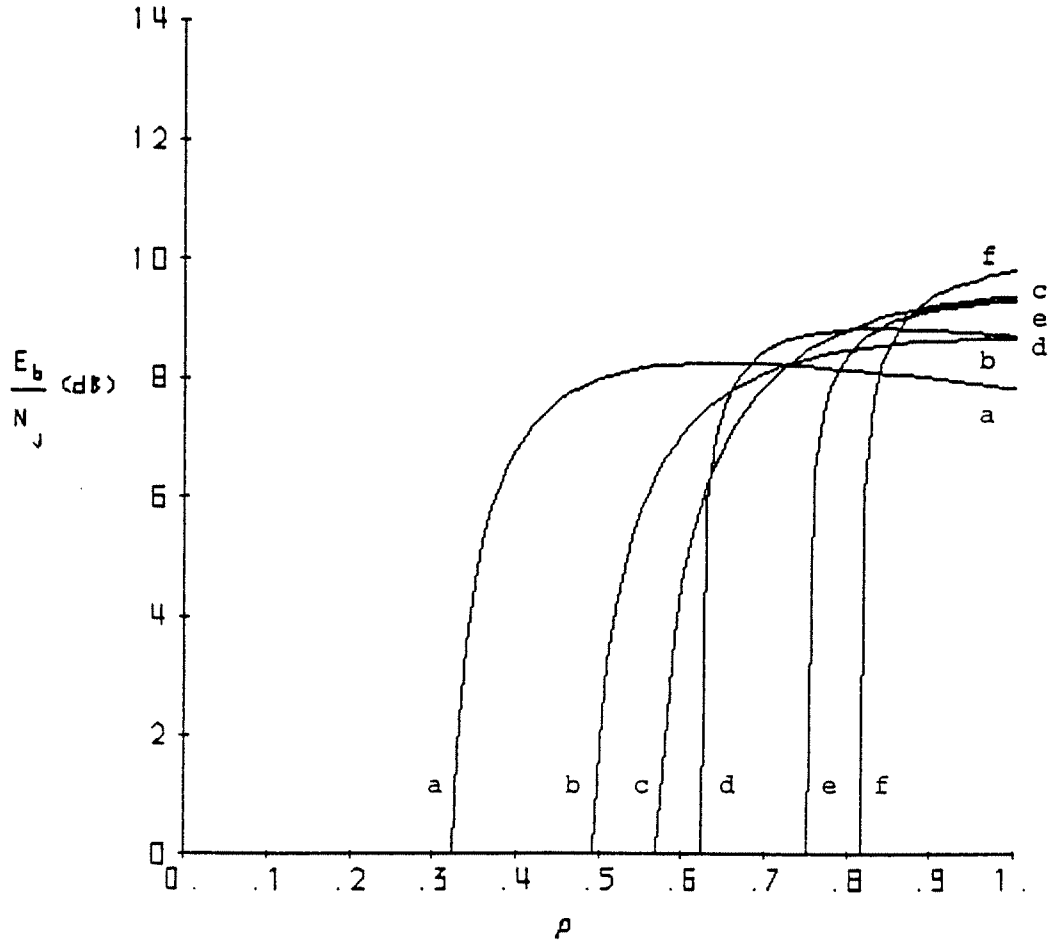

Figure 5.18 $P_b=10^{-4}$, $(32,16)R$-S, Decoders D and E: (a) D, $L=3$; (b) D, $L=5$; (c) D, $L=7$: (d) E, $L=3$; (e) E, $L=5$; (f) E, $L=7$

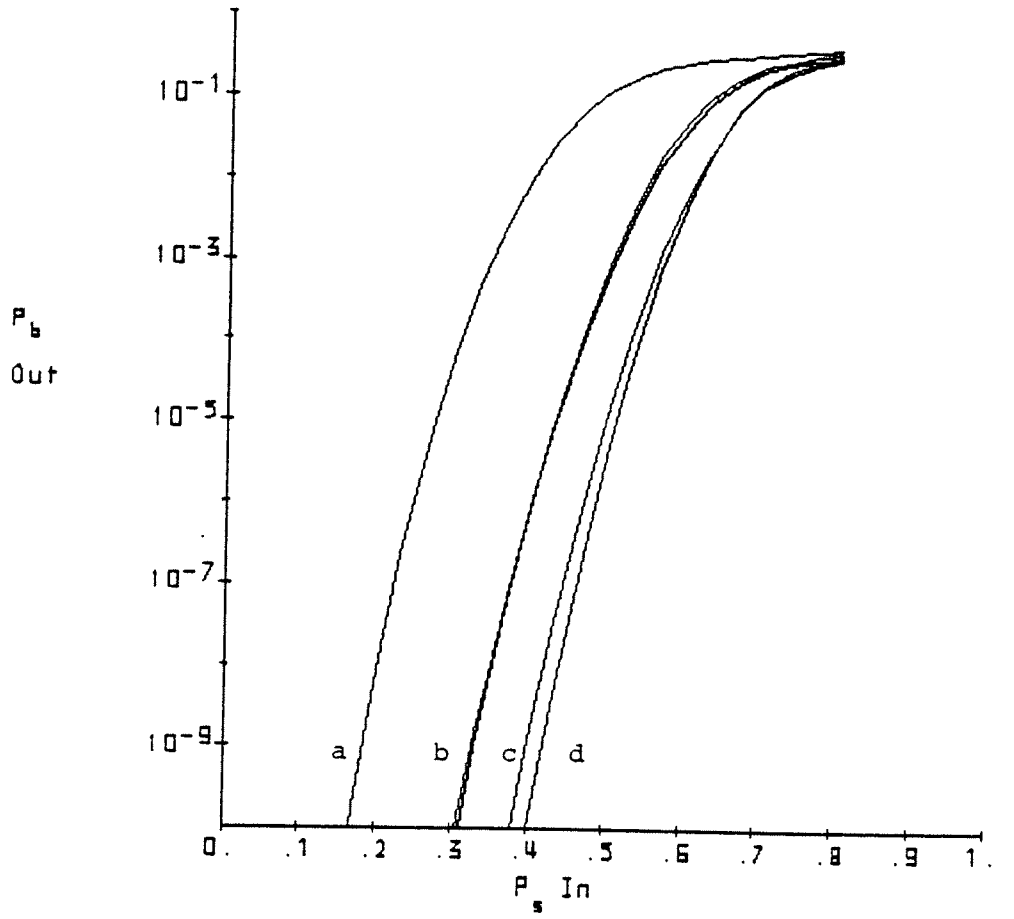

Figure 5.19 (32,16)R-S, Decoders C and D: (a) C, $L=3$, $T=2$ and C, $L=3$: (b) C, $L=5$, $T=2$ and D, $L=5$; (c) C, $L=7$, $T=2$; (d) D, $L=7$

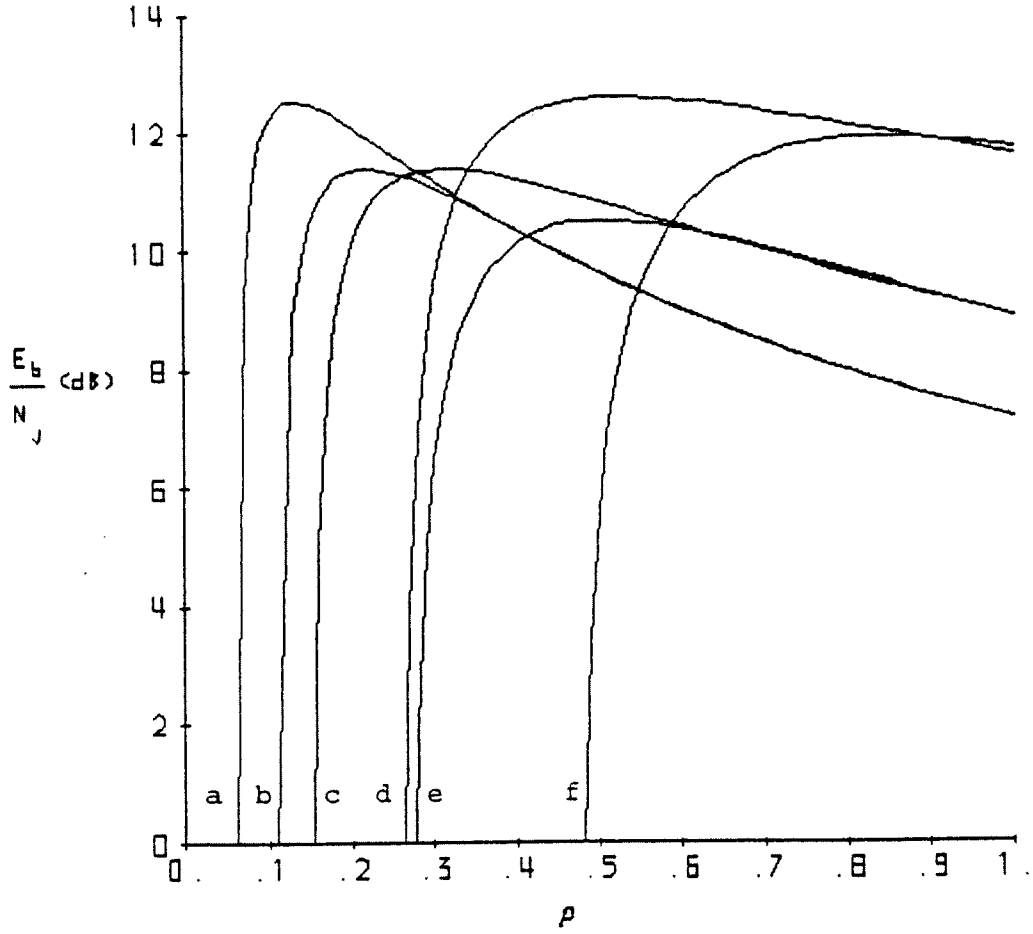

Figure 5.20 $P_b = 10^{-4}$, Decoder I: (a) I(1), (32,24)R-S; (b) I(0), (32,24)R-S; (c) I(1), (32,16)R-S; (d) I(0), (32,16)R-S; (e) I(1), (32,8)R-S; (f) I(0), (32,8)R-S

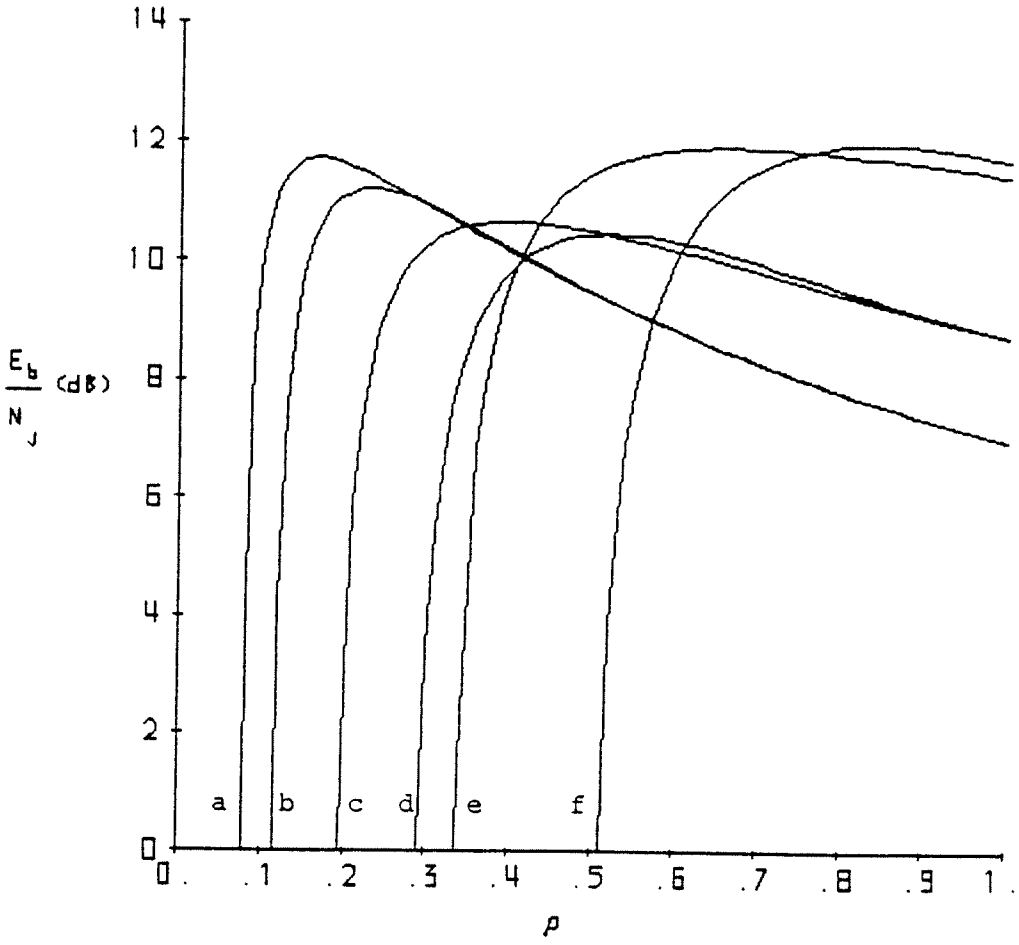

Figure 5.21 $P_b = 10^{-4}$, Decoder IIb: (a) IIb(1), (32,24)R-S; (b) IIb(0), (32.24)R-S; (c) IIb(1), (32,16)R-S; (d) IIb(0), (32.16)R-S; (e) IIb(1), (32,8)R-S; (f) IIb(0), (32,8)R-S

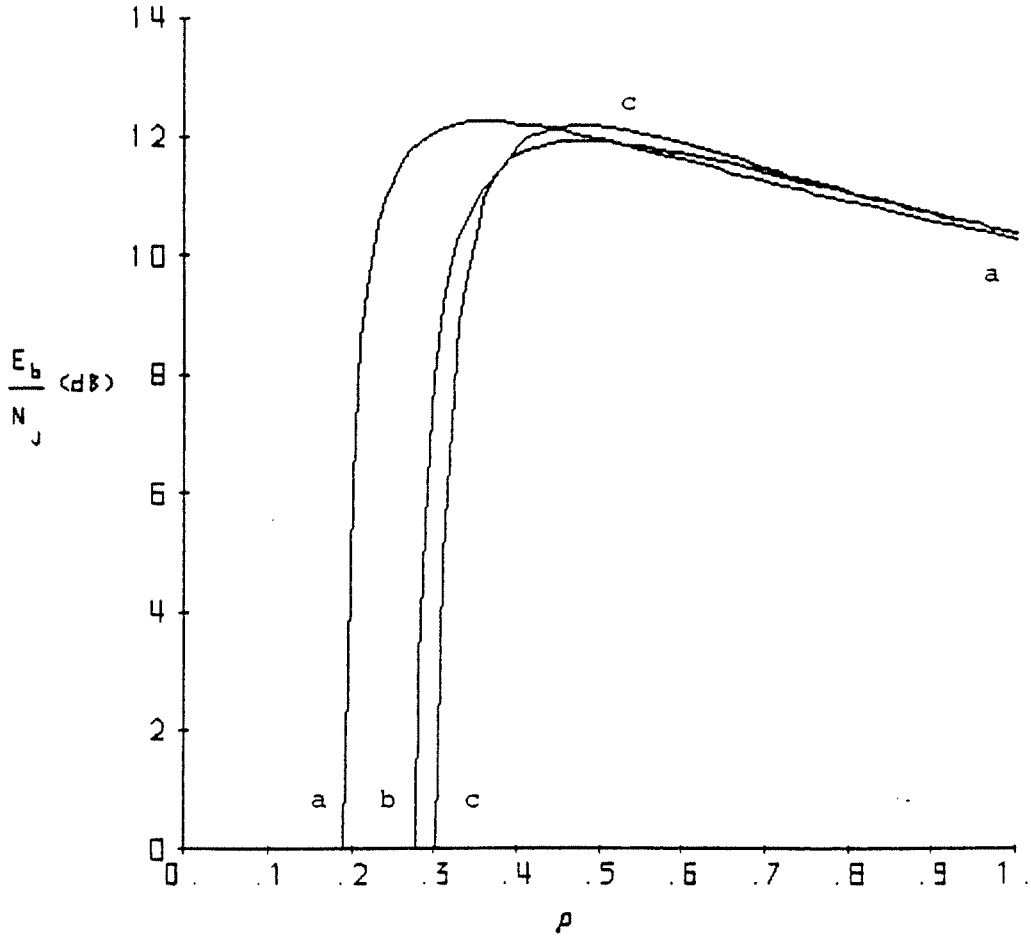

Figure 5.22 $P_b = 10^{-4}$, $(32,16)R\text{-}S$, Decoder III: (a) III(2); (b) III(1); (c) III(0)

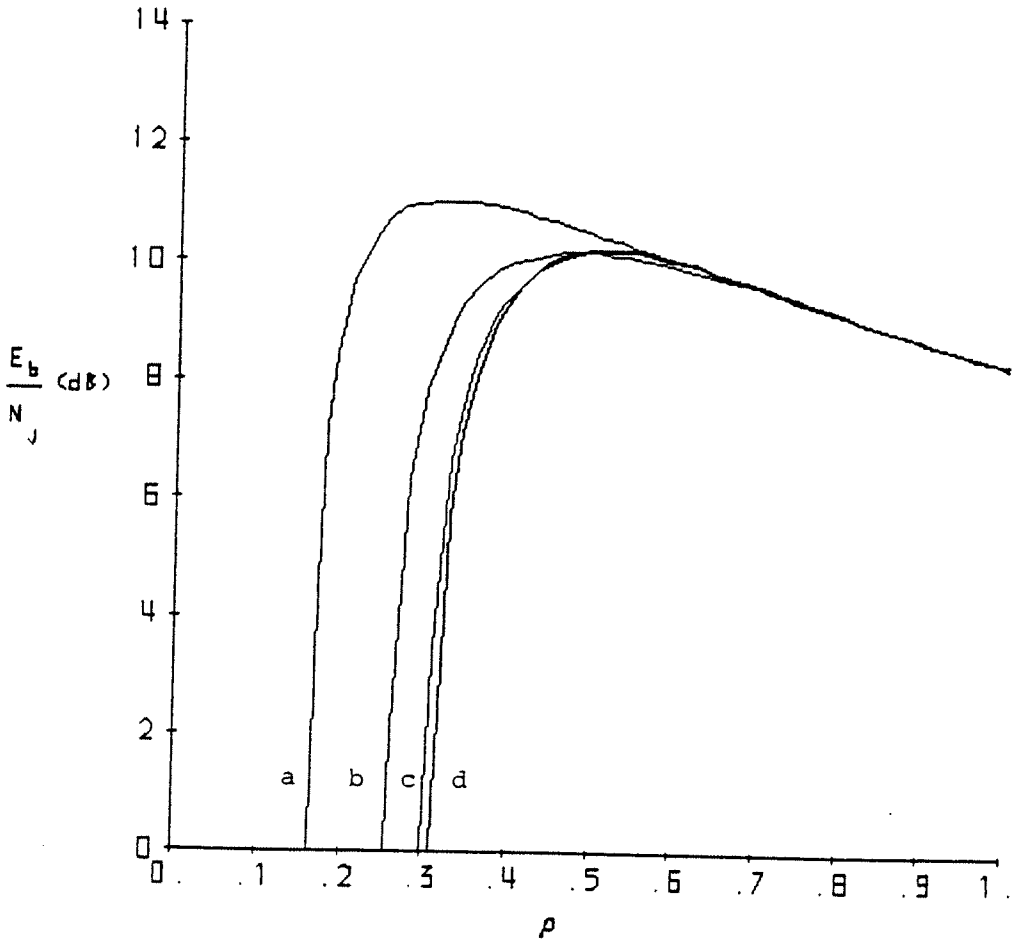

Figure 5.23 $P_b = 10^{-4}$, $(32,16)R\text{-}S$, Decoder IVb: (a) IVb(3); (b) IVb(2); (c) IVb(1); (d) IVb(0)

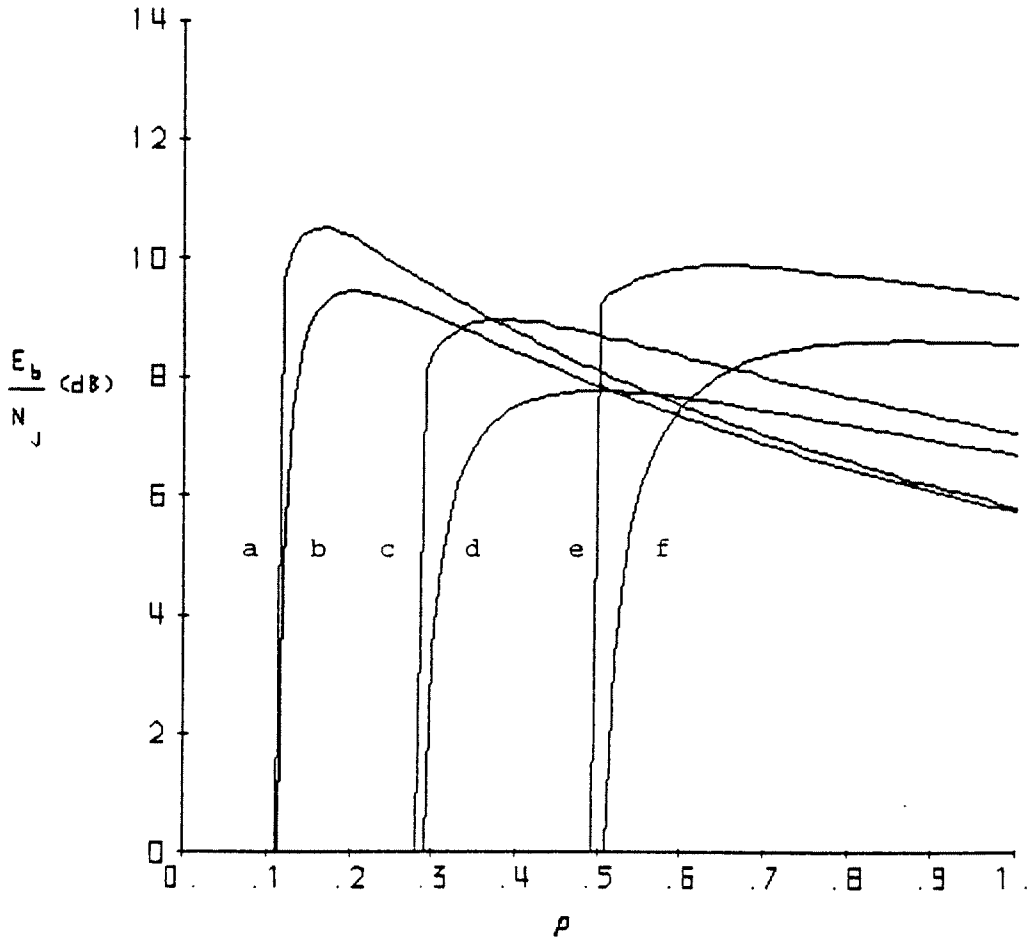

Figure 5.24 $P_b = 10^{-4}$, Decoder IIm: (a) IIm(1) $(32,24)R\text{-}S$; (b) IIm(0) $(32,24)R\text{-}S$; (c) IIm(1), $(32,16)R\text{-}S$; (d) IIm(0), $(32,16)R\text{-}S$; (e) IIm(1), $(32,08)R\text{-}S$; (f) IIm(0), $(32,08)R\text{-}S$

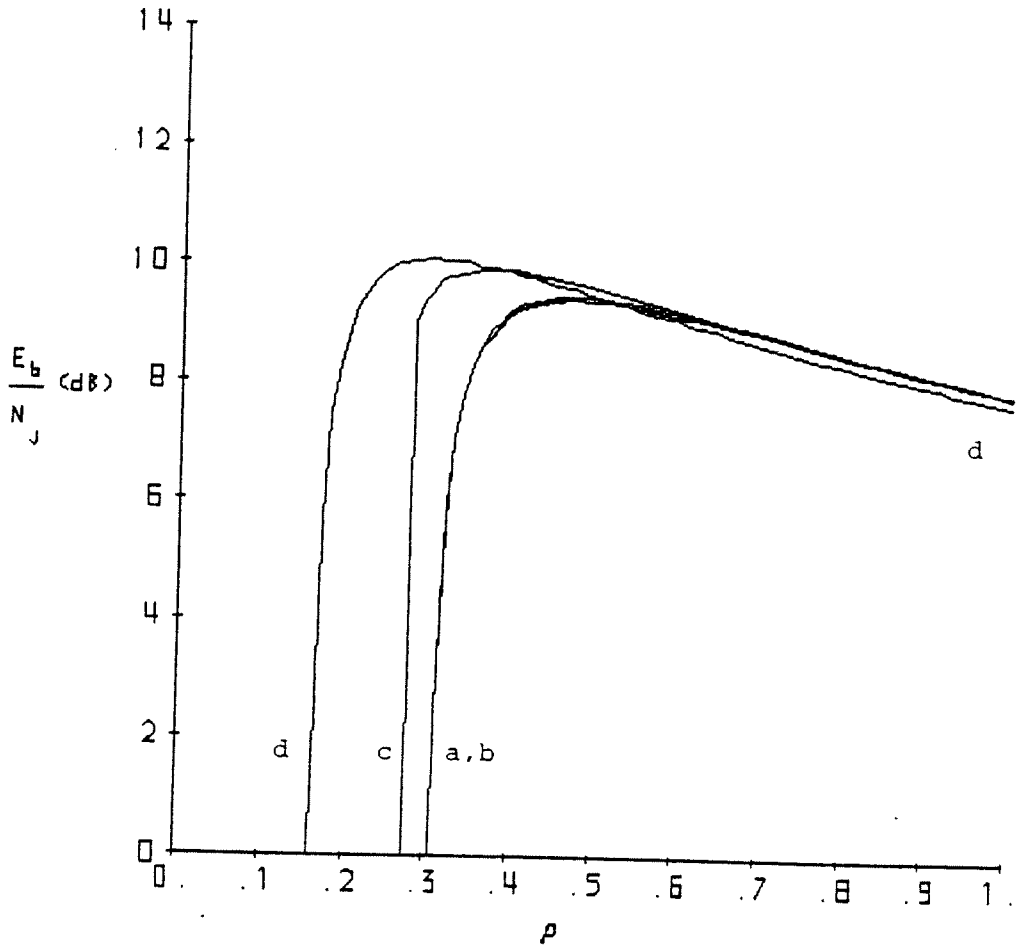

Figure 5.25 $P_b = 10^{-4}$, $(32,16)R\text{-}S$, Decoder IVm: (a) IVm(0); (b) IVm(1); (c) IVm(2); (d) IVm(3)

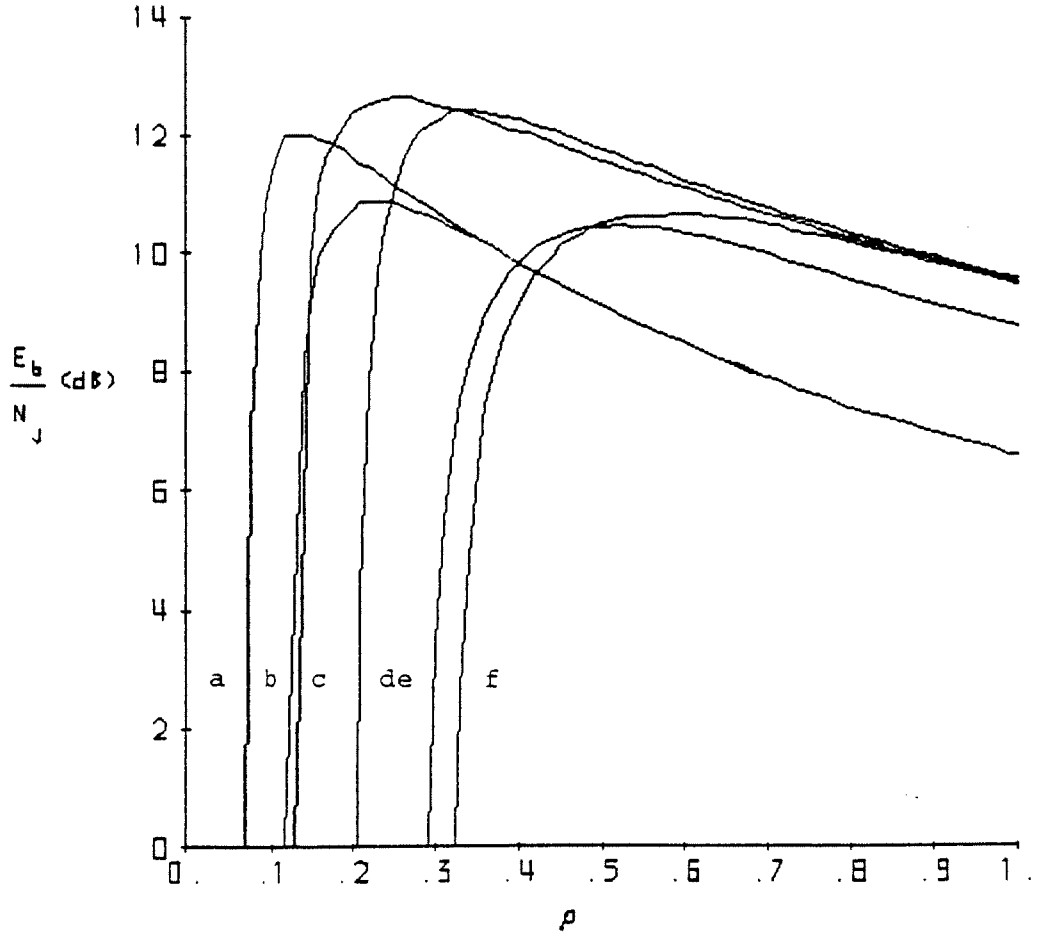

Figure 5.26 Comparison of Schemes with Binary Signalling and Approximately Equal Codes Rates R (in bits per dimension), $P_b = 10^{-4}$: (a) IVb(3), $(32,24)R\text{-}S$, $R = .125$; (b) IVb(1), $(32,24)R\text{-}S$, $R = .125$; (c) III(2), $(32,20)R\text{-}S$, $R = .120$; (d) III(0), $(32,20)R\text{-}S$, $R = .120$; (e) IIb(0), $(32,16)R\text{-}S$, $R = .125$; (f) I(0), $(32,14)R\text{-}S$, $R = .121$

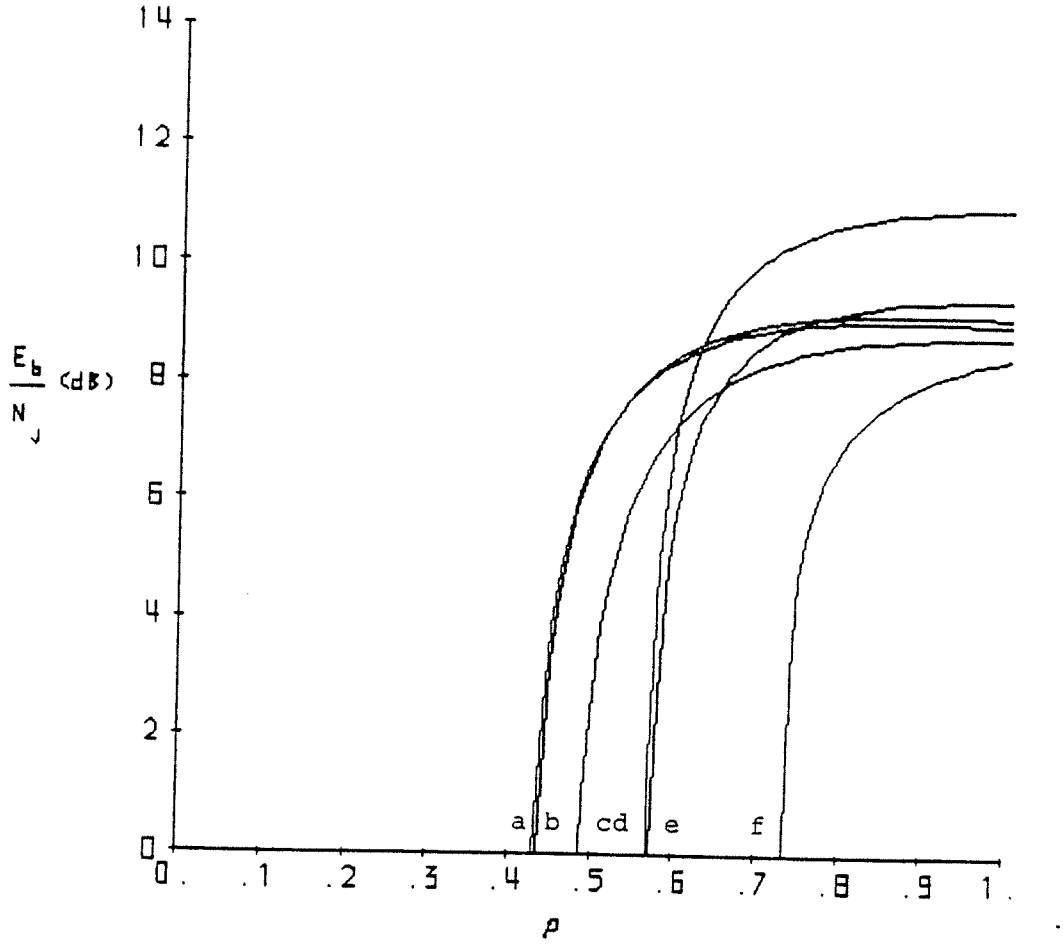

Figure 5.27 Comparison of Schemes with M-ary Signalling and Approximately Equal Codes Rates R (in bits per dimension), $P_b = 10^{-4}$: (a) C, $L=3$, $T=2$, $(32,10)R\text{-}S$, $R=.016$; (b) A_2 and B_2, $L=5$, $\theta=1.0$, $(32,16)R\text{-}S$, $R=.016$; (c) D, $L=7$, $(32,22)R\text{-}S$, $R=.015$; (d) B_2, $L=5$, $\theta=2.0$, $(32,16)R\text{-}S$, $R=.016$; (e) IIm(0), $(32,6)R\text{-}S$, $R=.015$; (f) E, $L=3$, $(32,10)R\text{-}S$, $R=.016$ and $L=5$, $(32,22)R\text{-}S$, $R=.015$

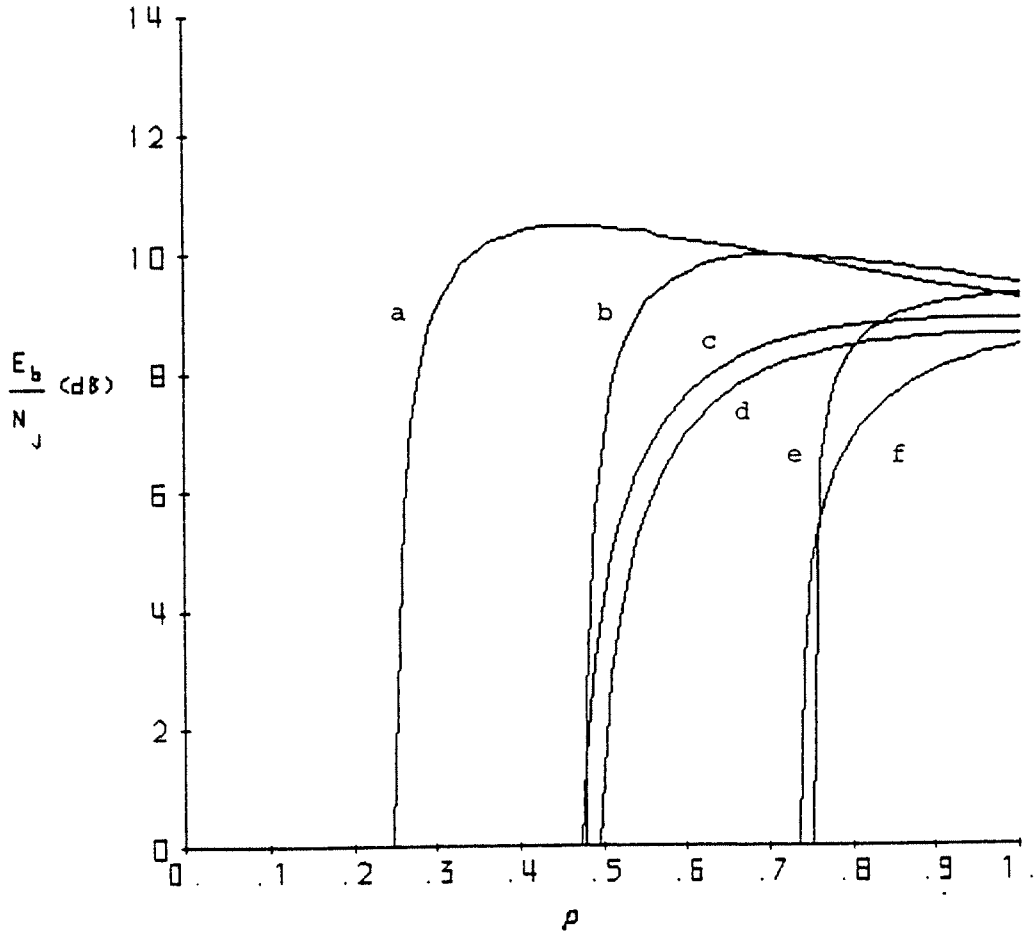

Figure 5.28 Comparison of Schemes with M-ary Signalling and Approximately Equal Codes Rates R (in bits per dimension), $P_b = 10^{-4}$: (a) IVm(3), (32,10)R-S, $R = .016$; (b) IVm(0), (32,10)R-S, $R = .016$; (c) C, $L = 7$, $T = 2$, (32,22)R-S, $R = .015$; (d) C, $L = 5$, $T = 2$, (32,16)R-S, $R = .016$; (e) E, $L = 5$, (32,16)R-S, $R = .016$; (f) E, $L = 3$, (32,10)R-S, $R = .016$ and $L = 5$, (32,22)R-S, $R = .015$

CHAPTER 6

SUMMARY AND CONCLUSIONS

In this thesis we have investigated the use of parallel decoding schemes to mitigate the effects of partial band Gaussian jamming for spread spectrum, M-ary orthogonal, frequency hopped communication systems which use concatenated coded error-correcting codes. The uniqueness of the parallel decoding technique and the concentration of our presentation has been on the design and analysis of the inner decoding system. We have presented a general analysis which may be used as a basis for evaluation of any decoding schemes which preserve symbol to symbol independence at the output of the inner decoder. We have also established the validity of the parallel decoding scheme via an analysis of the joint error rate of the Reed-Solomon outer decoders.

In Chapters 3 and 4 we have defined and derived performance statistics for seven decoding schemes which encompass use of L-diversity and general binary linear block inner codes. The results of computer analysis for many variations of inner codes are presented in Chapter 5. We have seen that performance gains are realizable with some very simple schemes (e.g., tie thresholding) while other very complex decoding algorithms (e.g., Algorithm A based on Viterbi ratio thresholding) yielded no appreciable improvements. The most significant performance was exhibited by the systems which used BCH inner codes.

This paper represents the culmination of only a segment of the research on parallel decoding algorithms. We have postulated additional problems for continuation of the research. Herein we have considered only a two state, partial band, Gaussian jammer in a thermal noise free environment. Addition of background noise is easily accommodated in the analysis and would likely result in commensurate increases in $E_s N_J^*$ and decreases in ρ^* as a function of the noise power density.

The optimal partial band Gaussian strategy against the parallel decoded system may involve a multi-state jammer with two or more nonzero power levels in segments of the band. Another constraint to be relaxed is the Gaussian assumption leading to consideration of fading and jamming together. A Rician fading channel model complicates the analysis by introducing symbol to symbol correlations which must be accounted for in the calculations leading to joint statistics at the outputs of both inner and outer decoders.

Our analysis considers numerous codes, with perfect side information, with derived side information, and with no side information. We concentrated on the use of binary linear block codes where the blocking of information bits was equal to the outer code symbol size and resulted in a single information symbol being transmitted per codeword. This constraint might be relaxed to allow multiple outer code symbols to be transmitted per inner code codeword. Finally, the analysis could be expanded to consider other than binary codes for the inner encoder.

APPENDIX A

DERIVATION OF RATIO THRESHOLDING RESULTS

A.1 Introduction

We present a ratio-thresholding technique as developed by Viterbi [18,19]. With this technique we produce a single bit quality measure of the symbol estimate in an M-ary FSK communication system. Although the procedure could be equally well applied to any M-ary estimation which compares signal amplitudes or powers, we will concentrate on non-coherent reception of FSK signals.

The results given in this Appendix are due to Viterbi and are presented for the purpose of completeness. On the other hand, the derivations were not provided in [18] or [19] and may be of interest to the reader. In some cases the derivations were not readily obvious to the author.

A.2 Ratio - Thresholding

The generic receiver for non-coherent reception of M-ary FSK signals is given in Figure A.1. We assume that the receiver is synchronized to the frequency hopping pattern and that during any hop interval the frequency separations of the M candidate signals are integer multiples of $(2T_S)^{-1}$. Equivalently, the M candidate signals are orthogonal where T_S is the information symbol time.

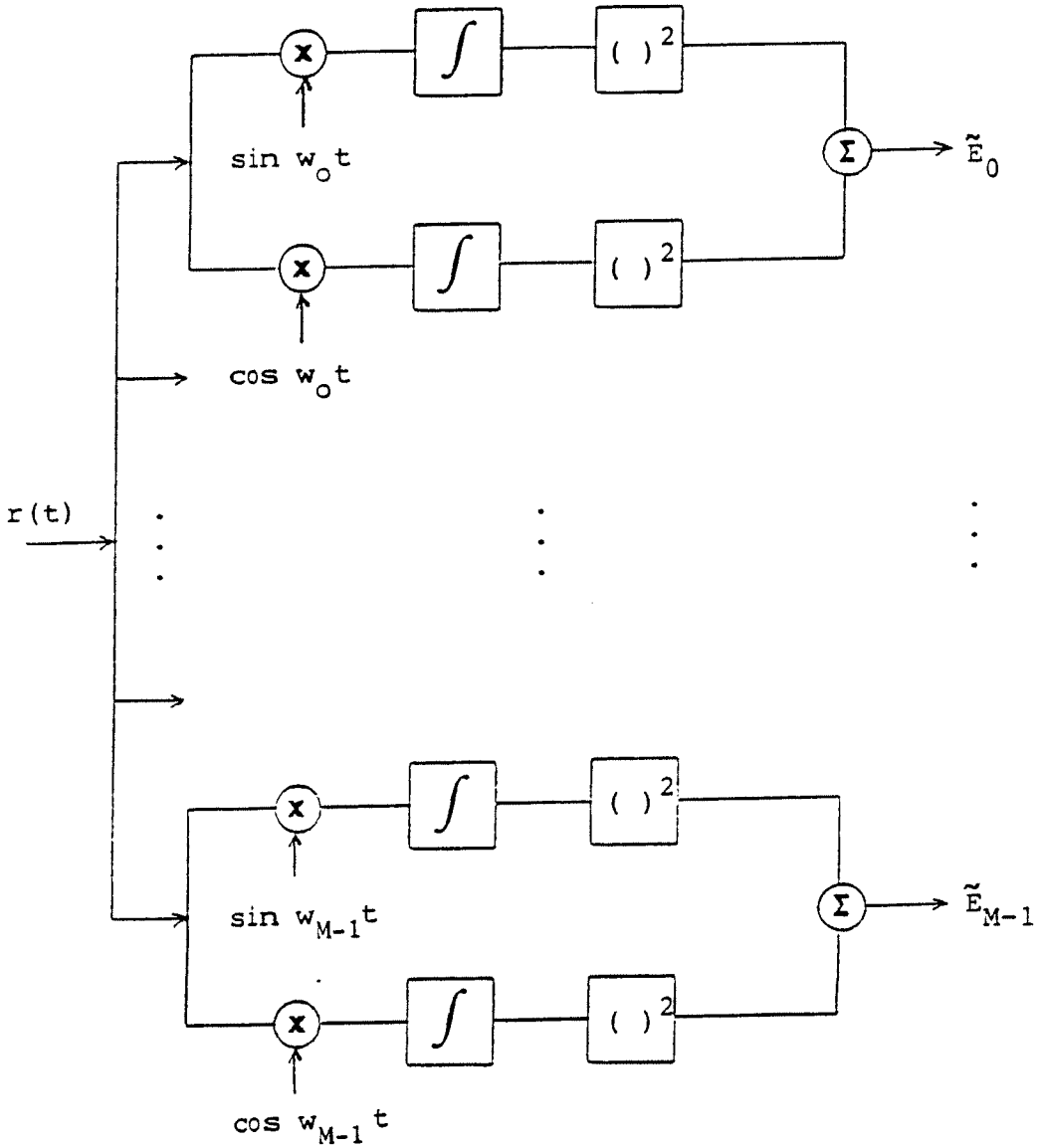

Figure A.1 Non-Coherent *M*-ary FSK Receiver

We will concentrate on the effects of the jammer and hence will assume the only channel noise is that due to the jammer. Furthermore, the jammer is modeled as a partial band jammer which jams a fraction ρ of the hopping bandwidth with uniform power density N_J/ρ. The received signal is either totally within or external to the jammed bandwidth.

Assuming symbol k is transmitted and that the signal lies within a jammed portion of the bandwidth, standard calculations (e.g., [6,Vol.I, Sec.4.7] and [11, Sec.4.3.2]) yield the following probability distributions on the matched filter outputs.

$$P_{\tilde{E}_j}(\alpha) = \begin{cases} \dfrac{\rho}{4E_S N_J}\, e^{-\frac{\rho\alpha}{4E_S N_J}} & j \neq k \\ \dfrac{\rho}{4E_S N_J}\, e^{-\frac{\rho\alpha}{4E_S N_J}} e^{-\frac{\rho E_S}{N_J}} I_0\left(\dfrac{\rho\sqrt{\alpha}}{N_J}\right) & j = k \end{cases} \tag{A.1}$$

I_0 is the 0^{th}-order modified Bessel function; the first distribution is exponential and the second is non-central chi-square with two degrees of freedom.

The receiver decides symbol k is transmitted if

$$\tilde{E}_k = \max_{0 \le j \le M-1} \{\tilde{E}_j\} \tag{A.2}$$

The Viterbi ratio threshold test assigns a quality bit, q, to the decision as follows:

$$q = \begin{cases} 0 & \tilde{E}_k \ge \max\limits_{0 \le j \le M-1} \{\theta \tilde{E}_j\} \\ 1 & \text{otherwise} \end{cases} \tag{A.3}$$

where $\theta > 1$ is a real variable. Simply stated, the quality bit is zero if the ratio of the largest filter output to the second largest filter output is greater than the threshold θ.

With orthogonal, equal energy signalling the receiver statistics are independent of the transmitted symbol. Thus, without loss of generality we will assume symbol 0 was transmitted. The resulting discrete channel model is shown in figure A.2 where the transition probabilities are labeled consistent with [19]. We now derive expressions for $F_c(\theta)$, $F_E(\theta)$, $\Delta F_c(\theta)$ and $\Delta F_E(\theta)$.

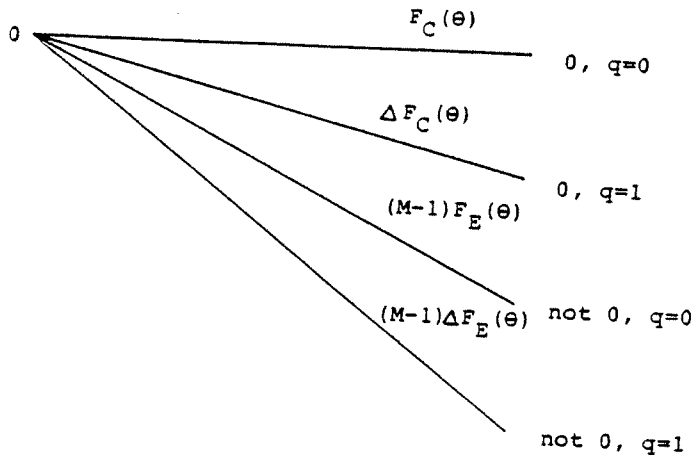

Figure A.2 Ratio-Threshold Discrete Channel

$$
\begin{aligned}
F_c(\theta) &= P\{\tilde{E}_0 \geq \theta \tilde{E}_j \quad j = 2, \ldots, M-1 \mid 0 \text{ sent}\} \\
&= P\{\tilde{E}_0 \geq \theta \tilde{E}_j \quad j = 2, \ldots, M \mid 0 \text{ sent, not jammed}\} P\{\text{not jammed} \mid 0 \text{ sent}\} \\
&\quad + P\{\tilde{E}_0 \geq \theta \tilde{E}_j \quad j = 2, \ldots, M \mid 0 \text{ sent, jammed}\} P\{\text{jammed} \mid 0 \text{ sent}\} \\
&= (1-\rho) + \rho P\{\tilde{E}_0 \geq \theta \tilde{E}_j \quad j = 2, \ldots, M-1 \mid 0 \text{ sent, jammed}\} \\
&= (1-\rho) + \rho \int_0^\infty P\{\tilde{E}_1 \leq \frac{\tilde{E}_0}{\theta}, \ldots, \tilde{E}_{M-1} \leq \frac{\tilde{E}_0}{\theta} \mid \tilde{E}_0, 0 \text{ sent, jammed}\} p_{\tilde{E}_0}(\alpha) d\alpha \\
&= (1-\rho) + \rho \int_0^\infty \left[\int_0^{\frac{\alpha}{\theta}} P_{\tilde{E}_1}(\beta) d\beta\right]^{M-1} P_{\tilde{E}_0}(\alpha) d\alpha
\end{aligned}
\tag{A.4}
$$

Where we have used: jamming is independent of the transmitted symbol; without jamming the symbol is received error free; with orthogonal signalling the error events are independent and identically distributed. The distribution of $P_{\tilde{E}_1}(\beta)$

is given by A.1a and thus,

$$\left[\int_0^{\frac{\alpha}{\theta}} P_{\tilde{E}_1}(\beta)\,d\beta\right]^{M-1} = \left[1 - e^{-\frac{\rho\alpha/\theta}{4E_S N_J}}\right]^{M-1}$$
$$= 1 + \sum_{k=1}^{M-1} \binom{M-1}{k} (-1)^k \, e^{-\frac{\rho k\alpha/\theta}{4E_S N_J}} \tag{A.5}$$

Comparing with A.4 and noting $p_{E_0}(\alpha)$ is given by A.16 we need to evaluate

$$\mathbf{I} = \int_0^{\infty} e^{-\frac{\rho k\alpha/\theta}{4E_S N_J}} \left[\frac{\rho}{4E_S N_J} \, e^{-\frac{\rho\alpha}{4E_S N_J}} e^{-\frac{\rho E_S}{N_J}} \mathbf{J}_0\left(\frac{\rho\sqrt{\alpha}}{N_J}\right)\right] d\alpha$$

Letting,

$$c = \frac{\rho}{4E_S N_J}\left[\frac{\theta + k}{\theta}\right]$$

$$d = \frac{\rho E_S}{N_J}\left[\frac{\theta}{\theta + k}\right]$$

$$\mathbf{I} = \frac{\rho}{4E_S N_J} \, e^{-\frac{\rho E_S}{N_J}} \, \frac{1}{c} \, e^{d} \int_0^{\infty} c e^{-c\alpha} e^{-d} I_0(2\sqrt{cd\,\alpha})\,d\alpha$$

The integrand is recognized as the general form for a non-central Chi-square distribution with two degrees of freedom. Thus, the integral is unity and A.4 becomes

$$F_c(\theta) = 1 + \rho \sum_{k=1}^{M-1} \binom{M-1}{k} (-1)^k \frac{\theta}{\theta+k} \, e^{-\frac{\rho E_S}{N_J}\left(\frac{k}{\theta+k}\right)} \tag{A.6}$$

$F_E(\theta)$ is the probability an erroneous symbol is received with quality bit 0. With equal energy, orthogonal signalling this probability is the same for all $M - 1$ incorrect symbols. Hence, we will evaluate the probability of receiving symbol 1 with $q = 0$.

$$
\begin{aligned}
F_{\tilde{E}}(\theta) &= P\{\tilde{E}_1 \geq \theta \tilde{E}_j \quad j = 0,2, \ldots, M-1 \mid 0 \text{ sent}\} \\
&= \rho\, P\{\tilde{E}_1 \geq \theta \tilde{E}_j \quad j = 0,2, \ldots, M-1 \mid 0 \text{ sent, jammed}\} \\
&= \rho \int_0^\infty P\{\tilde{E}_0 \leq \frac{\tilde{E}_1}{\theta}, \tilde{E}_2 \leq \frac{\tilde{E}_1}{\theta}, \ldots, \tilde{E}_{M-1} \leq \frac{\tilde{E}_1}{\theta} \mid \tilde{E}_1, 0 \text{ sent, jammed}\} P_{\tilde{E}_1}(\alpha) d\alpha \\
&= \rho \int_0^\infty \left[\int_0^{\frac{\alpha}{\theta}} P_{\tilde{E}_0}(\beta) d\beta \right] \left[\int_0^{\frac{\alpha}{\theta}} P_{\tilde{E}_1}(\gamma) d\gamma \right]^{M-2} P_{\tilde{E}_1}(\alpha) d\alpha
\end{aligned}
$$

Where we have used the same reasoning as led to equation A.4. The second inner integral is the same form as A.5 and absorbing the "1" in the summation we have:

$$
\left[\int_0^{\frac{\alpha}{\theta}} P_{E_1}(\gamma) d\gamma \right]^{M-2} = \sum_{k=0}^{M-2} \binom{M-2}{k} (-1)^k \, e^{-\frac{\rho k \alpha / \theta}{4E_S/N_J}}
$$

Now, using [11,Equation 1.1.121] and [13,Appendix A]

$$
\begin{aligned}
\left[\int_0^{\frac{\alpha}{\theta}} P_{E_0}(\beta) d\beta \right] &= 1 - Q\left(\sqrt{\frac{2E_S\rho}{N_J}}, \sqrt{\frac{\rho\alpha/\theta}{2E_S N_J}} \right) \\
&= e^{-\frac{E_S\rho}{N_J}} \, e^{-\frac{\rho\alpha/\theta}{4E_S/N_J}} \sum_{m=1}^{\infty} \left(\frac{1}{2E_S} \sqrt{\frac{\alpha}{\theta}} \right)^m \mathbf{J}_M\left(\frac{\rho}{N_J} \sqrt{\frac{\alpha}{\theta}} \right)
\end{aligned}
$$

Combining all the terms we arrive at an integral much like **I** above except that the integral is put in the form of a non-central Chi-square distribution with $2m - 1$ degrees of freedom. Again the integral is unity and we are left with

$$
F_{\tilde{E}}(\theta) = \rho \sum_{k=0}^{M-2} \binom{M-2}{k} (-1)^k \, e^{-\frac{E_S\rho}{N_J}\left[\frac{k+\theta}{1+k+\theta}\right]} \left(\frac{\theta}{1+k+\theta} \right) \sum_{m=1}^{\infty} \left(\frac{1}{1+k+\theta} \right)^m
$$

Since $(1-k+\theta) > 1$, the inner sum is a geometric progression and is easily reduced. Finally, changing the range of summation we arrive at:

$$F_E(\theta) = \frac{\rho}{M-1} \sum_{k=1}^{M-1} \binom{M-1}{k} (-1)^{k-1} \frac{\theta}{k+\theta} \frac{k}{k+\theta-1} e^{-\frac{E_S \rho}{N_J}\left[\frac{k-\theta-1}{k+\theta}\right]} \tag{A.7}$$

Equations (A.6) and (A.7) are similar to [19, Equations 3.9 and 3.10]. Formulas for $\Delta F_c(\theta)$ and $\Delta F_E(\theta)$ are not derived in the references; however, we offer the derivations which follow. Again assuming symbol 0 was transmitted let

$A_1 =$ event $\tilde{E}_0 > \tilde{E}_j$ for all $j \in \{1, \ldots, M-1\}$ given 0 sent

$A_2 =$ event there exists at least one value of $j \in \{1, \ldots, M-1\}$ such that $\tilde{E}_0 < \theta \tilde{E}_j$ given 0 sent

then,

$$\begin{aligned} \Delta F_c(\theta) &= P\{A_1 \cap A_2\} \\ &= P\{A_1\} - P\{A_1 \cap A_2^c\} \end{aligned}$$

but,

$A_2^c =$ event $\tilde{E}_0 \geq \theta \tilde{E}_j$ for all $j \in \{1, \ldots, M-1\}$ given 0 sent

hence,

$$\begin{aligned} A_1 \cap A_2^c &= A_2^c \\ \Delta F_c(\theta) &= P\{A_1\} - P\{A_2^c\} \\ &= F_c(1) - F_c(\theta) \end{aligned} \tag{A.8}$$

Similarly, if we let

$B_1 =$ event $\tilde{E}_1 > \tilde{E}_j$ for all $j \in \{0,2,3, \ldots, M-1\}$ given 0 sent

$B_2 =$ event there exist at least one value of $j \in \{0,2,3, \ldots, M-1\}$ such that $\tilde{E}_1 < \theta \tilde{E}_j$ given 0 sent

by the same argument as above

$$\begin{aligned} \Delta F_E(\theta) &= Pr\{B_1 \cap B_2\} \\ &= F_E(1) - F_E(\theta) \end{aligned} \tag{A.9}$$

APPENDIX B

ENUMERATION TECHNIQUE AND FORMULAS

B.1 Introduction

For analysis of the parallel decoding configurations with L-diversity inner codes, we use one of two models for the discrete channel between the output of the inner encoders and the inputs to the inner decoders. The first model is the M input, $2M$ output channel which results from using the ratio threshold technique described in Appendix A. Figure A.2 illustrates the transition probabilities for this channel where symbol 0 is assumed transmitted and where the $M-1$ error events of each type (good and bad quality bits) are lumped together. The channel has symmetry in that the four event types and transition probabilities of figure A.2 are identical regardless of which symbol is transmitted.

The second channel of interest is the conventional M input, M output M-ary symmetric channel illustrated in Figure B.1 where symbol 0 is assumed transmitted. We use the transition probabilities $p/(M-1)$ and $q = 1-p$ throughout this thesis.

To evaluate the performance of the parallel decoders with L-diversity inner encoders, we will often be concerned with calculation of the probability that specific combinations of outputs occur. For example, with $L = 5$ we might ask what the probability is that we receive symbol 0 twice and no other symbol more than twice assuming symbol 0 was transmitted 5 times.

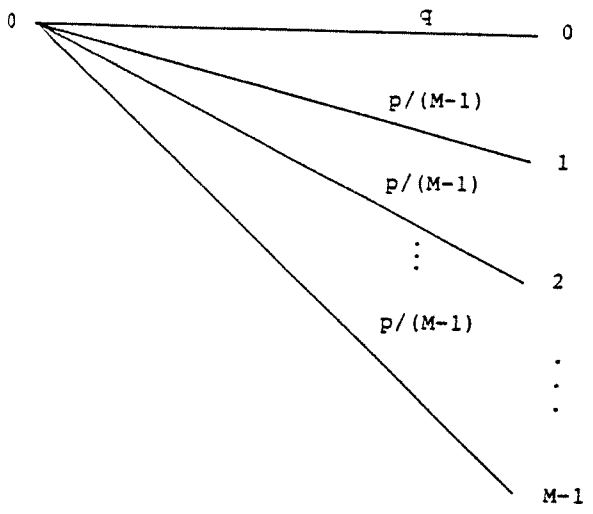

Figure B.1 M-ary Symmetric Channel

To start with we know that any single event which has two symbols 0 and three symbols not 0 being received has probability

$$q^2 \left(\frac{p}{M-1} \right)^3 \tag{B.1}$$

Hence, we merely need to enumerate (or count) the number of events which satisfy the desired condition and multiply this number by (B.1). In this appendix we present a general approach for evaluating probabilities of events like given in the example above. We also give a compact form for expressing probabilities of this type which we call enumeration formulas or equations. We will describe the technique by example, deriving the probability of error for an L-diversity code on an M-ary symmetric channel. We conclude the appendix by giving sample evaluations of ten enumeration formulas used in Chapter 3.

B.2 Probability of Error for L-diversity Codes

The probability of error for an L-diversity code on an M-ary alphabet used over an M-ary symmetric is evaluated, for example, in [16,Appendix A] for $L = 3,4, \ldots, 7$. However, we know of no published algorithm, suitable for computer automation, which will derive a solution for arbitrary L. The enumeration procedure described herein provides such an algorithm.

We begin by considering specific events to help motivate the general solution. Let $L = 5$ and consider the case when 3 correct symbols are received. The probability of receiving 3 correct symbols and any two specific incorrect symbols

$$\binom{5}{3} q^3 \left(\frac{p}{M-1} \right)^2 = 10q^3 \left(\frac{p}{M-1} \right)^2$$

The two incorrect symbols may be the same $(M-1)$ ways and may be different $(M-1)(M-2)$ ways. Thus, the total probability of receiving 3 correct and two incorrect symbols is

$$[(M-1) + (M-1)(M-2)]10q^3 \left(\frac{p}{M-1} \right)^2 = 10q^3p^2 \qquad \text{(B.2)}$$

as in [16]. Equation (B.2) is also the probability of receiving 3 correct symbols and correctly decoding.

Now, consider the probability of receiving two correct symbols and correctly decoding. The probability of receiving 2 correct symbols and three specific incorrect symbols is

$$\binom{5}{2} q^2 \left(\frac{p}{M-1} \right)^3 = 10q^2 \left(\frac{p}{M-1} \right)^3$$

We cannot count the case when all three incorrect symbols are the same since then the decoder will make an error. We can select two of $(M-1)$ incorrect symbols to fill

the three error positions by using one of the symbols twice. To count the ways this may be done proceed as follows: (1) select the two incorrect symbols in $\binom{M-1}{2}$ ways; (2) choose one of the two symbols to use twice in two ways; (3) choose 2 of the 3 error position to locate the identical incorrect symbols in $\binom{3}{2}$ ways. Finally, note that in each case the decoder will have to choose between the two incorrect symbols and the two correct symbols. With probability $1/2$ the correct symbol will be chosen. Hence, the total probability for this event is

$$\binom{M-1}{2}(2)\binom{3}{2}\frac{1}{2}10q^2\left(\frac{p}{M-1}\right)^3 = 15\frac{M-2}{(M-1)^2}\,q^2p^3 \qquad \text{(B.3a)}$$

Finally, we can choose three distinct incorrect symbols and fill the three error positions in $(M-1)(M-2)(M-3)$ ways. The total probability of this event is

$$(M-1)(M-2)(M-3)10q^2\left(\frac{p}{M-1}\right)^3 = 10\frac{(M-2)(M-3)}{(M-1)^2}\,q^2p^3 \qquad \text{(B.3b)}$$

The sum of (B.3a) and (B.3b) is the probability two correct symbols are received and decoded correctly which also matches [16].

We can now consider the general case for evaluating the probability of correct decoding for L-diversity codes on M-ary symmetric channels. The probability of error will be one minus this quantity. If one or more correct symbols are received and if n_c is the number of correct symbols received, we write

$$P(\text{correct}) = \sum_{n_c=1}^{L}\left[\sum_{Y} G(Y,n_c)\binom{L}{Y}\right] q^{n_c}\left(\frac{p}{M-1}\right)^{L-n_c} \qquad \text{(B.4)}$$

where the role of the bracketed quantity is to enumerate all events which contribute to the desired probability.

We let $Y = (m_1, m_2, \ldots, m_\alpha)$ where $m_1 \geq m_2 \geq \cdots \geq m_\alpha > 0$ be a generic configuration of received symbols not constrained by an external sum. For example, in (B.4) there are $L - n_c$ positions to be filled by m_1 of symbol A, m_2 of symbol B, etc. Here the symbols are different and $\sum_{i=1}^{\alpha} m_i = L - n_c$. For the case of calculating the probability of correct decoding the L-diversity codes we also introduce the constraint $n_c \geq m_1$ otherwise a correct decision couldn't be made.

We next define the values $n_1, \ldots, n_\beta$ as follows

$n_1 =$ the number of terms in the largest grouping of equal terms in Y.

$n_2 =$ the number of terms in the next largest grouping of equal terms in Y.

$\vdots$

n_β the number of terms in the smallest grouping of equal terms in Y.

We note $n_1 + n_2 + \cdots + n_\beta = \alpha$

To illustrate, we will repeat an example given in Chapter 3. Let $L = 5$, $M = 4$, the symbol set $\{a, b, c, d\}$. If a is sent, the configuration $Y = (2,1)$ accounts for the received L-tuples *aabbc*, *aabbd*, *aaccd*, *aabcc*, *aabdd*, and *aacdd* (without respect to order). In this example $\alpha = 2$, $n_1 = 1$, $n_2 = 1$, $\beta = 2$. The configuration $Y = (1,1,1)$ accounts for the L-tuple *aabcd* (without respect to order). In this case $\alpha = 3$, $n_1 = 3$, $\beta = 1$.

The term $\binom{L}{Y}$ in (B.4) is a shorthand notation for the multinomial coefficient:

$$\binom{L}{m_1\ m_2 \cdots m_\alpha} = \frac{L!}{m_1!m_2! \cdots m_\alpha!\left(L - \sum_{i=1}^{\alpha} m_i\right)!} \tag{B.5}$$

This term provides the number of ways of choosing $m_1, m_2, \ldots, m_\alpha$ and n_c positions in the received L-tuple. There are $\binom{M-1}{\alpha}$ ways to choose the α symbols to fill these positions and

$$\binom{\alpha}{n_1\ n_2 \cdots n_{\beta-1}}$$

ways to assign each group of α symbols to the generic configuration.

Finally, we need to account for random choices made by the decoder in case of ties. Define N_e as the number of terms in Y which equal n_c. Then the probability the correct symbol is chosen is given by $1/(N_e+1)$. We note, if $N_e = 0$ this probability is unity.

Thus, putting all these terms together we arrive at:

$$\begin{aligned} G(Y,n_c) &= \binom{1}{N_e+1}\binom{M-1}{\alpha}\binom{\alpha}{n_1, \ldots, n_{\beta-1}} \\ &= \binom{1}{N_e+1}\frac{(M-1)(M-2)\cdots(M-\alpha)}{n_1!n_2! \cdots n_\beta!} \end{aligned} \tag{B.6}$$

For a final example, consider $L = 7$ and $n_c = 3$. We know

$$q^{n_c}\left(\frac{p}{M-1}\right)^{L-n_c} = q^3\left(\frac{p}{M-1}\right)^4$$

for all terms, hence, we will calculate the bracketed quantity of (B.4). There are four possible generic configuration which meet the constraints set above

(1) $Y_1 = (1,1,1,1)$

$$\alpha = 4\ ,\ n_1 = 4\ ,\ \beta = 1\ ,\ N_e = 0$$

$$G(Y_1,3) = \frac{(M-1)(M-2)(M-3)(M-4)}{4!} \begin{pmatrix} 7 \\ 1,1,1,1 \end{pmatrix}$$

$$= 35(M-1)(M-2)(M-3)(M-4)$$

(2) $Y_2 = (2,1,1)$

$$\alpha = 3\ ,\ n_1 = 2\ ,\ n_2 = 1\ ,\ \beta = 2\ ,\ N_e = 0$$

$$G(Y_2,3) = \frac{(M-1)(M-2)(M-3)(M-4)}{2!\ 1!} \begin{pmatrix} 7 \\ 2,1,1 \end{pmatrix}$$

$$= 210(M-1)(M-2)(M-3)$$

(3) $Y_3 = (2,2)$

$$\alpha = 2\ ,\ n_1 = 2\ ,\ \beta = 1\ ,\ N_e = 0$$

$$G(Y_3,3) = \frac{(M-1)(M-2)}{2!} \begin{pmatrix} 7 \\ 2,2 \end{pmatrix}$$

$$= 105(M-1)(M-2)$$

(4) $Y_4 = (3,1)$

$$\alpha = 2\ ,\ n_1 = 1\ ,\ n_2 = 1\ ,\ \beta = 2\ ,\ N_e = 1$$

$$G(Y_4,3) = \frac{1}{2}\ \frac{(M-1)(M-2)}{1!\ 1!} \begin{pmatrix} 7 \\ 31 \end{pmatrix}$$

$$= 70(M-1)(M-2)$$

Combining (1)-(4), the full term for $n_e = 3$ is

$$\frac{35}{(M-1)^3} \left[5(M-2) + 6(M-2)(M-3) + (M-2)(M-3)(M-4) \right] \qquad \text{(B.7)}$$

which also agrees with [16].

B.3 Sample Evaluations of Enumeration Formulas

This section provides evaluations of ten of the enumeration formulas of Chapter 3 for sample values of L and appropriate thresholds. To allow more compact presentation of the formulas define

$$m_{ij} = \prod_{k=i}^{j} (M-i) \tag{B.8}$$

for example, $m_{13} = (M-1)(M-2)(M-3)$

Equation (3.7) [let $q_1 = F_c(1)$, $p_1 = F_E(1)$]

(1) $L = 3$

$$P(E_2 \cap E_d) = 2m_{12}q_1p_1^2 + m_{13}p_1^3 \tag{B.9a}$$

(2) $L = 5$

$$\begin{aligned} P(E_2 \cap E_d) = {} & 15m_{12}q_1^2p_1^3 + (4m_{14}+30m_{13}+15m_{12})q_1p_1^4 \\ & + (m_{15}+10m_{14}+15m_{13})p_1^5 \end{aligned} \tag{B.9b}$$

(3) $L = 7$

$$\begin{aligned} P(E_2 \cap E_d) = {} & 70m_{12}q_1^3p_1^4 \\ & + (105m_{14}+420m_{13}-210m_{12})q_1^2p_1^5 \\ & + (6m_{16}+105m_{15}-595m_{14}+525m_{13}-70m_{12})q_1p_1^6 \\ & + (m_{17}+21m_{16}+140m_{15}+315m_{14}+175m_{13})p_1^7 \end{aligned} \tag{B.9c}$$

Equation (3.18) [F_c, F_E, F_z defined in section 3.3]

(1) $L = 3$

$$\begin{aligned} p_2 = {} & \frac{M-1}{M} F_z^3 + 3m_{11}F_EF_z^2 + 3m_{12}F_E^2F_z \\ & + 3m_{11}F_cF_EF_z + m_{13}F_E^3 \end{aligned} \tag{B.10a}$$

(2) $L = 5$

$$
\begin{aligned}
p_2 = \frac{M-1}{M}\ & F_x^5 + 5m_{11}F_E F_x^4 + 10(m_{11}+m_{12})F_E^2 F_x^3 \\
& + 10m_{11}F_c F_E^2 F_x^2 + (10m_{13}+30m_{12})F_E^3 F_x^2 \\
& + (20m_{12}+30m_{11})F_C F_E^2 F_x^2 \\
& + (5m_{14}+30m_{13}+15m_{12})F_E^4 F_x \\
& + (15m_{13}+16m_{12})F_C F_E^3 F_x + 15m_{11}F_C^2 F_E^2 F_x \\
& + (m_{15}+10m_{12}+15m_{13})F_E^5 \\
& + (4m_{14}+30m_{13}+15m_{12})F_C F_E^4 + 15m_{12}F_c^2 F_E^3
\end{aligned}
\qquad \textbf{(B.10b)}
$$

Equation (3.26) [let $q_3 = q$, $p_3 = \dfrac{P}{M-1}$, $\mu(\ \ ) =$ unit step function]

(1) $L = 3$

$$
\begin{aligned}
p_2 = & \left[\ m_{13} + 3m_{12}\mu(T-3)\ \right] p_3^3 \\
& + \left[2m_{12}+3m_{11}\mu(T-3)\ \right] q_3 p_3^2
\end{aligned}
\qquad \text{(B.11a)}
$$

(2) $L = 5$

$$
\begin{aligned}
p_2 = & \left[\ m_{15}+10m_{15}+15m_{13}+10(m_{13}+m_{12})\mu(T-4) + 5m_{12}\mu(T-5)\right] p_3^5 \\
& + \left[4m_{14}+30m_{13}+15m_{12}+20m_{12}\mu(T-4) + 5m_{1}\mu(T-5)\ \right] q_3 p_3^4 \\
& + \left[15m_{12}+10m_{11}\mu(T-4)\ \right] q_3^2 p_3^3
\end{aligned}
\qquad \text{(B.11b)}
$$

(3) $L = 7$

$$
\begin{aligned}
p_2 = & \left[\ m_{17}+21m_{16}+140m_{15}+315m_{14}+175m_{13}\right. \\
& \quad + (35m_{14}+105m_{13}+35m_{12})\mu(T-5) \\
& \quad \left. + (21m_{13}+21m_{12})\mu(T-6) - 7m_{12}\mu(T-7)\ \right] p_3^7 \\
& + \left[6m_{16}+105m_{15}+455m_{14}+525m_{13}+70m_{12}\right. \\
& \quad \left. + (35m_{14}+105m_{13})\mu(T-5) + 42m_{12}\mu(T-6)+7m_{11}\mu(T-7)\ \right] q_3 p_3^6 \\
& + \left[105m_{14}+420m_{13}+210m_{12}+150m_{12}\mu(T-5) + 21m_{11}\mu(T-6)\ \right] q_3^2 p_3^5 \\
& + \left[70m_{12} + 35m_{11}\mu(T-5)\ \right] q_3^3 p_3^4
\end{aligned}
\qquad \text{(B.11c)}
$$

Equation (3.29) [use q_3, p_3 as defined above]

(1) $L = 5,\ T = 2$

$$p_{1b} = (10m_{14}+15m_{13})p_3^5 + (30m_{13}+15m_{12})q_3p_3^4 + 3.75m_{12}q_3^2p_3^3 \tag{B.12a}$$

(2) $L = 7,\ T = 3$

$$p_{1b} = (35m_{15}+210m_{14}-175m_{13})p_3^7 + (210m_{13}-210m_{12})p_3^2q_3^5 - (140m_{14}-420m_{13}-70m_{12})p_3q_3^6 + 35m_{12}p_3^3q_3^4 \tag{B.12b}$$

(3) $L = 7,\ T = 2$

$$p_{1b} = (21m_{16}+140m_{15}-315m_{14}-175m_{13})p_3^7 + (105m_{15}+445m_{14}+525m_{13}+70m_{12})q_3p_3^6 + (52.5m_{14}+350m_{13}+210m_{12})q_3^2p_3^5 + 35m_{12}q_3^3p_3^4 \tag{B.12c}$$

Equation (3.31) [use q_3, p_3]

(1) $L = 5,\ T = 2$

$$p_2 = m_{15}p_3^5 + 4m_{14}q_3p_3^4 \tag{B.13a}$$

(2) $L = 7,\ T = 3$

$$p_2 = (m_{17}+21m_{16}+105m_{15}+105m_{14})p_3^7 + (6m_{16}+105m_{15}-315m_{14}+105m_{13})q_3p_3^6 + (105m_{14}-210m_{13})q_3^2p_3^5 \tag{B.13b}$$

(3) $L = 7,\ T = 2$

$$p_2 = m_{17}p_3^7 + 6m_{16}q_3p_3^6 \tag{B.13c}$$

Equation (3.3.2) [use q_3, p_3]

(1) $L = 5,\ T = 2$

$$p_{eb} = [\text{ equation (B.12a) }] + 3.75m_{12}q_3^2p_3^3 \tag{B.14a}$$

(2) $L = 7,\ T = 3$

$$p_{eb} = [\text{ equation (B.12b) }] + 35m_{12}q_3^3p_3^4 \tag{B.14b}$$

(3) $L = 7,\ T = 2$

$$p_{2b} = [\text{ equation (B.12c) }] + 35m_{12}q_3^3p_3^4 + (52.5m_{14}+70m_{13})q_3^2p_3^5 \tag{B.14c}$$

Equation (3.3.3) [use q_3, p_3]

(1) $L = 5,\ T = 2$

$$P(E_{J_z}) = [\text{ equation (B.13a) }] + m_{14}q_3p_3^4 \tag{B.15a}$$

(2) $L = 7,\ T = 3$

$$P(E_{I_z}) = [\text{ equation (B.13b) }] + m_{16}q_3p_3^6 + (21m_{15}+105m_{14}+105m_{13})q_3^2p_3^5 \tag{B.15b}$$

(3) $L = 7,\ T = 2$

$$P(E_{I_z}) = [\text{ equation (B.13c) }] + m_{16}q_3p_3^6 \tag{B.15c}$$

Equation (3.4.2) [use q_3, p_3]

$L = 3$

$$p_{1b} = 0 \tag{B.16a}$$

$L = 5$

$$p_{1b} = 10m_{14}p_3^5 + 30m_{13}q_3p_3^4 \tag{B.16b}$$

$L = 7$

$$p_{1b} = (21m_{16}+210m_{15}+1260m_{14}+630m_{13})p_3^7 + (105m_{15}+35m_{14}+105m_{13})q_3p_3^6 + (210m_{13}+210m_{12})q_3^2p_3^5 \tag{B.16c}$$

Equation (3.43) [use q_3, p_3]

$L = 3$

$$p_2 = 2m_{12}q_3p_3^2 + m_{13}p_3^3 \tag{B.17a}$$

$L = 5$

$$p_2 = 15m_{12}q_3^2p_3^3 + (15m_{12}+4m_{14})q_3p_3^4 + (15m_{13}+m_{15})p_3^5 \tag{B.17b}$$

$L = 7$

$$p_2 = 70m_{12}q_3^3p_3^4 + (105m_{14}+210m_{13})q_3^2p_3^5 + (70m_{12}+105m_{13}+315m_{14}+6m_{16})q_3p_3^6 + (70m_{13}-105m_{14})105m_{15}+m_{17})p_3^7 \tag{B.17c}$$

Equation (3.44) [use q_3, p_3]

$L = 3$

$$p_5 = m_{12}q_3p_3^2 \tag{B.18a}$$

$L = 5$

$$p_5 = m_{14}q_3p_3^4 + 15m_{12}q_3^2p_3^3 \tag{B.18b}$$

$L = 7$

$$p_5 = m_{16}q_3p_3^6 + (105m_{14}+105m_{13})q_3^2p_3^5 + 70m_{12}q_3p_3^4 \tag{B.18c}$$

APPENDIX C

CODE AND COSET WEIGHT DISTRIBUTIONS

In this appendix we give binary and M-ary weight enumerators or equivalently weight distributions for Codes I, II, III, and IV as defined in Chapter 4.

In the tables that follow the weight distributions start at weight 1 in the left-most column and increment by 1 each position from left to right. For example, consider the code weight distribution for the (9,5) code. There are no vectors of weight one or two, 7 vectors of weight three, 9 of weight four, etc. Note that the tables do not account for the weight zero vector which must lie in both the code and coset weight distributions.

For binary weights, with reference to Section 4.3, the "Code Weight Distribution" corresponds to A_i enumerator values, the "Coset Leader Weight Distribution" corresponds to L_i enumerator values, "Weight Distribution of Cosets" corresponds to C_{ji} enumerator values excldlng the coset leaders, and the "Weight vs Bit Error Matrix" corresponds to the values $N(w,j)$.

For M-ary weight distributions the correspondences are the same except references are to the primed values A'_i, L'_i, C'_{ji}, and $N'(w,j)$ of Section 4.4.

WEIGHT DISTRIBUTIONS FOR (9,5) CODE

BINARY WEIGHTS - CODE I

CODE WEIGHT DISTRIBUTION

0	0	7	9	6	6	3	0	0

COSET LEADER WEIGHT DISTRIBUTION

9	6	0	0	0	0	0	0	0

WEIGHT DISTRIBUTION OF COSETS

WGT=1	0	21	36	72	81	45	18	6	0
WGT=2	0	9	41	45	39	33	15	3	1
WGT=3	0	0	0	0	0	0	0	0	0

WEIGHT VS BIT ERROR MATRIX

#ERRS=1	0	15	24	30	11	0	0	0	0
#ERRS=2	0	8	32	41	52	20	6	1	0
#ERRS=3	0	6	24	42	32	38	14	4	0
#ERRS=4	0	1	4	13	29	19	12	2	0
#ERRS=5	0	0	0	0	2	7	4	2	1

WEIGHT DISTRIBUTIONS FOR (10,5) CODE

BINARY WEIGHTS - CODE IIb

CODE WEIGHT DISTRIBUTION

0	0	0	16	0	12	0	3	0	0

COSET LEADER WEIGHT DISTRIBUTION

10	15	6	0	0	0	0	0	0	0

WEIGHT DISTRIBUTION OF COSETS

WGT=1	0	0	64	0	168	0	72	0	6	0
WGT=2	0	30	0	194	0	198	0	42	0	1
WGT=3	0	0	50	0	84	0	48	0	4	0
WGT=4	0	0	0	0	0	0	0	0	0	0

WEIGHT VS BIT ERROR MATRIX

#ERRS=1	0	15	35	50	45	15	0	0	0	0
#ERRS=2	0	14	63	95	86	50	11	1	0	0
#ERRS=3	0	0	11	48	81	92	63	20	5	0
#ERRS=4	0	1	5	17	40	48	35	14	0	0
#ERRS=5	0	0	0	0	0	5	11	10	5	1

M-ARY WEIGHTS (M=5) - CODE IIm

CODE WEIGHT DISTRIBUTION

1	30

COSET LEADER WEIGHT DISTRIBUTION

26	5

WEIGHT DISTRIBUTION OF COSETS

BWGT=1	12	298
BWGT=2	18	447
BWGT=3	5	181
BWGT=4	0	0

WEIGHT VS BIT ERROR MATRIX

#ERRS=1	10	146
#ERRS=2	10	301
#ERRS=3	4	307
#ERRS=4	12	145
#ERRS=5	0	32

WEIGHT DISTRIBUTIONS FOR (13,5) CODE

BINARY WEIGHTS - CODE III

CODE WEIGHT DISTRIBUTION

0	0	0	0	8	10	4	3	4	2	0	0	0

COSET LEADER WEIGHT DISTRIBUTION

13	78	134	30	0	0	0	0	0	0	0	0	0

WEIGHT DISTRIBUTION OF COSETS

WGT=1	0	0	0	40	60	92	94	60	35	16	6	0	0
WGT=2	0	0	80	150	404	504	536	420	204	90	24	6	0
WGT=3	0	0	72	423	611	910	882	668	404	138	40	5	1
WGT=4	0	0	0	72	204	200	200	136	68	40	8	2	0

WEIGHT VS BIT ERROR MATRIX

#ERRS=1	0	0	47	212	336	328	216	119	22	0	0	0	0
#ERRS=2	0	0	43	229	445	621	562	410	182	58	10	0	0
#ERRS=3	0	0	52	192	388	518	586	420	263	107	29	5	0
#ERRS=4	0	0	10	52	116	209	304	269	199	86	29	5	1
#ERRS=5	0	0	0	0	2	40	48	69	49	35	10	3	0

WEIGHT DISTRIBUTIONS FOR (15,5) CODE

BINARY WEIGHTS - CODE IVb

CODE WEIGHT DISTRIBUTION

0	0	0	0	0	0	15	15	0	0	0	0	0	0	1

COSET LEADER WEIGHT DISTRIBUTION

15	105	455	420	28	0	0	0	0	0	0	0	0	0	0

WEIGHT DISTRIBUTION OF COSETS

WGT=1	0	0	0	0	0	105	120	120	105	0	0	0	0	15
WGT=2	0	0	0	0	315	420	840	840	420	315	0	0	105	0
WGT=3	0	0	0	525	840	2520	2940	2940	2520	840	525	455	0	0
WGT=4	0	0	0	420	1680	1680	2520	2520	1680	1680	840	0	0	0
WGT=5	0	0	0	0	140	280	0	0	280	168	0	0	0	0

WEIGHT VS BIT ERROR MATRIX

#ERRS=1	0	0	0	161	641	961	1083	1062	696	362	154	0	0	0	0
#ERRS=2	0	0	0	322	1122	1796	2166	2124	1552	850	308	0	0	0	0
#ERRS=3	0	0	0	308	850	1552	2124	2166	1796	1122	322	0	0	0	0
#ERRS=4	0	0	0	154	362	696	1062	1083	961	641	161	0	0	0	0
#ERRS=5	0	0	0	0	0	0	0	0	0	28	420	455	105	15	1

M-ARY WEIGHTS (M=5) - CODE IVm

CODE WEIGHT DISTRIBUTION

0	0	31

COSET LEADER WEIGHT DISTRIBUTION

81	599	343

WEIGHT DISTRIBUTION OF COSETS

BWGT=1	0	15	450
BWGT=2	0	180	3075
BWGT=3	6	993	13106
BWGT=4	6	1027	11987
BWGT=5	0	69	799

WEIGHT VS BIT ERROR MATRIX

#ERRS=1	3	549	4564
#ERRS=2	3	591	9637
#ERRS=3	0	659	9572
#ERRS=4	6	485	4625
#ERRS=5	0	0	1024

BIBLIOGRAPHY

BIBLIOGRAPHY

[1] R.E. Blahut, *Theory and Practice of Error Control Codes,* Addison-Wesley Pub. Co., Massachusetts, 1983.

[2] K.G. Castor and W.E. Stark, "Performance of Diversity/Reed-Solomon Frequency-Hopped Communications with Errors and Erasures via Ratio Thresholding," *Proceedings of the 22nd Annual Allerton Conference on Communication, Control, and Computing,* pp.869-877, October 2-4, 1985.

[3] K.G. Castor and W.E. Stark, "Parallel Decoding of Diversity/Reed-Solomon Coded SSFH Communications with Repetition Thresholding," *Proceedings of the 20th Annual Conference on Information Sciences and Systems,* Princeton University, March 19-21, 1986.

[4] G.C. Clark Jr. and J.B. Cain, *Error-Correction Coding for Digital Communications,* Plenum Press, New York, 1982.

[5] Pil Joong Lee, "Performance of a Normalized Energy Metric Without Jammer State Information for an FH/MFSK System in Worst Case Partial Band Jamming," *IEEE Transactions on Communications,* pp.869-877, August 1985.

[6] B.K. Levitt and J.K. Omura, "Coding Tradeoffs for Improved Performance of FH/MFSK Systems in Partial Band Noise," *Record of the National Telecommunications Conference (NTC'81),* D9.1.1-5, November 1981.

[7] F.J. MacWilliams and N.J.A. Sloane, *The Theory of Error-Correcting Codes,* North-Holland Publishing Co., New York, 1977.

[8] R.J. McEliece, *The Theory of Information and Coding,* Addison-Wesley Pub. Co., Massachusetts, 1977.

[9] R.J. McEliece and L. Swanson, "On the Decoder Error Probability for Reed-Solomon Codes," unpublished paper.

[10] A.M. Michelson and A.H. Levesque, *Error-Control Techniques for Digital Communications,* John Wiley and Sons, New York, 1985.

[11] J.G. Proakis, *Digital Communications,* McGraw Hill Book Co., New York, 1983.

[12] M.B. Pursley and W.E. Stark, "Performance of Reed-Solomon Coded Frequency-Hop Spread Spectrum in Partial Band Interference," *IEEE Transactions on Communications,* pp.767-774, August, 1985.

[13] M. Schwartz, W.R. Bennett, and S. Stein, *Communication Systems and Techniques,* McGraw-Hill Book Co., New York, 1966.

[14] M.K. Simon, J.K. Omura, R.A. Scholtz, and B.K. Levitt, *Spread Spectrum Communications, Vol. I, Vol. II, Vol. III,* Computer Science Press, Maryland, 1985.

[15] W.E. Stark, "Coding for Frequency-Hopped Spread Spectrum Channels with Partial Band Interference," Ph.D. Dissertation, University of Illinois, 1982.

[16] W.E. Stark, "Coding for Frequency-Hopped Spread Spectrum Communication with Partial Band Interference — Part II: Coded Performance," *IEEE Transactions on Communications,* pp.1045-1057, October 1985.

[17] A.J. Viterbi, *Principles of Coherent Communication,* McGraw-Hill Book Co., New York, 1966.

[18] A.J. Viterbi, "A Robust Ratio Threshold Technique to Mitigate Tone and Partial Band Jamming in Coded MFSK Systems," *Proceedings of the 1982 IEEE Military Communications Conference,* pp.22.4.1-5, October 1982.

[19] A.J. Viterbi, "Robust Decoding of Jammed Frequency Hopped Modulation," submitted to *IEEE Transactions on Communications.*

[20] A.J. Viterbi and J.K. Omura, *Principles of Digital Communications and Coding,* McGraw-Hill Book Co., New York, 1979.

[21] J.K. Wolf, A.M. Michelson, and A.L. Levesque, "On the Probability of Undetected Error for Linear Block Codes," *IEEE Transactions on Communications,* pp.317-324, February 1982.